# A NEW Vs30 PREDICTION STRATEGY TAKING GEOLOGY, TERRAIN, AND SATURATION INTO ACCOUNT: APPLICATION TO TÜRKİYE

A THESIS SUBMITTED TO
THE GRADUATE SCHOOL OF NATURAL AND APPLIED SCIENCES
OF
MIDDLE EAST TECHNICAL UNIVERSITY

BY

HAKAN BORA OKAY

IN PARTIAL FULFILLMENT OF THE REQUIREMENTS
FOR
THE DEGREE OF MASTER OF SCIENCE
IN
GEOLOGICAL ENGINEERING

AUGUST 2022

Approval of the thesis:

**A NEW Vs30 PREDICTION STRATEGY TAKING GEOLOGY, TERRAIN, AND SATURATION INTO ACCOUNT: APPLICATION TO TÜRKİYE**

submitted by **HAKAN BORA OKAY** in partial fulfillment of the requirements for the degree of **Master of Science** i**n Geological Engineering, Middle East Technical University** by,

Prof. Dr. Halil Kalıpçılar
Dean, Graduate School of **Natural and Applied Sciences** _____

Prof. Dr. Erdin Bozkurt
Head of the Department, **Geological Engineering** _____

Assoc. Prof. Dr. Atilla Arda Özacar
Supervisor, **Geological Engineering, METU** _____

**Examining Committee Members:**

Prof. Dr. Erdin Bozkurt
Geological Eng, METU _____

Assoc. Prof. Dr. Atilla Arda Özacar
Geological Eng, METU _____

Prof. Dr. Mehmet Lütfi Süzen
Geological Eng, METU _____

Prof. Dr. Zeynep Gülerce
Civil Eng., METU _____

Assoc. Prof. Dr. Tolga Görüm
Eurasia Institute of Earth Sciences, İstanbul Teknik Uni. _____

Date: 26.08.2022

**I hereby declare that all information in this document has been obtained and presented in accordance with academic rules and ethical conduct. I also declare that, as required by these rules and conduct, I have fully cited and referenced all material and results that are not original to this work.**

Name Last name : Hakan Bora Okay

Signature :

# ABSTRACT

## A NEW Vs30 PREDICTION STRATEGY TAKING GEOLOGY, TERRAIN, AND SATURATION INTO ACCOUNT: APPLICATION TO TÜRKİYE

Okay, Hakan Bora
Master of Science, Geological Engineering
Supervisor: Assoc. Prof. Dr. Atilla Arda Özacar

August 2022, 87 pages

Various parameters are used for geotechnical characterization of site conditions. Among them, most widely used one is average shear wave velocity in upper 30 meters (Vs30). So far, many different proxy-based approaches are proposed to predict Vs30 across large-scale areas where geophysical measurements are limited or absent. In this study, elevation and slope of Vs30 measurement locations in Türkiye and California are determined using high-resolution digital elevation model along with their geologic unit and terrain classes. Their correlation with measurements indicate that Vs30 is sensitive to various site properties and thus should be treated as multi-factor dependent parameter.

In order to improve accuracy, new Vs30 prediction strategy is developed. In this approach, geologic units are classified into 4 sedimentary rock classes according to their ages (Quaternary-Pliocene, Miocene, Paleogene, Pre-Paleogene) and 3 non-sedimentary rock classes (Intrusive, Extrusive, Metamorphic).Vs30 measurements from Quaternary-Pliocene rocks are most abundant and characterized by large data scatter thus further divided into 2 terrain classes (Mountain/Hill, Plain/Terrace). Since reduction in Vs30 due to fluid saturation is pronounced especially in unconsolidated young units, Quaternary-Pliocene rocks are also differentiated as

saturated if water table less than 30 m and unsaturated otherwise. In the absence of borehole measurements, flat areas with height difference less than 30 m from surface water bodies (sea, lake, and major rivers) are mapped out in Türkiye as saturated using water level rise analysis. After elimination of outliers, slope and elevation based Vs30 prediction equations are developed separately for sub-classes of Quaternary-Pliocene, Miocene, and Paleogene aged sedimentary rocks using linear regression with multivariable while Vs30 is fixed to class average in others. Our prediction strategy performed better in young units than others and provided a new, more accurate Vs30 map of Türkiye.

Keywords: Vs30 Prediction, Topographic Slope, Elevation, Morphological Terrain, Geologic Rock Classification, Saturation, Water Level Rise Analysis, Türkiye, California

# ÖZ

## JEOLOJİ, ARAZİ VE DOYGUNLUĞU DİKKATE ALAN YENİ Vs30 TAHMİN STRATEJİSİ: TÜRKİYE UYGULAMASI

Okay, Hakan Bora
Yüksek Lisans, Jeoloji Mühendisliği
Tez Yöneticisi: Doç. Dr. Atilla Arda Özacar

Ağustos 2022, 87 sayfa

Saha koşullarının jeoteknik karakterizasyonu için çeşitli parametreler kullanılmaktadır. Bunlardan en yaygın kullanılanı yüzeyin ilk 30 metresine ait ortalama kesme dalgası hızı (Vs30) değeridir. Şimdiye kadar,jeofizik ölçümlerin sınırlı olduğu veya bulunmadığı geniş alanlarda Vs30 tahmin etmek için farklı öncül tabanlı yaklaşımlar önerilmiştir. Bu çalışmada, Türkiye ve Kaliforniyadaki Vs30 ölçüm noktalarının yükseklik ve eğimleri, jeolojik birim ve arazi sınıfları ile birlikte yüksek çözünürlüklü sayısal yükseklik modeli kullanılarak belirlenmiştir. Ölçümlerle korelasyonları, Vs30'un çeşitli saha özelliklerine duyarlı olduğunu ve çok faktöre bağlı bir parametre olarak ele alınması gerektiğini göstermektedir.

Tahmin tutarlılığını artırmak için yeni Vs30 tahmin stratejisi geliştirilmiştir. Buna göre jeolojik birimler, yaşlarına göre 4 tortul kayaç sınıfına (Kuvaterner-Pliyosen, Miyosen, Paleojen, Pre-Paleojen) ve 3 tortul olmayan kayaç (iç püskürük, dış püskürük, başkalaşım) sınıfına ayrılmıştır. Vs30 ölçümlerinin çoğunluğu, dağınık veri dağılımı sergileyen Kuvaterner-Pliyosen kayaçlarda olduğundan, bu kayaçlar ayrıca 2 arazi sınıfına (Dağ/Tepe, Ova/Teras) ayrılmıştır. Özellikle pekişmemiş genç birimlerde akışkan doygunluğuna bağlı Vs30'daki azalma belirgin olduğundan,

Kuvaterner-Pliyosen kayaçlar su tablası derinliği 30 m'den az ise doymuş, aksi halde doymamış olarak ayırtlanmıştır. Sondaj ölçümlerinin yokluğunda, yüzey su kütlelerinden (deniz,göl ve büyük nehirler) yükseklik farkı 30 m'den az olan düz alanlar, su seviyesi yükselme analiziyle Türkiye genelinde doygun alanlar olarak haritalanmıştır. Aykırı değerlerin atılmasından sonra, Kuvaterner-Pliyosen alt sınıfları, Miyosen ve Paleojen yaşlı tortul kayaçlar için ayrı ayrı eğim ve yükselti tabanlı Vs30 tahmin denklemleri çok değişkenli lineer regresyon kullanılarak belirlenmiş, diğerleri ise Vs30 sınıf ortalamasına sabitlenmiştir. Tahmin stratejimiz genç birimlerde diğerlerinden daha iyi performans gösterdi ve Türkiyenin yeni, daha doğru bir Vs30 haritası oluşturuldu.

Anahtar Kelimeler: Vs30 Tahmini, Topografik Eğim, Yükseklik, Morfolojik Arazi, Jeolojik Kaya Sınıflandırması, Doygunluk, Su Seviyesi Yükselme Analizi, Türkiye, California

To Our Untimely and Preventable Losses

# ACKNOWLEDGMENTS

First, I would be glad to express my deepest gratitude to my supervisor Assoc. Prof. Dr. Atilla Arda Özacar for his patience, criticism, and encouragement throughout the research. Thanks to his guidance, I believe I have succeeded in taking it to the next level. I am grateful to him for the opportunities he has created in my career.

I would also like to thank Prof. Dr. M. Lütfi Süzen for his suggestions, technical and moral support, and forward-carrying comments. I want to thank him for sharing not only academic life but also real life from our conversations. I am also grateful to my examining committee members Prof. Dr. Erdin Bozkurt, Prof. Dr. Zeynep Gülerce, and Assoc. Prof. Dr. Tolga Görüm for their critical reviews, shared knowledge, and forward-looking feedback.

I want to thank my friends and colleagues Yakup Betus, Utku Karakaya, Kaan Onat, and Akın Çil for their support for helping to think differently when a dead end comes. Our friends are the family that we can choose. I would also like to thank my chosen family, Ekin Özbek, U. Barış Asil, Ozan Sinoplu, Çağan Yılmaztürk, Özgür Mutlu, Hasan Sezai Sevindik, İsmet Gökhan, Cem Gökağaçlı and whoever feels like a part of this family. I also miss my friend Samet Albasar, whom I lost untimely during this period. I'm sure you're in the place you deserve and at peace, brother.

I am sincerely grateful to my lovely and devoted mother for his endless and unconditional love and endeavor. I would also like to express my deepest love and appreciation to my father and sister, whose love and support have strengthened me.

Most importantly, I would like to thank my wife Büşra Karagöz, whose love, support and presence I have always felt beside me and in my mind. I can't express my gratitude to her, who found a way to lift me up every time I fell and my companion on this long journey, my biggest confidant and my only playmate in this life. We are two crazy trying to make our dreams come true. I'm glad you're the lifelong psychologist of this madman. Your madman is here for you until the end.

## TABLE OF CONTENTS

## LIST OF TABLES

## LIST OF FIGURES

## LIST OF ABBREVIATIONS

AFAD: Disaster and Emergency Management Presidency

CASGEM: California Statewide Groundwater Elevation Monitoring

DEM: Digital Elevation Model

DSFZ: Dead Sea Fault Zone

DWR: Department of Water Resources

EAFZ: East Anatolian Fault Zone

FAO: Food and Ahriculture Organization

GIS: Geographic Information Systems

GSA: Geological Society of America

JAXA: Japan Aerospace Exploration Agency

MERIT: Multi-error-removed improved-terrain

NAFZ: North Anatolian Fault Zone

NASA: National Aeronautics and Space Administration

NEAFZ: Northeast Anatolian Fault Zone

NEHRP: National Earthquake Hazard Reduction Program

NGA: The National Geospatial-Intelligence Agency

SGMA: Sustainable Groundwater Management Act

SRTM: Shuttle Radar Topography Mission

TBDY: Türkiye Building Earthquake Code

USGS: United States Geological Survey

# CHAPTER 1

# INTRODUCTION

Earthquake is one of the most crucial and irrefutable facts of Türkiye and the World. Ground conditions have to be more deeply investigated to ensure the '*real risks*' of the earthquake and prevent the possible damages. Understanding seismic site characterization and soil-type classification for a specific region or area is crucial. The average seismic shear wave velocity of the top 30 meters from ground level (Vs30) is used for different ground condition classifications like Eurocode8:*Design of Structures for Earthquake Resistance* (CEN, 2004), *Türkiye Building Earthquake Code* (TBDY, 2019), and *National Earthquake Hazard Reduction Program* (NEHRP) (BSSC, 2004). Design parameters have to be selected appropriate to the seismic site conditions to build proper structures. Therefore, accurate mapping of Vs30, which is a widely accepted parameter for site characterization, is critical. From an engineering perspective, Vs30 has an essential role in seismic hazard mapping, ground motion prediction equations, and earthquake-resistant design.

Ground-based techniques often take a long time and involve much physical work. Therefore, some unconventional techniques are created to estimate Vs30 for unknown regions to investigate regional seismic hazard risk. This study investigates the performance of some available proxy-based approaches by using a collection of Vs30 measurements from Türkiye and California and develops a new Vs30 prediction strategy to improve the accuracy of Vs30 estimations.

## 1.1 Purpose and Scope

Seismic site conditions are essential to understanding the characterization of the ground under the effect of earthquake waves. The most common construction regulations with earthquake risk include Vs30 as one of the standard indicators for seismic site conditions. With this respect, a map that shows the distribution of Vs30 can be a good representative of seismic site conditions. The work detailed here aims to (a) examine the performance of the Vs30 estimating practice that is currently used in Türkiye and California and (b) enhance estimation ability for situations where measurements are not available to provide necessary seismic site conditions for further studies and design phases. The first stage aims to make a performance analysis of available Vs30 data. The second stage mainly focuses on creating a more accurate nationwide Vs30 map of Türkiye.

In order to achieve our first aim, we used a collection of Vs30 measurements from Türkiye and California. In Türkiye, Disaster and Emergency Management Presidency (AFAD) published a nationwide Vs30 database comprising measurements taken at strong ground motion stations located around Türkiye. The United States Geological Survey (USGS) collected and published 4389 Vs30 measurements across the United States, and 1358 were from the California region. Both databases are combined and used for the performance analysis stage of this study. The distribution of these measurements, which can be seen in Figure 1-1, is mainly present in residential areas of both Türkiye and California.

During the first phase, the conducted performance analysis allowed us to explore the inherit uncertainty associated to available proxy-based Vs30 prediction approaches. In the second phase, a comprehensive effort is spent to develop a formulation using accurate instruments that would improve the accuracy of Vs30 predictions at areas where seismic site conditions are unknown. In this direction, we investigated key factors, including surface geology, lithologies, water saturation, topographic slope, elevation, and morphological terrain classes for Vs30 parameter estimation. By

adding geological limitations to the topographical properties, we aim eventually to create a new enhanced Vs30 model of the entire Türkiye.

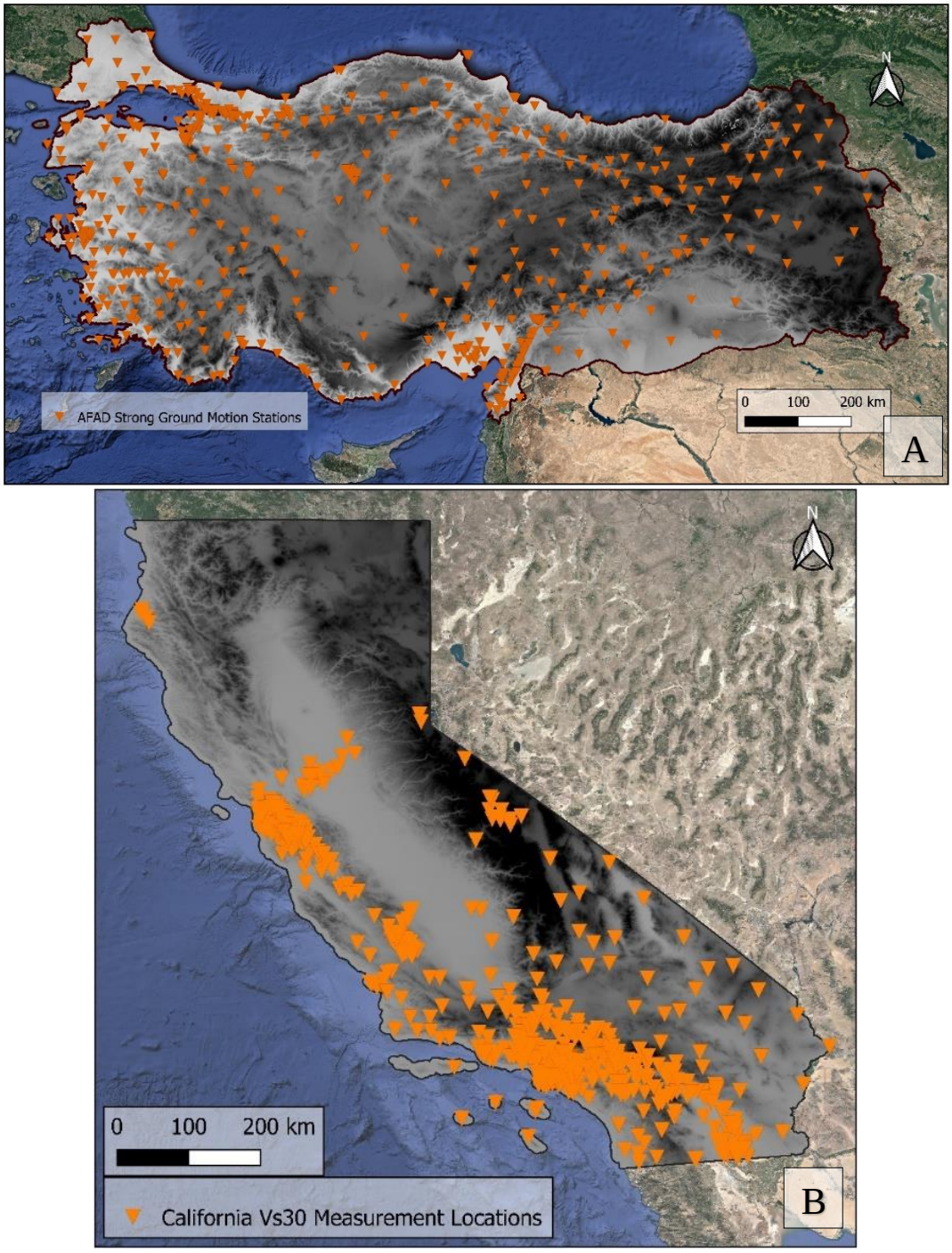


Figure 1-1: (A) Topographical map of Türkiye, showing AFAD strong ground motion station locations where Vs30 measurement is available. (B) Topographical map of California showing Vs30 measurement locations.

## 1.2 Background

Vs30 measurement by borehole logging and surface geophysical surveys is an expensive and time-consuming procedure; that is why numerous proxy-based Vs30 prediction methodologies have been developed to estimate Vs30 globally or nationwide. Global-scale research is based on a topographical slope, while local-scale research adds some extra predictors to their studies. Using topographic properties as proximity for Vs30 allows the creation of quick, cheap, and accessible data about seismic site conditions. However, global-scale Vs30 models should be treated with caution since they use only topographic data as a proxy for seismic site conditions (Allen & Wald, 2009; Heath et al., 2020; Wald & Allen, 2007)

There are also many regional studies aiming to improve the quality of Vs30 estimations. In California, Wills et al. (2000) created a site condition map based on geology and shear-wave velocity measurements. After their first study, they rearranged their geologic boundaries and developed a second study for California (Wills & Clahan, 2006). Another regional study was conducted by Stewart et al. (2014) in Greece and recommended using terrain, geologic age and gradation for Vs30 estimation. Another study conducted by Kwok et al. (2018) aims to create a Taiwan-specific Vs30 prediction model using slope gradient and elevation for younger sediments and geomorphic terrain for older deposits.

In addition to the geology and topographic properties, different methods are also used to increase the precision of Vs30 estimation. Karimzadeh et al. (2019) prepared a site classification map based on Vs30 estimation using convexity and morphology matrix. Recently, Mori et al. (2020) conducted and published a new study in which they derived a Vs30 map for Italy using geotechnical borehole data and global terrain classification (Iwahashi et al., 2018).

### 1.2.1 Site Characterization Based on Seismic Shear Wave Velocity

Ground amplification is a reason for most earthquake damages. This means ground conditions are as important as earthquake properties like earthquake magnitude or epicenter location in terms of intended regions. Vs30 is the best indicator for understanding ground stiffness, and it is an important criterion in building design. Material's resistance to deformation is called stiffness (Sheriff, 2002), and it is related to Young's modulus, which is resistance along the stress axis and shear modulus that shape the deformation resistance of the material. Seismic shear wave velocity is a direct indicator of material stiffness. Lower Vs30 values generally indicate greater ground amplification; thus, these regions are more prone to earthquake damage.

Vs30 is essential to understand the average properties of layered Earth, where material property changes significantly with depth. Although medium properties are considered homogeneous inside a layer, dynamic processes near the surface produce higher level of complexity resulting in faster property change at shallower depths. For this reason, taking the characteristics of the first 30 meters as a whole can give more robust results.

### 1.2.2 Usage and Calculation of Vs30

During the instrumental period, large volumes of seismic data become accessible for earthquake observations, and many studies are conducted to explain the amount of damage caused by earthquake phenomena. Vs30 is first introduced for estimating site response to design earthquake resistant structures (Borcherdt, 1994). During elastic wave propagation from hard rock to soft deposits, seismic waves slow down and amplify, possibly causing heavy structural damage. In this respect, Vs30 provides means for unbiased quantitative classification of site conditions needed for accurate computation of response spectra.

Vs30 is a widely accepted proxy for seismic amplification, but several works that question this proxy is also present (Castellaro et al., 2008; Pitilakis et al., 2013, 2019; Sandikkaya et al., 2013; Sandıkkaya & Dinsever, 2018). Common points of these studies are mainly focused on the usage of Vs30 as the only parameter for seismic site amplification. Despite the improvements in 3-D geological modeling and soil characterization techniques, Vs30 measurements are still widely used for site classification and utilized in most design codes (Table 1-1).

Table 1-1: Vs30 Classification table from universal handbooks NEHRP (BSSC, 2004), Eurocode8 - EN1998 (CEN, 2004), and local regulation Türkiye Building Earthquake Code (TBDY)

| ***Site Class (Type)*** | **NEHRP** | **EN1998** | **TBDY** |
|---|---|---|---|
| ***A*** | > 1500 | > 800 | > 1500 |
| ***B*** | 760 – 1500 | 360 – 800 | 760 – 1500 |
| ***C*** | 360 – 760 | 180 – 360 | 360 – 760 |
| ***D*** | 180 – 360 | < 180 | 180 – 360 |
| ***E*** | < 180 | Descriptive conditions* | < 180 |
| ***F (S1&S2 for Eurocode8)*** | < 180 (additional conditions) | $S_1$: < 100 (indicative)<br>$S_2$: Descriptive conditions* | Site-specific investigation and evaluation required* |

Several different methods are present to measure shear wave velocity. These methods can be grouped under two, as shown in Figure 1-2: surface and downhole methods (Hunter et al., 2002). Surface methods are classified as non-invasive, and they are relatively more accessible. On the other hand, downhole methods are “in-situ” that measure vertical shear wave velocity and require borehole logging. During this process, a borehole is drilled, and measurements are conducted for further investigation.

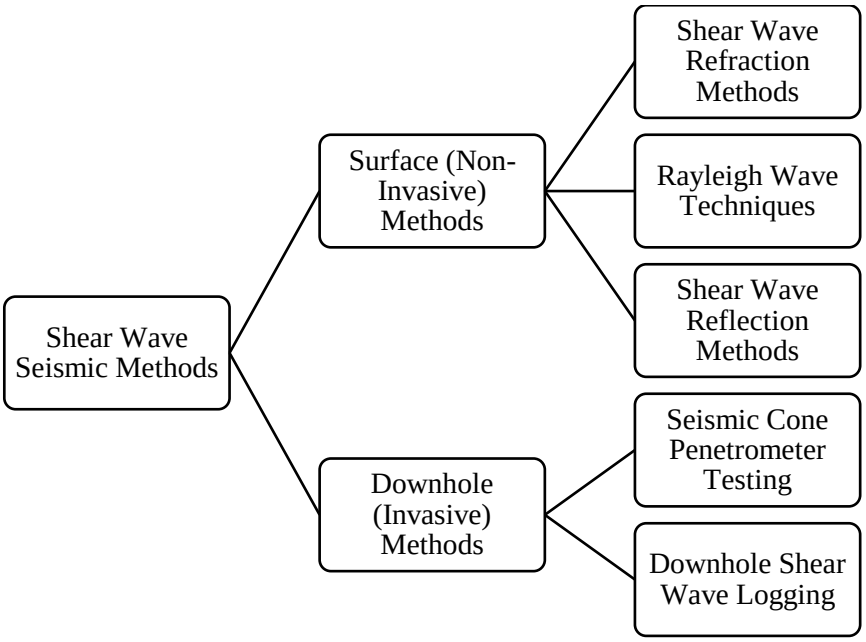


Figure 1-2: Summary of seismic shear wave velocity measurement techniques (Hunter et al., 2002)

In general, the total time taken for shear waves to travel from a depth of 30 meters to the ground surface defines the Vs30 value. In a simple multi-layered earth model where layers are assumed horizontal, Vs30 is calculated by dividing 30 meters to the summed ratio of the thickness (H) to shear wave velocity (Vs) of each in individual layer (i) within the top 30 meters depth (Figure 1-3).

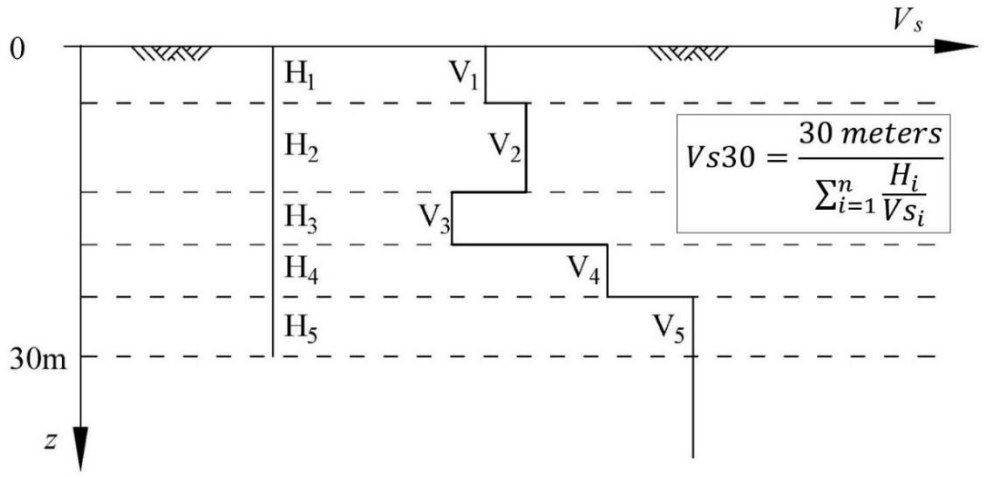


Figure 1-3: Equation and schematic illustration of Vs30 calculation in a simple earth model containing multiple horizontal layers (Borcherdt, 1994).

# CHAPTER 2

# DATA AND RESOURCES

During the collection of data, several open sources are explored. First, we started with available Vs30 measurements around the World in addition to Türkiye data. Both Türkiye and California are characterized by widespread active tectonic processes producing a high level of earthquake activity. Two of the World's most active continental transform faults, the North Anatolian Fault (NAF) and San Andreas Fault (SAF) are also located within Türkiye and California, respectively. Since California and Türkiye have similar geologic and tectonic attributes, we decided to combine Vs30 measurements available from California, the USA, with the Turkish nationwide Vs30 database. In order for both regions to have the same resolution and quality, the Shuttle Radar Topography Mission (SRTM) 1 arc-second (approximately 30 meters) resolution digital elevation model (DEM) was used for elevation data and derivatives like slope and aspect. On the other hand, surface geology, hydrological features, and Vs30 measurements are combined from separate databases for each region.

## 2.1 Surface Geology

In this study, the surface geology of Türkiye is digitized from 1/500,000 scale geological maps prepared by the General Directorate of Mineral Research and Exploration (MTA) and California's surface geology from Wills et al. (2000).

The Geology of Türkiye is mainly shaped by the complex collision between Gondwana and Laurasia that formed multiple suture zone separating various geologic terranes (Okay, 2008). More recently, Türkiye shows westward escape due

to the collision between the Arabian, African and Eurasian plates. This position creates different types of faults and different seismotectonic regions in Türkiye. Major active tectonic elements of Türkiye is simply shown in Figure 2-1. In the east, an ongoing continental collision between Arabian and Eurasian plates translates to large lateral motions along major continental transform faults (North Anatolian Fault and East Anatolian Fault), while processes associated to the northward subduction of the African plate mainly leads to active extension in the west (e.g. Bozkurt & Mittwede, 2001). It is worth noting that this stunning complexity creates large variety in geology; thus, Türkiye is an ideal location for new geologic studies.

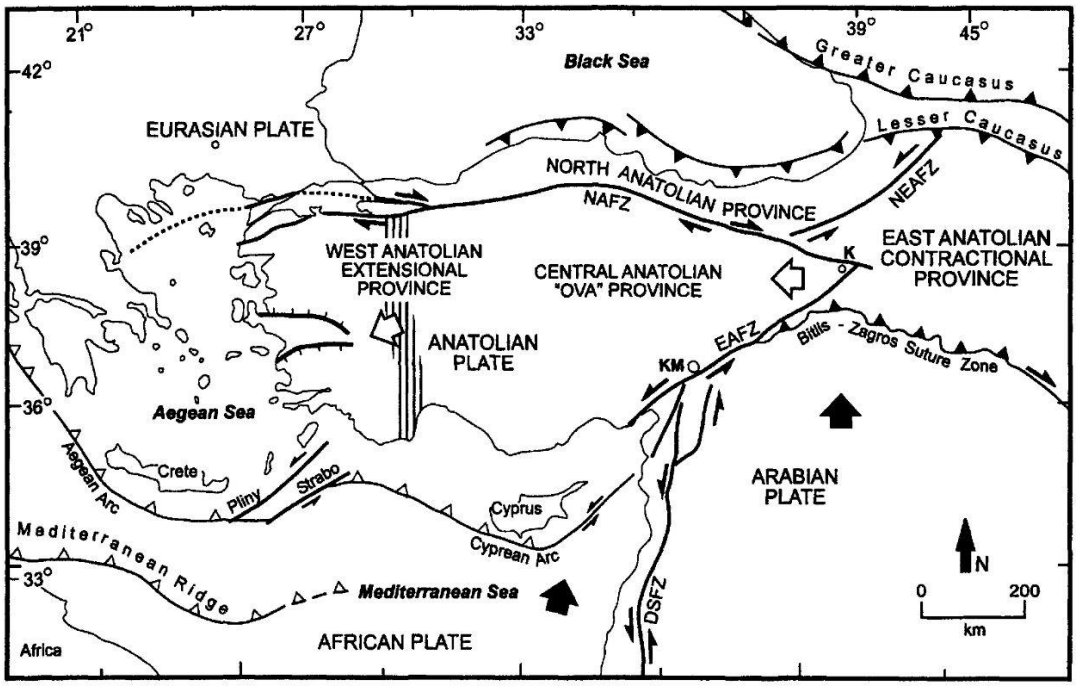


Figure 2-1: Simplified tectonic map of Türkiye that indicates neotectonic structures and provinces (directly taken from Bozkurt & Mittwede, 2001; Bozkurt & Oberhänsli, 2001)

Similarly, California displays a very complex geologic evolution that resulted in the formation of various tectonic terrains (Prothero, 2016). Throughout its history, the initially passive continental margin became an active subduction margin which ended with the demise of the Farallon Plate, initiating the formation of a transform plate boundary associated with the San Andreas Fault plate. As a result, California

consists of eleven major provinces separated by their geologic and geomorphic properties (Figure 2-2).

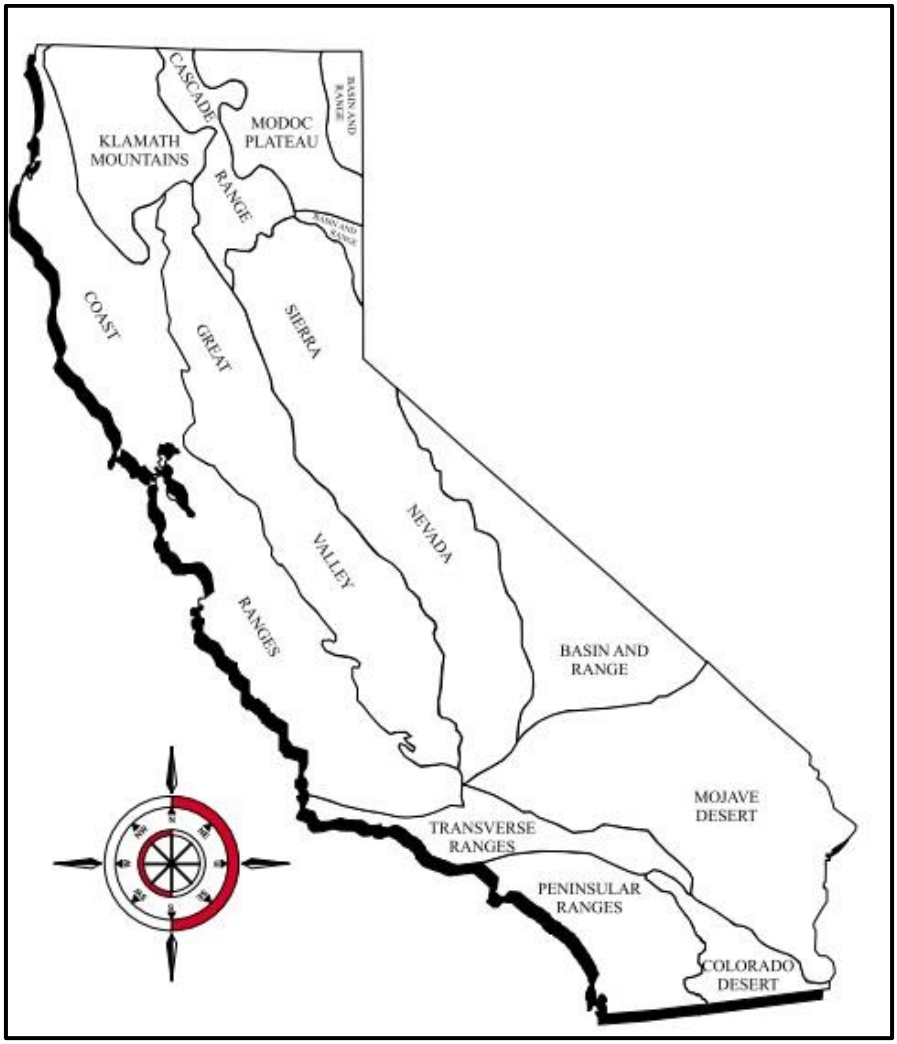


Figure 2-2: Geomorphic provinces of California (California Geological Survey)

After we had compiled all data about the surface geology of Türkiye and California, we created digital geologic maps of these two regions and observed the geologic units' distribution according to their age (Figure 2-3). The surface geology of both regions is mainly dominated by Quaternary basins and mountain ranges surrounding them. In this respect, there are some noticeable similarities and differences in morphology and deposition environments.

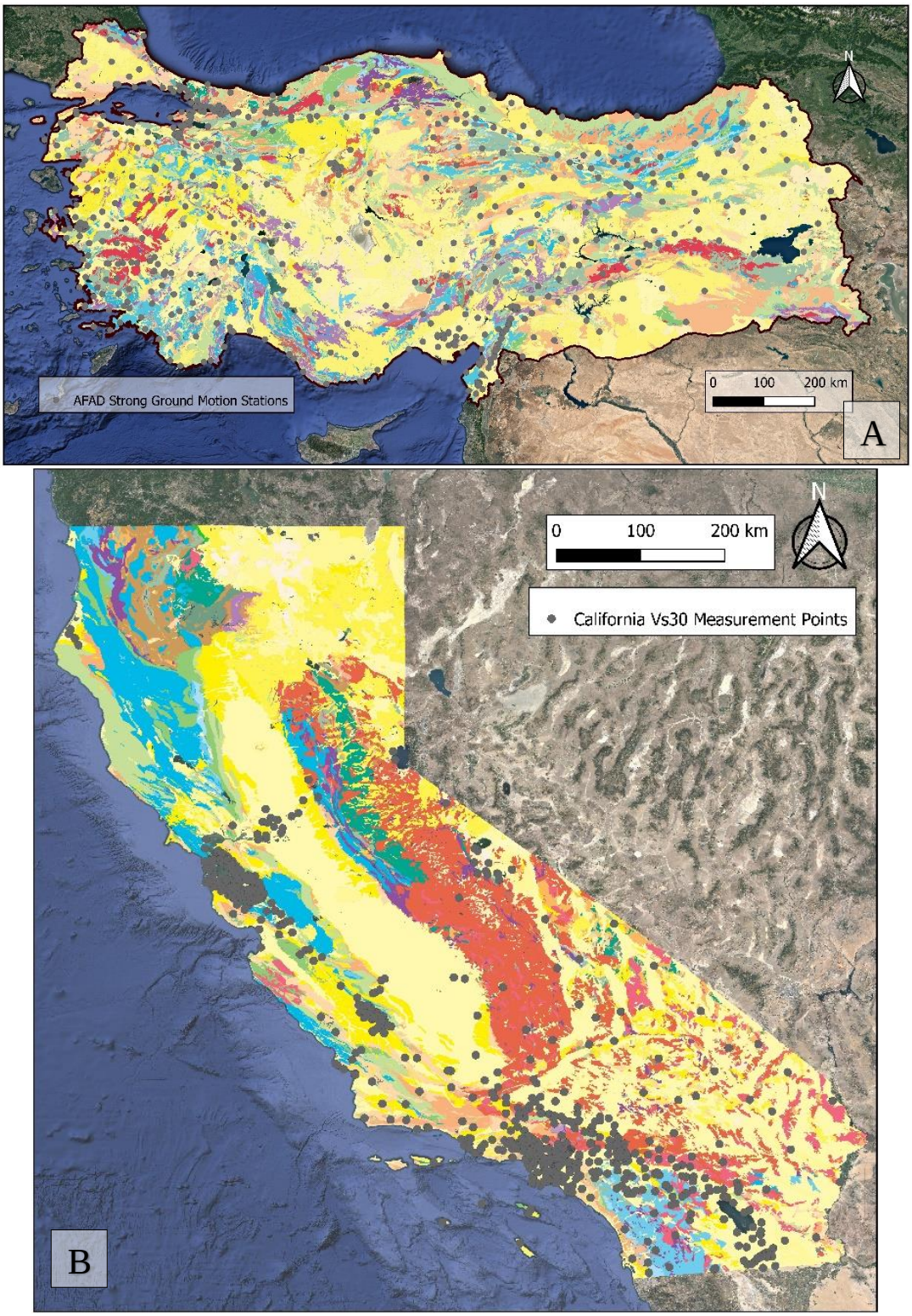


Figure 2-3: Geology maps of Türkiye (A) and California (B) with Vs30 measurement locations (GSA geologic time scale color-coded)

## 2.2 Digital Elevation Model

Both Türkiye and California have various geomorphological features, including various land shapes. In order to explore this rich topography in detail, we used the same high-resolution digital elevation model (DEM) for both regions. With this respect, Shuttle Radar Topography Mission (SRTM) data is the most suitable digital elevation data source with 1 arc-second resolution. It is widely accepted and has worldwide coverage.

SRTM, whose partners are '*The National Geospatial-Intelligence Agency* (NGA)' and the '*National Aeronautics and Space Administration* (NASA)', has an objective of producing digital topographic data for land surfaces between 60° north and 56° south latitude (80% of Earth's surface) with 16 meters of absolute vertical accuracy at 90% confidence, and 1 arc-second, which is approximately 30 meters, resolution (USGS eros archive - digital elevation - shuttle radar topography mission (SRTM) 1 ARC-second global, 2018). Information associated with the used SRTM is listed in Table 2-1.

Table 2-1: Summary information about SRTM

| | |
|---|---|
| **Mission Start Date** | 11/02/2000 – Space Shuttle "*Endeavour*" |
| **Data Projection** | Geographic |
| **Horizontal Datum** | World Geodetic System 1984 – WGS84 |
| **Vertical Datum** | Earth Gravitational Model 1996 – EGM96 |
| **Data Coverage** | 60° North – 56° South |
| **Spatial Resolution** | 1 arc-second (~ 30 meters) |
| **Raster Size** | 1-degree tiles |

Resolution is key in creating different elevation derivatives like slope or aspect. As shown in Figure 2-4, both regions have 1 arc-second resolution DEM which gives the advantage of examining land shapes and morphology in more detail.

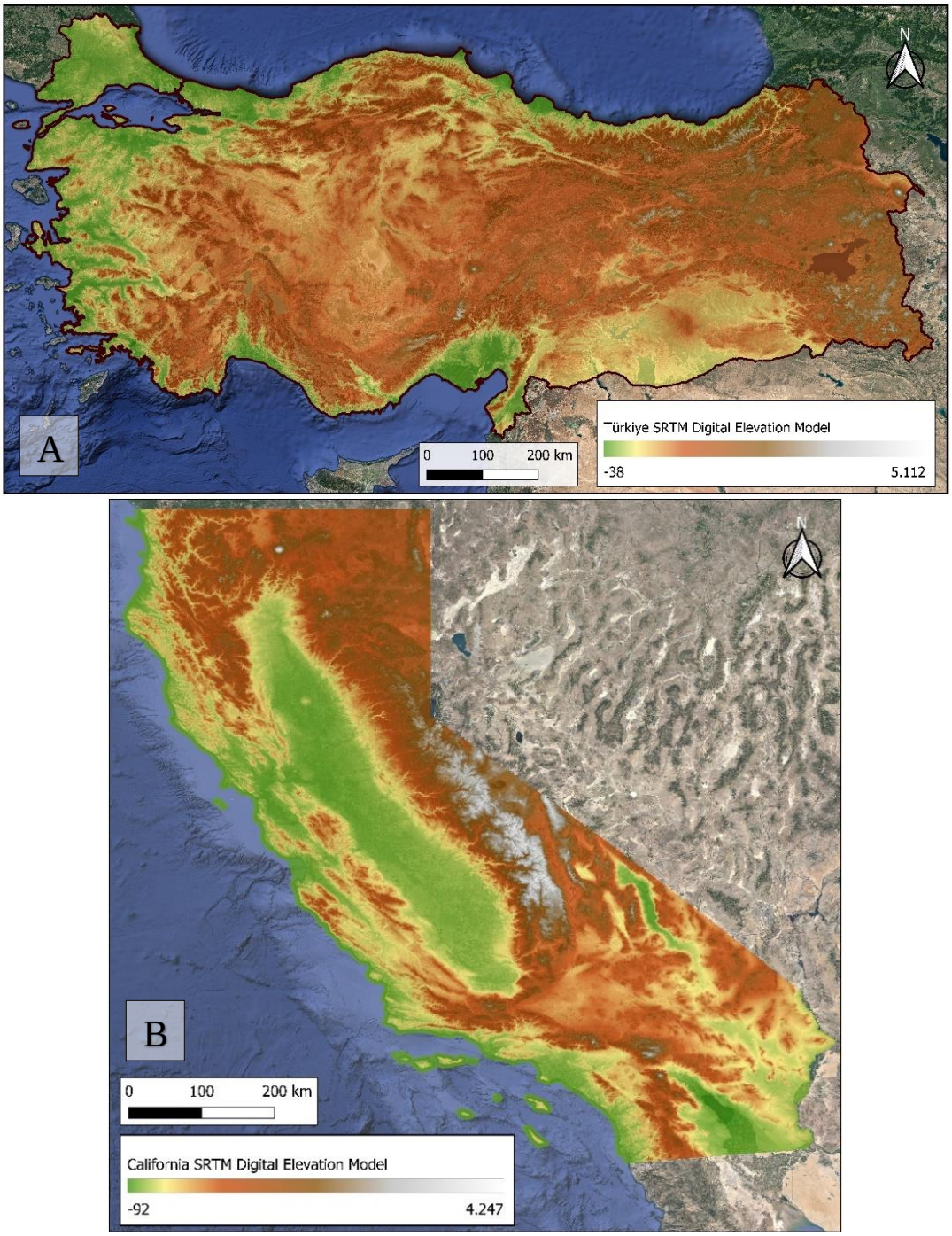


Figure 2-4: Shuttle Radar Topography Mission (SRTM) digital elevation model for (A) Türkiye and (B) California, USA

Figure 2-5 shows the resolution difference between 1 arc-second and 30 arc-second DEMs. As it is clearly seen, 30 arc-second DEM with approximately 1 km resolution provides a rather coarse elevation map that is not much suitable for mapping parameters in high spatial resolution. On the other hand, 1 arc-second DEM effectively reveals topographic details that are critical for mapping.

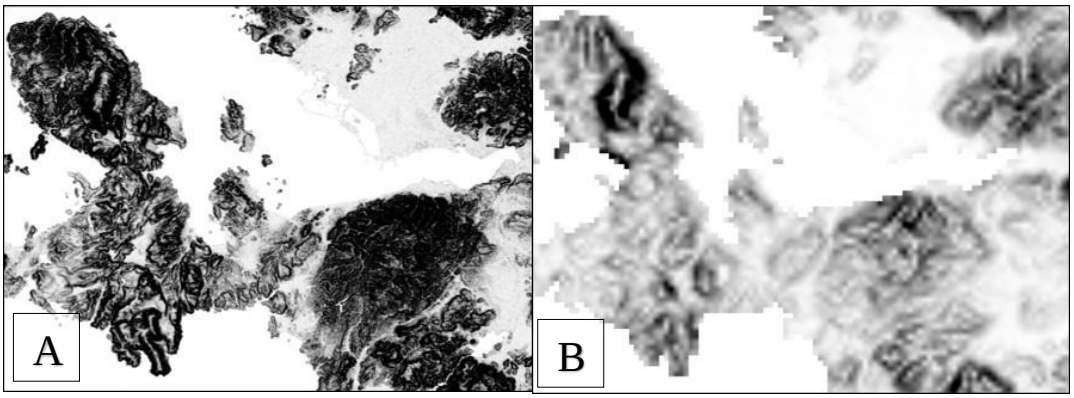


Figure 2-5: 1 arc-second (A) and 30 arc-second (B) SRTM DEMs showing near vicinity of İzmir, Türkiye.

## 2.3 Water Bodies and River Data

River metadata for Türkiye is collected from Regional IM Working Group – Europe, the Food and Agriculture Organization of the United Nations (FAO), which was last updated in January 2022. The resolution of this nationwide data is 1/1,000,000. Unlike river data, available nationwide lake data is improved by the digitization of the new dam lakes and seasonal lakes. At this stage, very small lakes that are unsuitable for robust mapping are eliminated to optimize data performance. The river and lake bodies that are used in this study are shown in Figure 2-6.

In Türkiye river map (Figure 2-6a), we used Strahler Method to get information about the importance of rivers for further calculations. Strahler Method is a quantitative method to measure the size and form of a river in a drainage basin. This method is conducted with order analysis which means the smallest tributaries are designated as Order-1, and when Order-1 channels join, Order-2 segment of this river

formed; and so forth (Strahler, 1957). In addition to them, DEM is used to identify zero elevation for the coastline of both Türkiye and California.

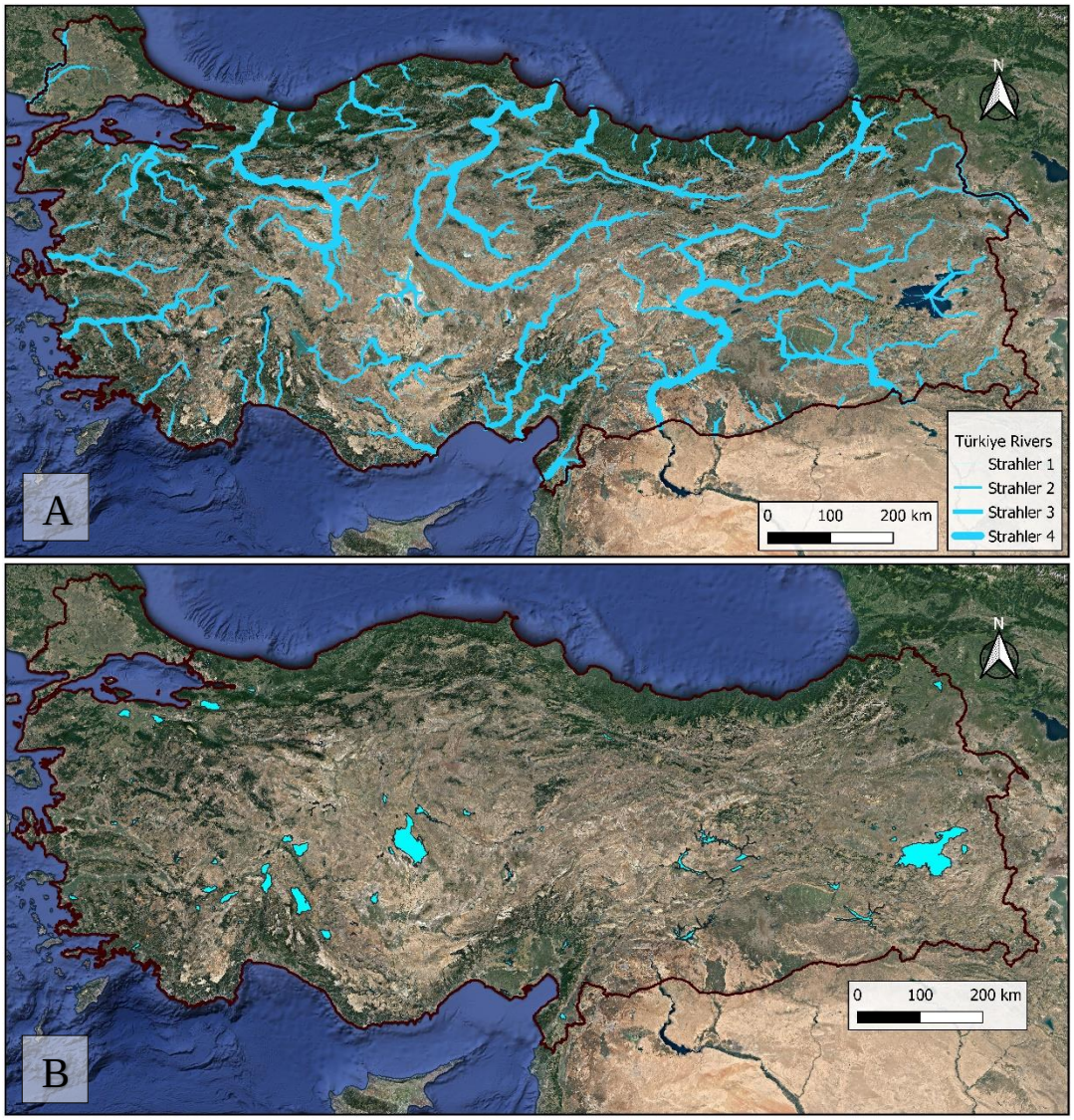


Figure 2-6: Maps of rivers with strahler categories (A) and lakes (B) in Türkiye.

In California, we collected river and lake data using publicly available open data sources published by National Atlas of the Unites States and the United States Geological Survey (U.S. National Atlas Water Feature Lines 2018). Then we create the drainage pattern of California, as shown in Figure 2-7.

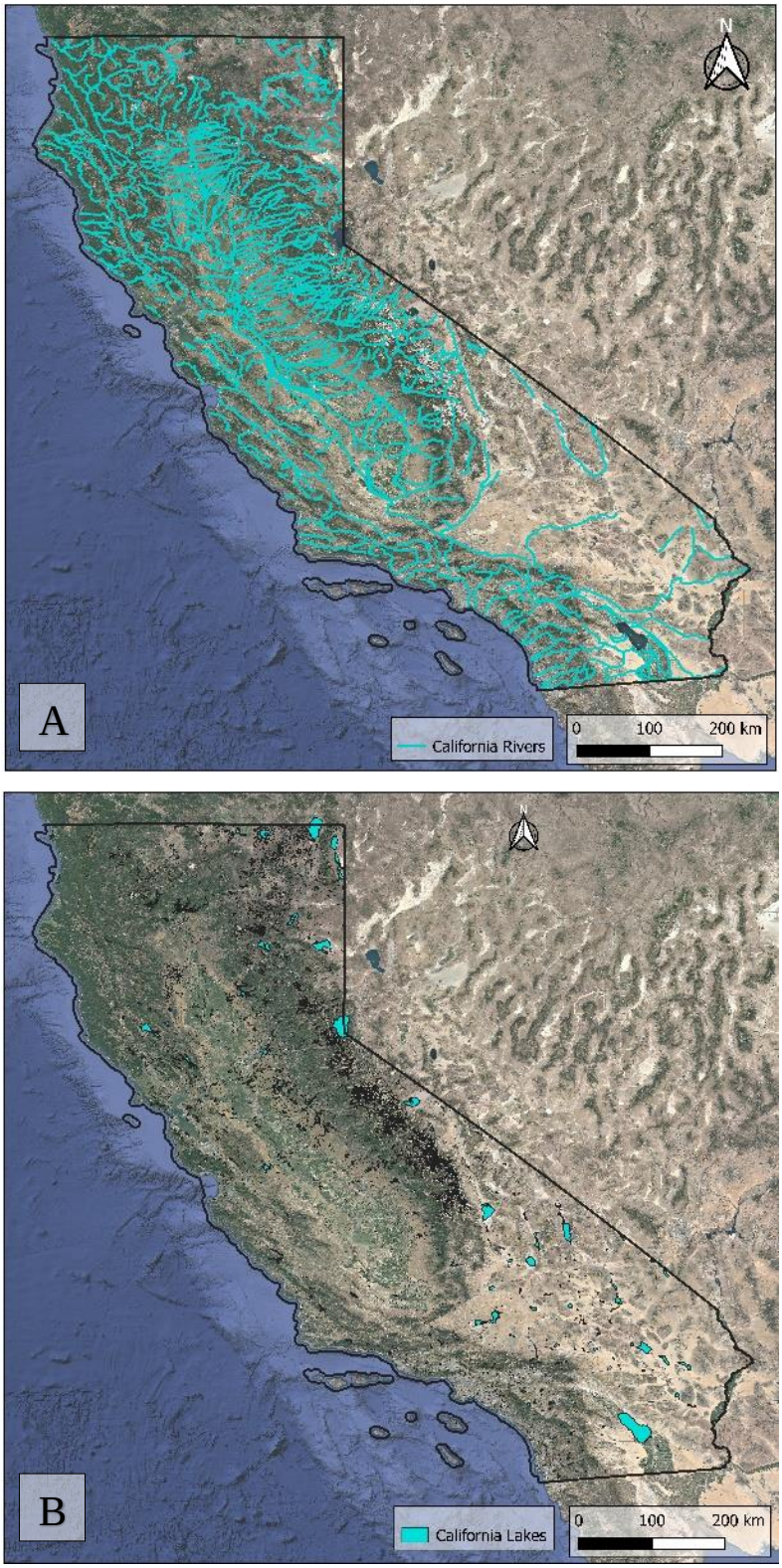


Figure 2-7: Maps showing rivers (A) and lakes (B) in California.

In California, the Department of Water Resources (DWR) Periodic Groundwater Levels collection includes seasonal and long-term groundwater level measurements taken in groundwater basins around the state by the DWR and partner organizations. Additionally, it contains information gathered by the California Statewide Groundwater Elevation Monitoring (CASGEM) Program and the Monitoring Network Module (MNM) of the Sustainable Groundwater Management Act (SGMA) Portal (Periodic groundwater level measurements, 2018). The measurement locations of these rather dense sets of observations are shown in Figure 2-8. Note that each well's average ground water level is used to eliminate seasonal fluctuations.

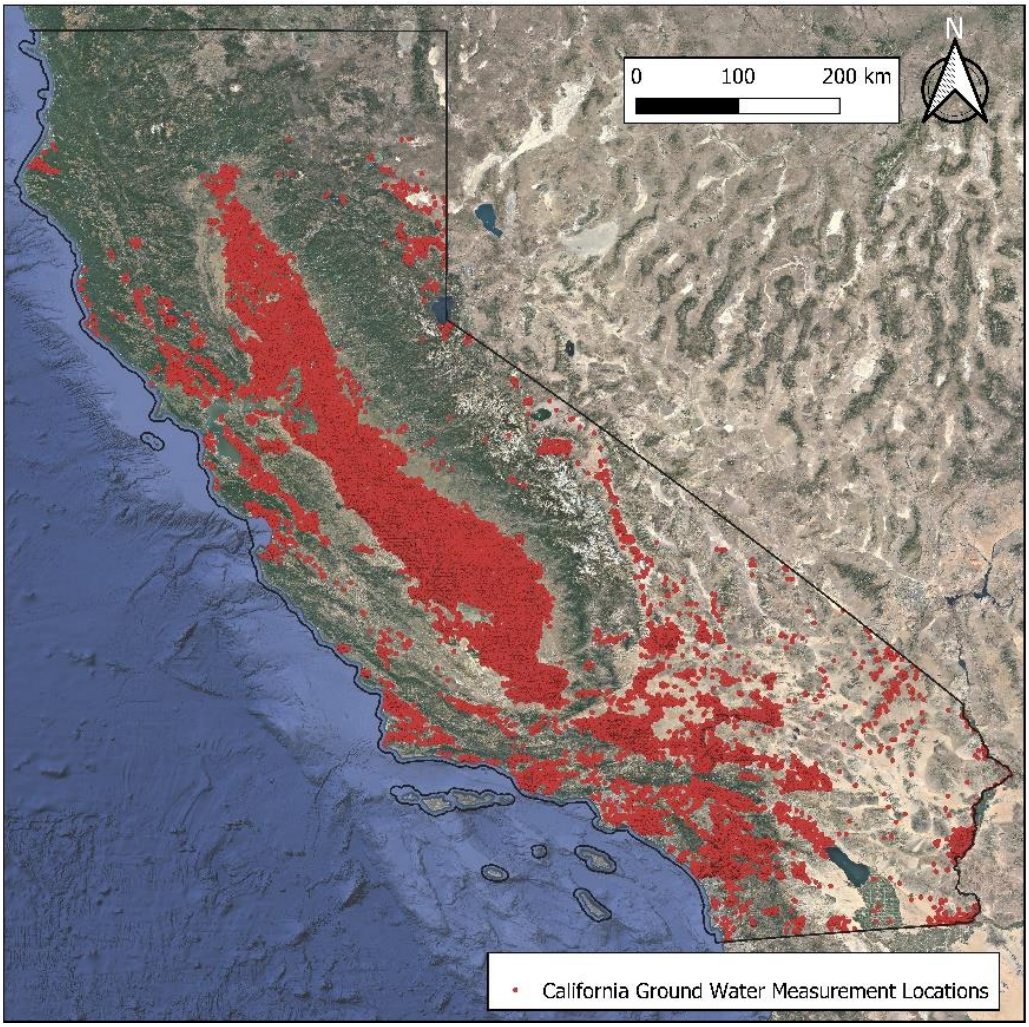


Figure 2-8: Map showing groundwater level measurement locations in California.

## 2.4 Terrain Classification

Classification of continuous topography is a complex topic on a worldwide scale. Topographic or terrain classification is a spatial operation for a surface form. Different approaches, including geology, soil, or hydrology, can be helpful in dividing terrain into categories. One of the very first examples of terrain classification is the study of Hammond (1964) which uses slope gradient, local relief, and surface profile. This initial quantitative approach was extensively used throughout the United States and later modified by several studies. As a result of this study, a total of 96 subclasses are identified, from which 24 classes are generated and mapped in the United States.

Within the scope of this study, we investigated several global terrain classifications and we decided to use the most recent study of Iwahashi et al. (2018). Global terrain classification is conducted by Iwahashi et al. (2018) with MERIT (Multi-error-removed improved-terrain) DEM (Yamazaki et al., 2017), which is the composition of Shuttle Radar Topography Mission (SRTM) 3 arc-sec DEM, Japan Aerospace Exploration Agency (JAXA) AW3D-30 m DEM and Viewfinder Panoramas DEM. This terrain classification is based on slope, local convexity, and surface texture. It has 15 groups from mountain to alluvial planes from 40 different clusters as shown in Table 2-2. Iwahashi et al. (2018) uses geological and geomorphological information from Japan and provides results in higher resolution than previous study (Iwahashi & Pike, 2007).

All distinguished terrain classes are present in both Türkiye and California, as shown in Figure 2-9. This indicates a variety in the geomorphologic background in the studied regions. It is also worth noting that rather than 15 groups, especially five main groups ( (1) bedrock mountain, (2) hills, (3) large highland slope, (4) plateau, terrace, large lowland slope, and (5) plain) is more accurate globally (Iwahashi et al., 2018).

Table 2-2: Terrain classification of Iwahashi et al. (2018).

| Main Groups | Terrain Group | Landform Pattern |
|---|---|---|
| Bedrock Mountain | **1A** | Steep Mountain (Rough) |
| | **1B** | Steep Mountain (Smooth) |
| | **2A** | Moderate Mountain (Rough) |
| | **2B** | Moderate Mountain (Smooth) |
| Hills | **3A** | Hills (Rough on a small and large scale) |
| | **3B** | Hills (Smooth on a small scale, rough on a large scale) |
| Large Highland Slope | **4** | Upper Large Slope |
| | **5** | Middle Large Slope |
| Plateau, Terrace, Large Lowland Slope | **6** | Dissected Terrace – Moderate Plateau |
| | **7** | Slope in and around Terrace or Plateau |
| | **8** | Terrace – Smooth Plateau |
| | **9** | Alluvial Fan – Pediment – Bajada – Pediplain |
| Plain | **10** | Alluvial Plain – Pediplain |
| | **11** | Alluvial or Coastal Plain – Pediplain |
| | **12** | Alluvial or Coastal Plain (Gentlest) – Lake Plain – Playa |

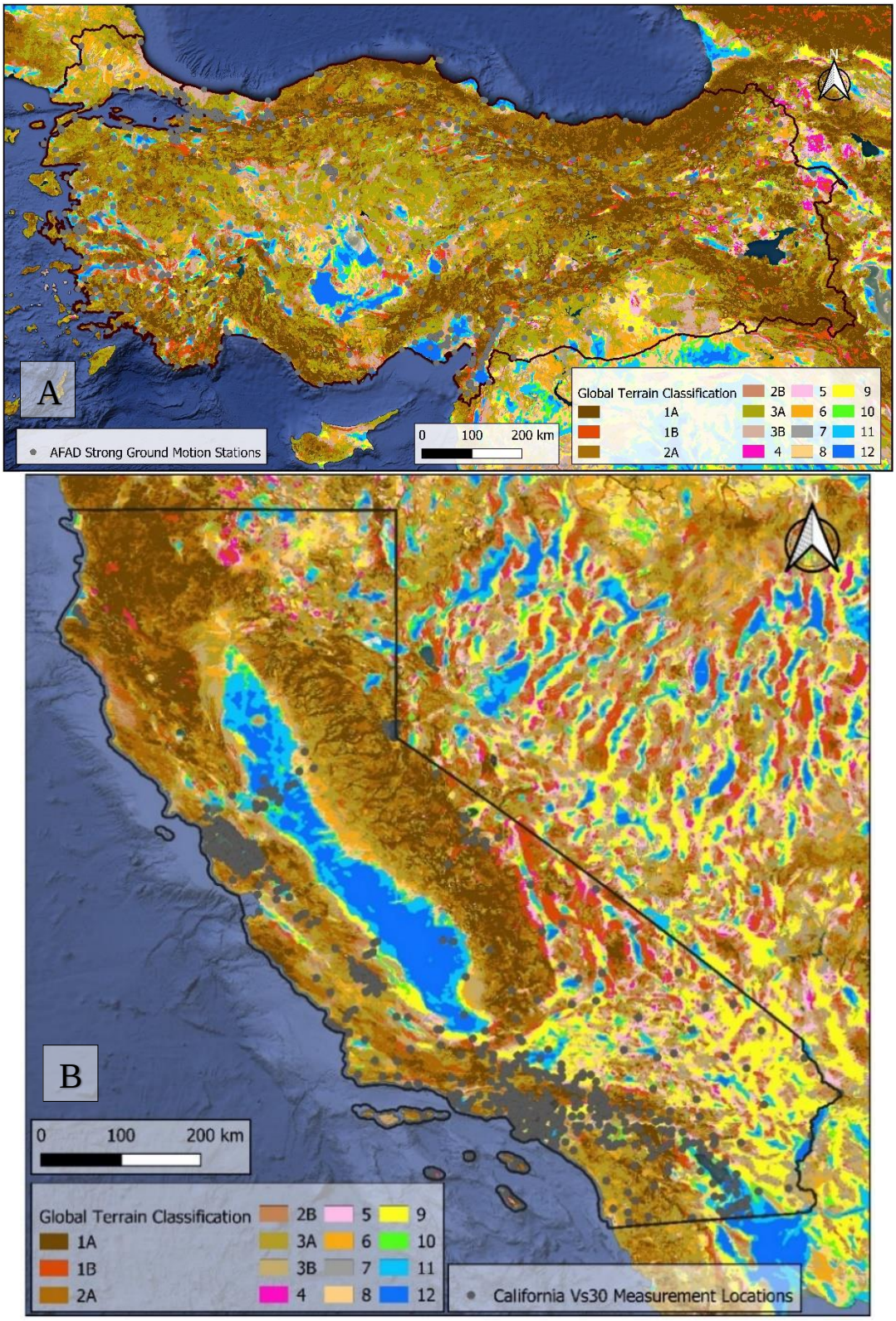


Figure 2-9: Terrain classification map of Türkiye (A) and California, USA (B) (taken from Iwahashi et al., 2018)

## 2.5 Measured Vs30 Data

As mentioned in the previous chapter, field borehole logging and/or surface geophysical surveys provide accurate Vs30 estimates and thus needed for model verification and performance analysis of proxy-based Vs30 prediction models. Fortunately, there are a significant amount of individual Vs30 measurement points across Türkiye and California, which makes this study viable.

AFAD provided a total of 573 individual Vs30 measurements taken at the strong ground motion station site throughout Türkiye. In this database, Vs30 measurements that fall in site classes C and D are the most abundant, while maximum and minimum measured Vs30 are 1862 m/s and 131 m/s, respectively (Figure 2-10a).

USGS has assembled Vs30 measurements from 4389 sites around the country that the USGS and other governmental organizations provided (McPhilips et al., 2020). In California, a total of 1358 individual Vs30 measurements are present. Compared to Türkiye, California has a more excessive Vs30 database, partly due to the systematic collection of measurements under one database. Unlike Türkiye, a large collection of local Vs30 measurements came from locally conducted engineering works, including soil investigation. That is why their measurements are generally more accumulated around cities. Similarly, Vs30 measurements fall in site classes C and D more abundantly, while maximum and minimum measured Vs30 are 1760 m/s and 106 m/s, respectively (Figure 2-10b).

The majority of Vs30 data of AFAD are measured by using the Multi-Channel Analysis of Surface Waves (MASW) while Refraction Microtremor (ReMi) technique was the second most abundant method in the database. When we examined the derived Vs profiles of stations in Türkiye, we notice that some of the data had anomalies at very shallow depths. The reason for these anomalies can be artificial local factors or measurement errors. In California, The Vs30 data has been compiled from various sources, thus measurements are derived from many different techniques. Even more than one technique has been employed in some sites, and the

Vs30 calculation has made use of a multi-technique approach. Array Microtremor (AM), Horizontal-to-Vertical Spectral Ratio (HVSR), Cone Penetrometer Test (CPT), Spectra Analysis of Surface Waves (SASW), MASW, interferometric MASW (iMASW), and ReMi are methodologies that have been employed. The observed scatter in the combined database including data from both Türkiye and California may be enhanced due to utilization of many different Vs30 measurement methods compared to the use of a single method. In this study, no subjective filtering and elimations were made during the use of measurements, and care was taken to use the reported Vs30 values as it is.

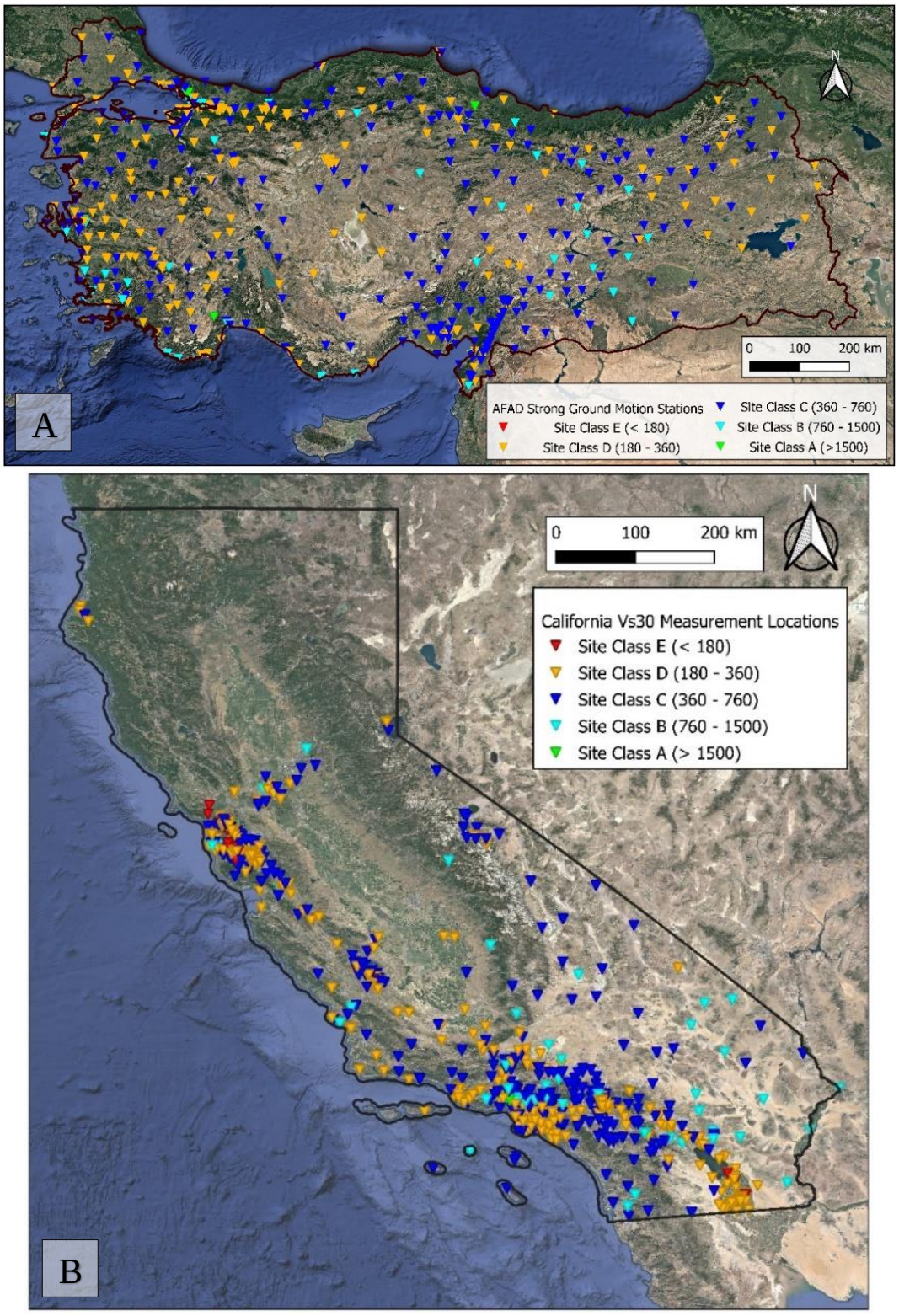


Figure 2-10: Maps of Türkiye (A) and California (B) showing Vs30 measurements in color according to NEHRP site classes.

# CHAPTER 3

# AVAILABLE Vs PREDICTION MODELS AND THEIR PERFORMANCE ANALYSIS

## 3.1 Available Vs Prediction Models

Off-site studies can offer much greater applicability; a typical method is to find widely accessible proxy variables that have correlations with Vs30. Globally, Vs30 prediction methods differ from region to region. Surface geology and slope are the most common of these proxies, but new ones are starting to become popular (e.g. Foster et al., 2019; Heath et al., 2020; Karimzadeh et al., 2019; Kwok et al., 2018; Li et al., 2021; Mori et al., 2020; Stewart et al., 2014; Vilanova et al., 2018; Wills et al., 2015). New studies are trying to estimate the Vs30 value for an entire region or country using specific proxies. These proxies are investigated to understand their sensitivities to Vs30, which is critical for developing an accurate Vs30 prediction model.

### 3.1.1 Vs30 Prediction Based on Topographic Slope

The topographic slope is a widely accepted proxy for Vs30 estimation. One well-known and globally available slope-based study is Wald & Allen (2007). In their study, they create a relationship based on separate regression analyses conducted within shear wave velocity bins further classified from NEHRP site classes with some modifications applied to bins at the edges (Allen & Wald, 2007). For the creation of the global Vs30 map, tectonically active and passive regions are treated separately.

Initially, the topographic slope is calculated by Wald & Allen (2007) using lower resolution (30 arc-second) DEM, which may alter the results. After the release of new digital elevation models for active tectonic and stable continental regions, new correlations are created by Allen & Wald (2009). They used the National Elevation Dataset (NED) of the U.S. Geological Survey Earth Resources Observation and Science (EROS) for high-resolution elevation data when arranging their slope ranges. As it is clearly seen in Table 3-1, the choice of DEM made a noticeable impact on the slope ranges proposed for different NEHRP site classes in these studies, which may affect regression results and thus the resultant Vs30 prediction.

Table 3-1: Subdivided NEHRP Vs30 categories used by Allen & Wald (2009)

| **Class** | **Vs30 Range (m/s)** | **9 arc-second Slope Range (m/m) - Active Tectonic** | **9 arc-second Slope Range (m/m) - Stable Continent** | **Modified 30 arc-second Slope Range (m/m) – Active Tectonic** |
|---|---|---|---|---|
| **E** | < 180 | $< 3.0x10^{-4}$ | $< 1.0x10^{-4}$ | $< 3.0x10^{-4}$ |
| **D** | 180 – 240 | $3.0x10^{-4} – 3.5x10^{-3}$ | $1.0x10^{-4} – 4.5x10^{-3}$ | $3.0x10^{-4} – 3.5x10^{-3}$ |
| | 240 – 300 | $3.5x10^{-3} – 0.010$ | $4.5x10^{-3} – 8.5x10^{-3}$ | $3.5x10^{-3} – 0.010$ |
| | 300 – 360 | 0.010 – 0.024 | $8.5x10^{-3} – 0.013$ | 0.010 – 0.018 |
| **C** | 360 – 490 | 0.024 – 0.08 | 0.013 – 0.022 | 0.018 – 0.050 |
| | 490 – 620 | 0.08 – 0.14 | 0.022 – 0.03 | 0.050 – 0.10 |
| | 620 – 760 | 0.14 – 0.20 | 0.03 – 0.04 | 0.10 – 0.14 |
| **B** | > 760 | > 0.20 | > 0.04 | > 0.14 |

Elevation has also been studied as part of multiple linear regression, but slope and elevation together correlate relatively well, while elevation alone is a weaker predictor for Vs30 and, therefore, not used (Wald & Allen, 2007). As we can see in Figure 3-1, the global Vs30 estimation of Wald & Allen (2007) was made publicly available. Recently, a new hybrid global Vs30 map database has been created using regional datasets inserted smoothly with weighting formulation (Heath et al., 2020).

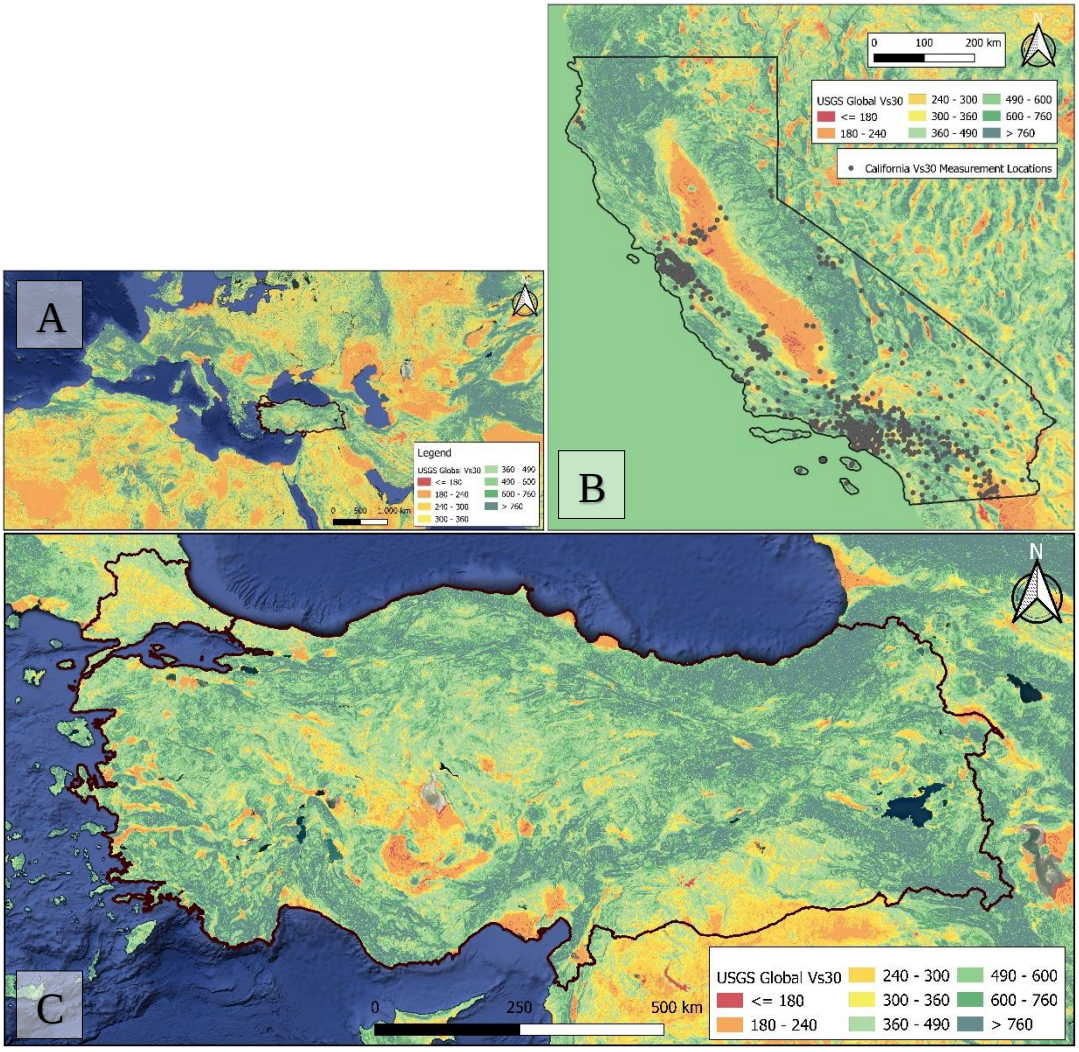


Figure 3-1: Predicted Vs30 maps of part of the globe (A), California, USA (B), Türkiye (C) (taken from *USGS Vs30 Map Viewer*)

### 3.1.2 Vs30 Prediction Based on Geology

One of the simplest ways to estimate site conditions is to use surface geology and shear wave velocity together. There are several studies present using only geology or geology with other proxies. As an example, Vilanova et al. (2018) defined geological units around Portugal, calculated the probability distribution of Vs30, and finally merged their units with statistical results. They used 3 arc-second resolution for topographic slope, classified their geology into 6 preliminary geologic units (P1-Igneous and Metamorphic rocks, P2-Old [Mesozoic/Paleogene] sedimentary rocks, P3-Miocene units, P4-Pliocene units, P5-Pleistocene units and P6-Holocene aged units) and then they reduced it from 6 groups to 3 final geologic groups (F1-Igneous, metamorphic and old sedimentary rocks, F2-Neogene and Pleistocene units and F3-Holocene units).

Later, Wills et al. (2000) prepared site categorization using geological similarities and 566 Vs30 measurements from San Francisco Area, and they divided 7 distinct Vs30 categories; as a result, 74% of the measured Vs30 measurements were found compatible with their predicted ranges. Finally, they used NEHRP site classification by adding some mid-categories to it (Table 3-2) and created a geology-based Vs30 map categorized into site classes, as shown in Figure 3-2. Their study shows that geology can be a fairly good estimator of Vs30 itself but is still open to development.

After this study, they examined larger-scale geology maps close to all of the strong-motion recording station locations in California to find misclassified sites, and changed the Vs30 ranges of the site conditions categories. As a result, they differentiated geologic groups and revised their map Wills & Clahan (2006). They did not change any of the original polygons but assigned a new geological categorization alternative to the NEHRP-based site classification (Figure 3-3).

After creating a geology based Vs30 map, Wills et al. (2015) improved their study by using the slope to subdivide younger alluvium and detailed geologic maps to create a new map of California.

Table 3-2: Summary table of site condition map of Wills et al. (2000)

| Site Category | Explanation | Vs30 Range |
|---|---|---|
| B | - Plutonic and metamorphic rocks<br>- Volcanic rocks<br>- Cretaceous and older age sedimentary rocks | > 760 |
| BC | - Franciscan Complex rocks (except mélange and serpentine)<br>- Crystalline rocks of the Transverse Ranges<br>- Cretaceous aged siltstones and mudstones | 555 – 1000 |
| C | - Franciscan mélange and serpentine<br>- Oligocene to Cretaceous age sedimentary rocks<br>- Younger aged coarse-grained sedimentary rocks | 360 – 760 |
| CD | - Miocene or younger sedimentary rocks<br>- Plio-Pleistocene alluvial units | 270 – 555 |
| D | - Holocene alluvium | 180 – 360 |
| DE | - Artificial fill material over mud<br>- Fine-grained alluvial | 90 – 270 |
| E | - Bay mud and intertidal mud | < 180 |

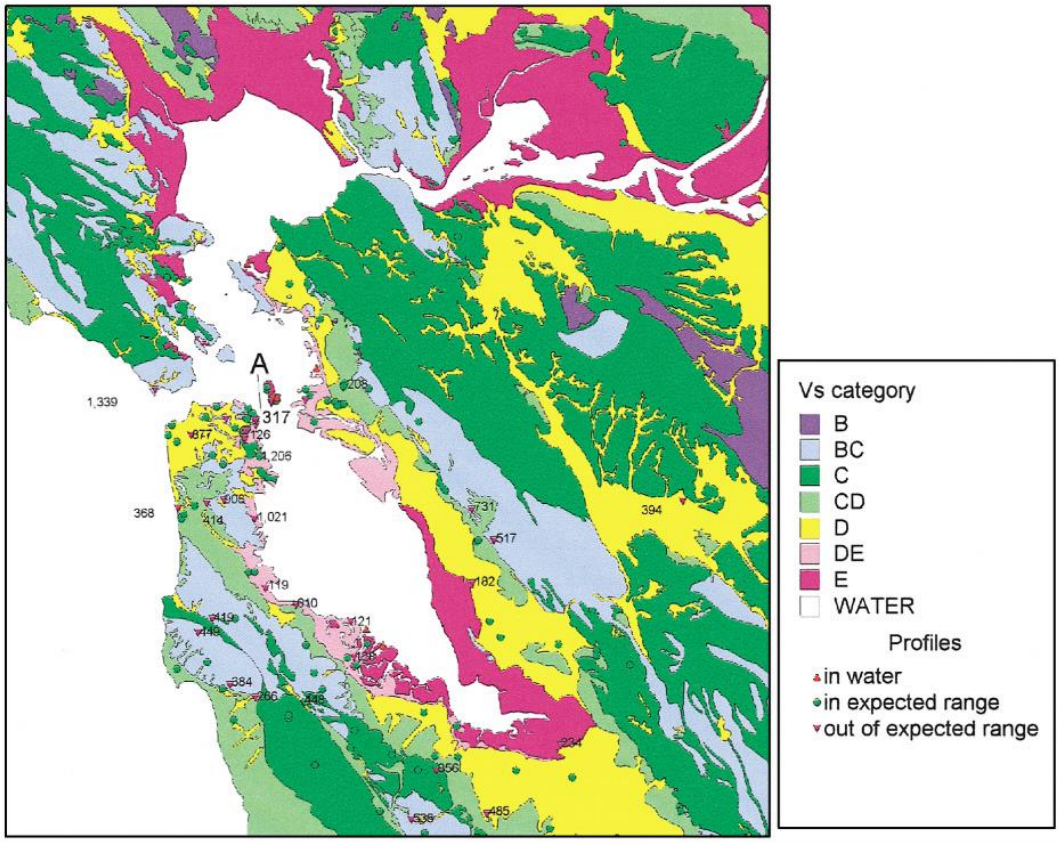


Figure 3-2: Geology based Vs30 classification map of San Fransisco area, California conducted by using average Vs30 of geologic categories and their associated site classes (directly taken from Wills et al. (2000)

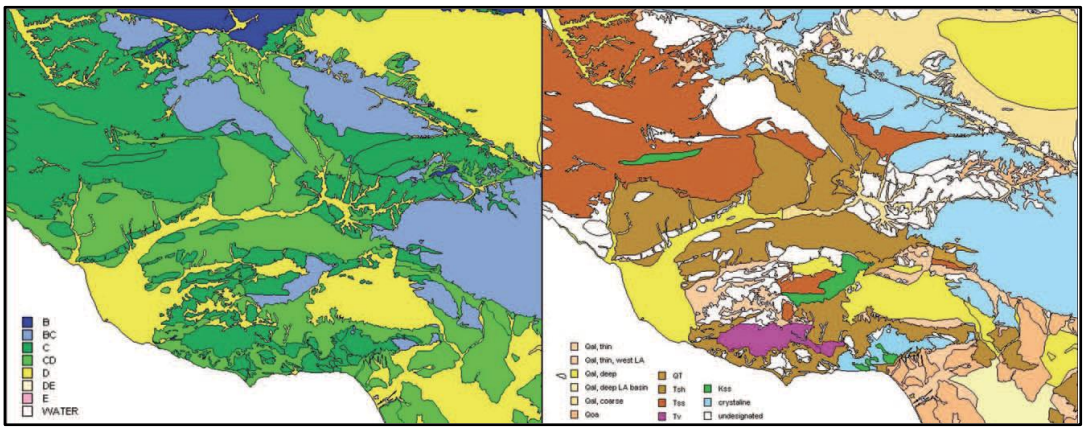


Figure 3-3: California site condition map of Wills et al. (2000) on the left, and revised map of Wills & Clahan (2006) that showing geology based Vs30 categories on the right. (directly taken from Wills & Clahan (2006))

### 3.1.3 Combined Vs30 Prediction Models

Instead of using only one proxy, some local studies use secondary pieces of information to create more accurate Vs30 estimation maps. Their goal is to minimize uncertainty on Vs30 using more than one parameter. Geotechnical, geological, morphological, and elevation data are the most common data for secondary parameters. If there is enough data, the use of secondary predecessors can improve the Vs30 prediction model accuracy.

#### 3.1.3.1 Combined Vs30 Model of Greece

Geology is one of the most critical indicators of Vs30. Seismic velocity differs from one unit to another unit. Stewart et al. (2014) developed a local relationship using the geology of Greece and the collected Vs30 profiles. They developed a geology-based Vs30 estimation model using slope gradient as summarized in Table 3-3.

Stewart et al. (2014) developed geologic categories based on age, gradation, and depositional environment and found a statistical correlation between slope and Vs30 for Quaternary and Tertiary units while no effect on Mesozoic units.

Table 3-3: Summary table of recommended geology-based approach for Vs30 estimation (Stewart et al., 2014). In the equation, 's' represents the slope.

**Equation:** $\overline{\ln(Vs30)} = a_0 + a_1 \ln(s)$

| Age | Explanation | Equation Constants |
|---|---|---|
| Quaternary | Gradation group: Coarse | $a_0 = 6.690\ ;\ a_1 = 0.184$<br>$\sigma_{lnV} = 0.426$ |
| | Gradation group: Mixed | $a_0 = 6.430\ ;\ a_1 = 0.188$<br>$\sigma_{lnV} = 0.365$ |
| Pleistocene | Gradation group: Coarse | $a_0 = 6.835\ ;\ a_1 = 0.184$<br>$\sigma_{lnV} = 0.426$ |
| | Gradation group: Mixed | $a_0 = 6.575\ ;\ a_1 = 0.188$<br>$\sigma_{lnV} = 0.365$ |
| | Gradation is unknown | $a_0 = 6.560\ ;\ a_1 = 0.138$<br>$\sigma_{lnV} = 0.378$ |
| Quaternary or Holocene | Gradation is unknown | $a_0 = 6.510\ ;\ a_1 = 0.181$<br>$\sigma_{lnV} = 0.402$ |
| Tertiary | Rock sites | $a_0 = 6.560\ ;\ a_1 = 0.138$<br>$\sigma_{lnV} = 0.378$ |
| Mesozoic | Rock sites | Category mean: 589 m/s<br>(Equivalent to: $a_0 = 6.378\ ;\ a_1 = 0$) |

#### 3.1.3.2 Taiwan Specific Combined Vs30 Prediction Model

Nearly half of Taiwan lacks the geophysical measurements necessary for seismic site classification (Kwok et al., 2018). This situation creates a need to develop a Vs30 prediction model. The Taiwan-specific Vs30 model consists of more than one proxy. They employed three broad, age-based geologic groups for the youngest category of Holocene and Quaternary undivided sediments and proposed models based on gradient, elevation, and adaptation of a geomorphic terrain-based approach,

producing two Vs30-prediction models (Kwok et al., 2018). The resultant Taiwan specific Vs30 prediction model that is conditioned to multiple proxies is given in Table 3-4. Note that the elevation ranges established for Taiwan are more representative of an island country and not seem as applicable globally.

Table 3-4: Summary table of Taiwan-specific model of Kwok et al. (2018)

$$\ln(Vs30) = b_0 + b_1 \ln(s) \quad s_{min} = 0.0008 \text{ (m/m)}$$

| **Geologic Category** | **Elevation Range** | **$b_0$** | **$b_1$** | **Hybrid Geology Proxy Weight** | **Terrain Proxy Weight** |
|---|---|---|---|---|---|
| Holocene + Quaternary | < 20 | 6.42 | 0.16 | 0.57 | 0.43 |
| | 20 – 35 | $\frac{lnV_2(s) - lnV_1(s)}{15\ m}(Elev - 20) + lnV_1(s)$ | | | |
| | > 35 | 6.62 | 0.12 | | |
| Pleistocene | All | 6.47 | 0.07 | 1.00 | 0.00 |
| Pre-Quaternary | All | $\mu_{lnV}$ = 656 m/s | | 1.00 | 0.00 |
| | | $\sigma_{lnV}$ = 0.41 | | | |

### 3.1.3.3 Combined Vs30 Prediction Model of Italy

Mori et al. (2020) derived the Vs30 map using the global terrain classification of Iwahashi et al. (2018) based on slope, convexity, and surface texture to improve accuracy and precision. Their work is based on geotechnical data collected all around Italy. They combined terrain classification and geotechnical data containing 35,000 boreholes and 11,300 Vs profiles with slope and elevation proxies (Mori et al., 2020). Different from previous studies, they used 40 geomorphological clusters rather than 15 morphologic classes defined by Iwahashi et al. (2018).

First, they distributed their measurements according to geomorphological clusters and geotechnical classification using borehole data. They divided geomorphologic clusters using geotechnical borehole data into 4 different soil classifications: gravels, sands, silts, and geological bedrock.

After combining two datasets, they create slope and elevation dependent multilinear regression model to calculate equation coefficients for each geomorphological cluster and create a Vs30 distribution map as shown in Figure 3-4.

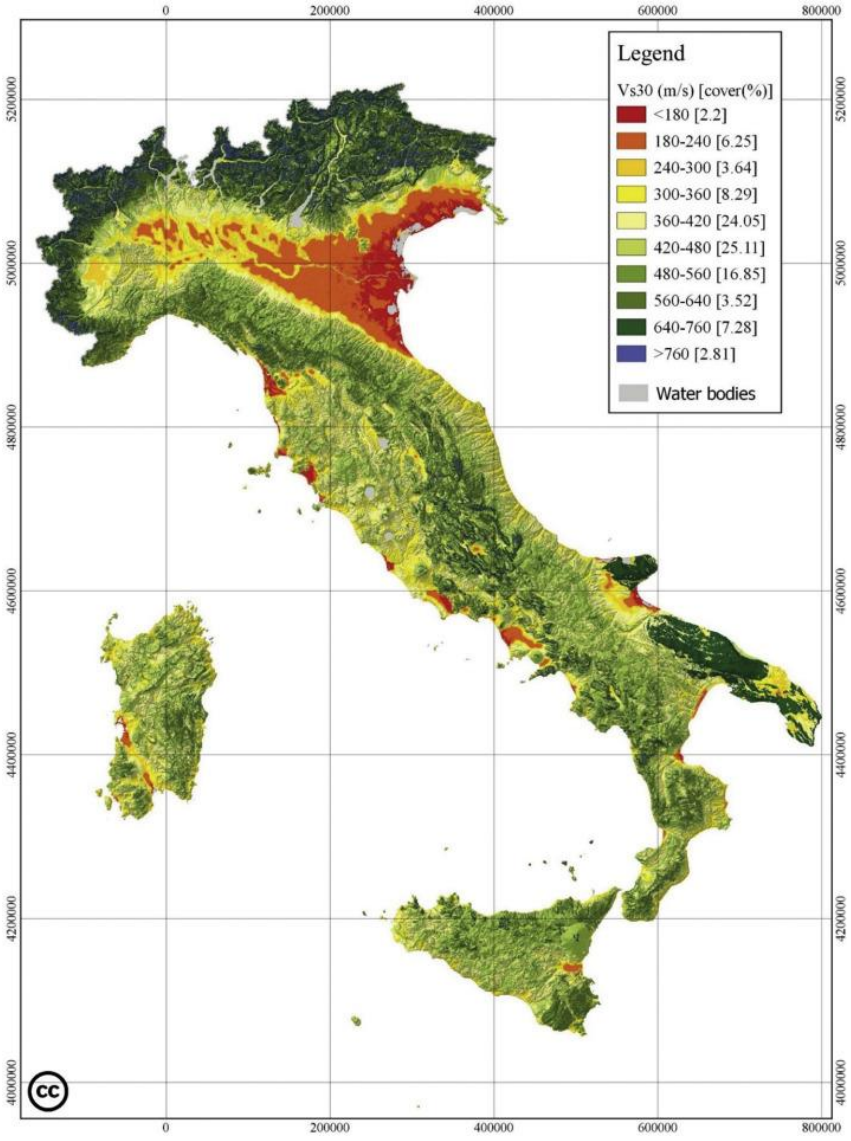


Figure 3-4: Predicted Vs30 map of Italy (directly taken from Mori et al., 2020)

## 3.2 Performance Analysis of Alternative Prediction Models

We chose two different methods to conduct performance analysis with Vs30 measurements combined from Türkiye and California. The first one is the global Vs30 model by Allen & Wald (2009) made available by USGS, which uses only slope as a proxy, and the second one is the Vs30 model developed for Italy by Mori et al. (2020) that includes a combination of terrain, slope, and elevation. By comparing predictions with actual data, we examine the accuracy of these proxy-based Vs30 estimates.

In order to conduct performance analysis, we collected Vs30 estimates from the global USGS Vs30 model for every measurement point in Türkiye and California. On the other hand, predictions based on the nationwide Vs30 model of Italy are computed by applying the proposed formulations of Mori et al., (2020) to our data points at which elevation and slope are calculated using 1 arc-degree SRTM DEMs.

First, we investigate the distribution of Vs30 measurements and predictions at discrete Vs30 bins in a histogram (Figure 3-5a). It is the simplest way to show the distribution difference of Vs30, and it can give an idea about prediction performance but not a "point-to-point" performance analysis.

Next, the difference between measured and predicted values are quantified for each Vs30 data point. Initially, the residual is computed using uses the logarithmic ratio of measured and predicted Vs30 following the equation below, and their binned distribution is shown in Figure 3-5b.

$$Residual = Log\left(\frac{Vs30_{Mea}}{Vs30_{Pred}}\right)$$

Additionally, assuming the log-normal distribution is present in Vs30 (Seyhan et al., 2014), residual analysis for each measurement is completed with the following equation and plotted in Figure 3-5c.

$$R_i = \ln(Vs30_{Measured}) - \ln(Vs30_{Predicted})$$

Finally, boxplots of residuals computed for alternative prediction approaches is constructed for further analysis (Figure 3-5d). It is worth noting that a narrower residual box centered at zero implies a good fit between measured and predicted values with a relatively low standard deviation.

According to our performance analysis, the nationwide Vs30 prediction model of Italy clearly overestimates Vs30 values since the number of predicted Vs30 values and residuals are systematically more concentrated on the higher Vs30 and residual bins (Figure 3-5). This observed systematic shift also reflects on the residual box that is centered at -160 rather than 0, with large bounds between -240 and -40. This result suggests that this nationwide Vs30 prediction model, developed by data from Italy, performs rather poorly in Türkiye and California and is not much suitable for global predictions.

In contrast, the global Vs30 model of USGS shows a relatively similar but slightly wider Vs30 distribution than the actual measurements, with residuals mainly centered at minimum (Figure 3-5). The resultant residual box is centered close to zero at -10 with bounds between -90 and 70. According to these results, the topographic slope based global Vs30 model of USGS performs relatively well in Türkiye and California, but its residuals are still widely distributed, and thus there is still room for improvement.

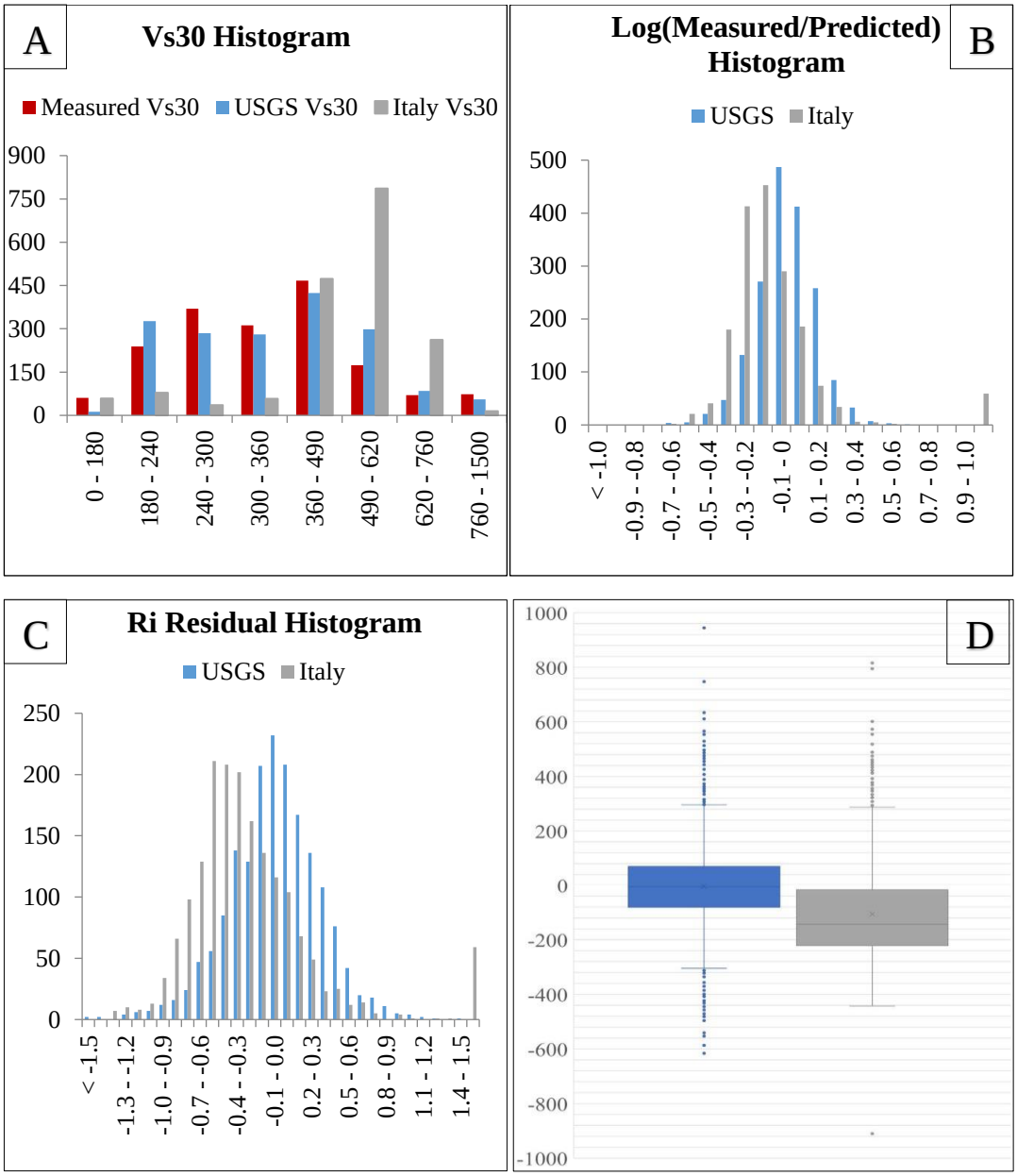


Figure 3-5: Histograms of measured and predicted Vs30 values (A), logarithmic ratio between measured and predicted Vs30 values (B), Ri - Residual (Seyhan et al., 2014) (C) and box plots of residuals (D).

# CHAPTER 4

# METHODOLOGY

When there is no Vs30 measurement, it is estimated by using different relationships as mentioned in previous chapters. Different proxies and techniques are proposed in the creation of regional or global Vs30 prediction models. In this chapter, we described our Vs30 prediction strategy involving data derivation and the development of prediction formulations conditioned to multiple proxies. First, proxies that will be tested are assigned to every Vs30 measurement point in the combined database containing data from both Türkiye and California. For this purpose, elevation and slope are derived from 1 arc-second SRTM DEMs along with their simplified geologic unit class, and terrain categories are taken from the global model of Iwahashi et al. (2018). In addition, the fluid saturation of young units is defined by using water table depths available in California and by using water level rise analysis in Türkiye. Overall workflow followed in this study is summarized within a flow chart plot given in Figure 4-1.

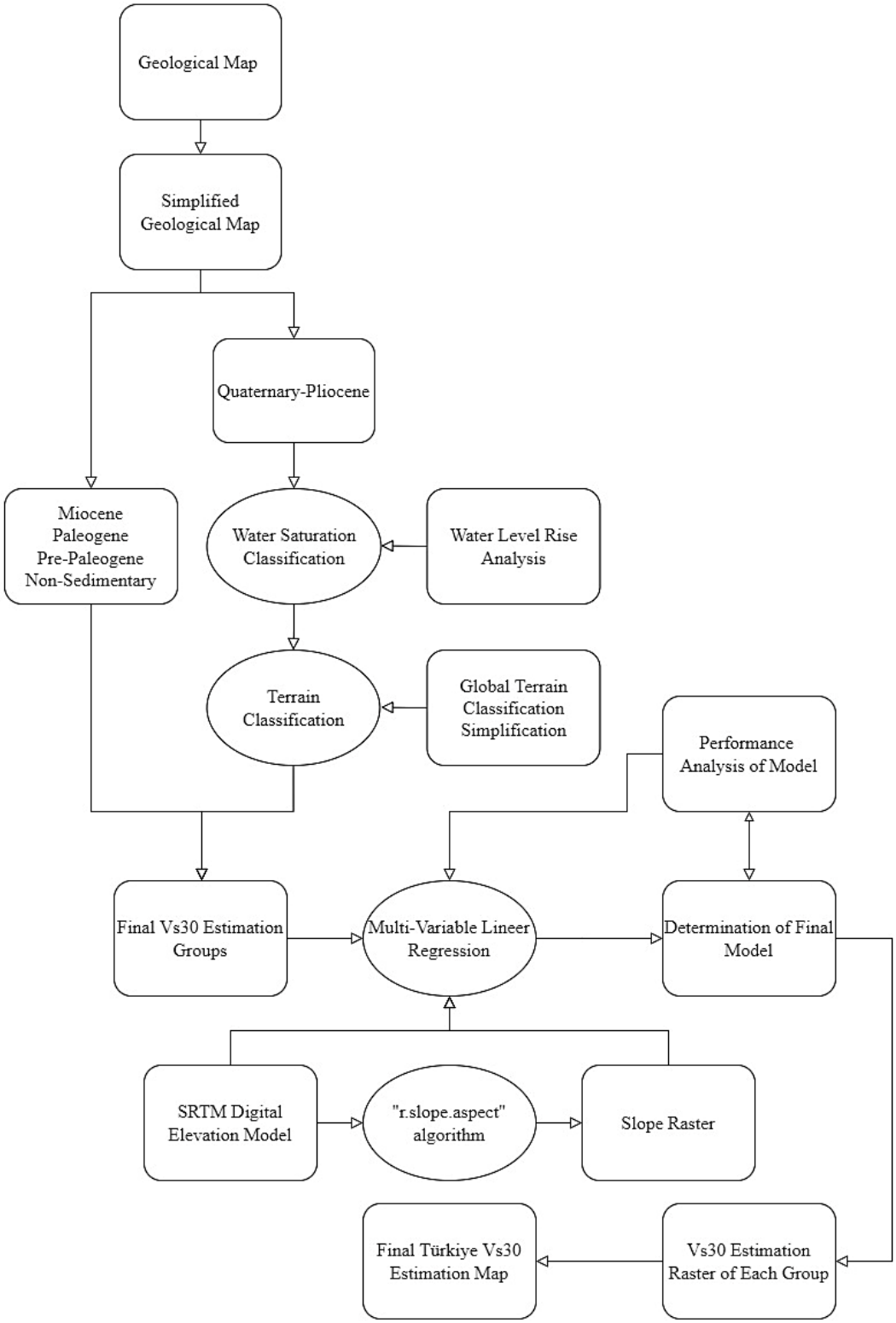


Figure 4-1: Simplified methodological flow chart of our Vs30 prediction strategy

## 4.1 Topographic Slope Determination

The slope and Vs30 relationship is first established with SRTM 30 arc-second data (Wald & Allen, 2007). As mentioned in the previous chapter, 30 arc second equals approximately 1 km pixel size. After they used 30 arc-second resolution, they found that higher resolution is more accurate in defining morphology, and they improved their study by using 9 arc-second resolution (Allen & Wald, 2009). A higher resolution is better for determining where the slope changes suddenly. Thus we have utilized 1 arc-second resolution DEM of SRTM, providing high resolution (~30 m) topography suitable for accurate calculation of slope.

Slope calculation is made with the "*r.slope.aspect*" algorithm of GRASS GIS in QGIS software. From an elevation raster map, this algorithm produces raster maps of a slope, aspect, curvatures, and partial derivatives. This calculation gives slope as a degree from the horizontal using input elevation raster. After compilation, the degree is converted to meter/meter to be consistent in other calculations. A sample calculation is given in Figure 4-2.

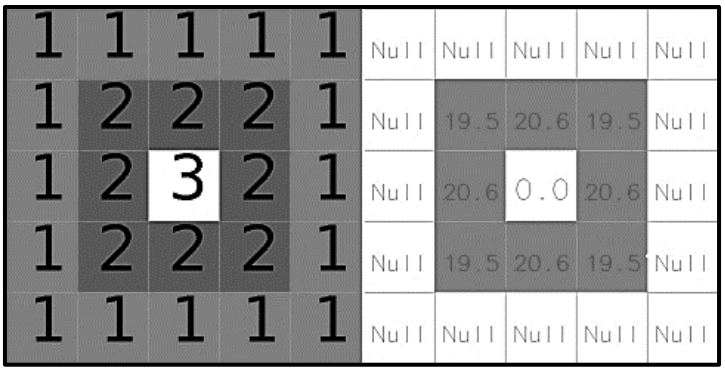


Figure 4-2: Example DEM and calculated slope in degree format of "*r.slope.aspect*" algorithm (Shapiro & Waupotitsch, 2022)

In Türkiye and California, the slope rarely exceeds 45°, and high values correlate with the mountain ranges (Figure 4-3). On the other hand, the basins, including major surface water bodies, are generally flat and characterized by minimal slope values (0°-2.5°). In this sense, slope reveals the spatial variation of geomorphic characteristics that correlate well with predefined tectonic provinces in both regions.

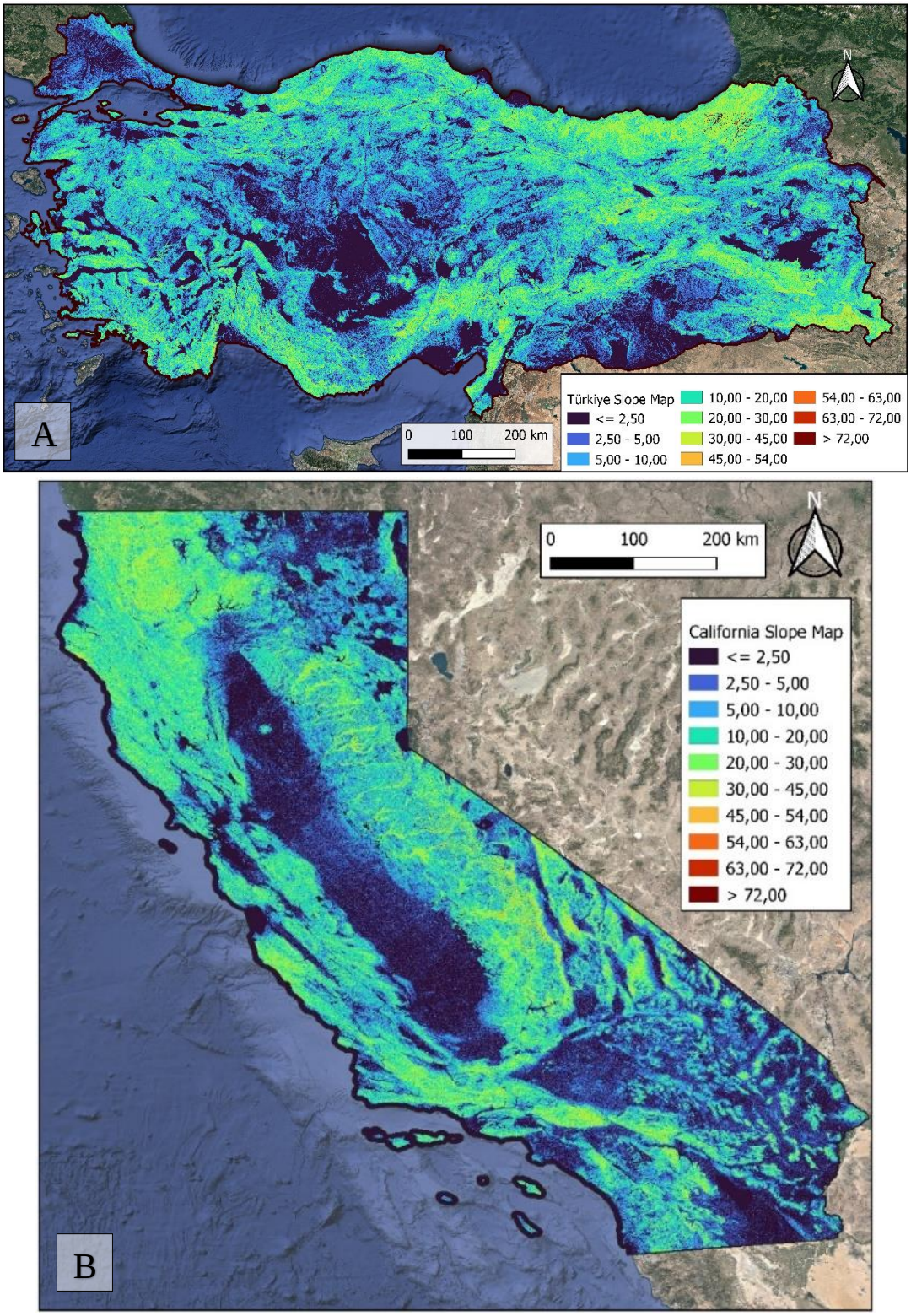


Figure 4-3: Slope map of Türkiye (A) and California (B) derived from 1 arc-sec SRTM DEM.

Figure 4-4 shows the distribution of slope and elevation with respect to Vs30 measurements. In the broad sense, slope indicates a positive correlation with Vs30 that may support the usage of slope as a proxy for Vs30 (Figure 4-4a). However, Vs30 values display wide scatters even within similar slope ranges. In this situation, a linear relation with a relatively limited goodness fit (r2) can be established with elevated error ranges using the entire slope range (check Figure 4-4a), but no statistically robust regression relations can be raised using our database for separate narrow slope bins derived from NEHRP site classes like as Wald & Allen (2007). Unlike global Vs30 models, our database only includes spatially well-distributed measurements from two tectonically active domains (Türkiye and California). Although this reduced data quantity may further limit our capacity to use multiple bins, developing statistically viable relations is highly unlikely since Vs30 measurements can scatter from around 100 m/s to over 1000 m/s even for almost identical slope values throughout the entire database. In short, Vs30 values show a noticeable positive correlation with slope, but the presence of a high degree of scattering throughout implies the need for other proxies that may reduce the present uncertainty.

Elevations of the measurement points display an uneven distribution. The majority of measurement points, which has elevations lower than 500 m, are especially clustered densely near sea level. This non-uniform concentration which occurs due to coastline settlements in Türkiye and California, is not much suitable for establishing the direct linear correlation between elevation and Vs30 values (Figure 4-4b). Even though coastal measurements are eliminated, no strong correlation emerges except a high level of scattering. In this respect, Vs30 values are more dependent to slope than elevation, and thus elevation should be used as a secondary proxy if needed.

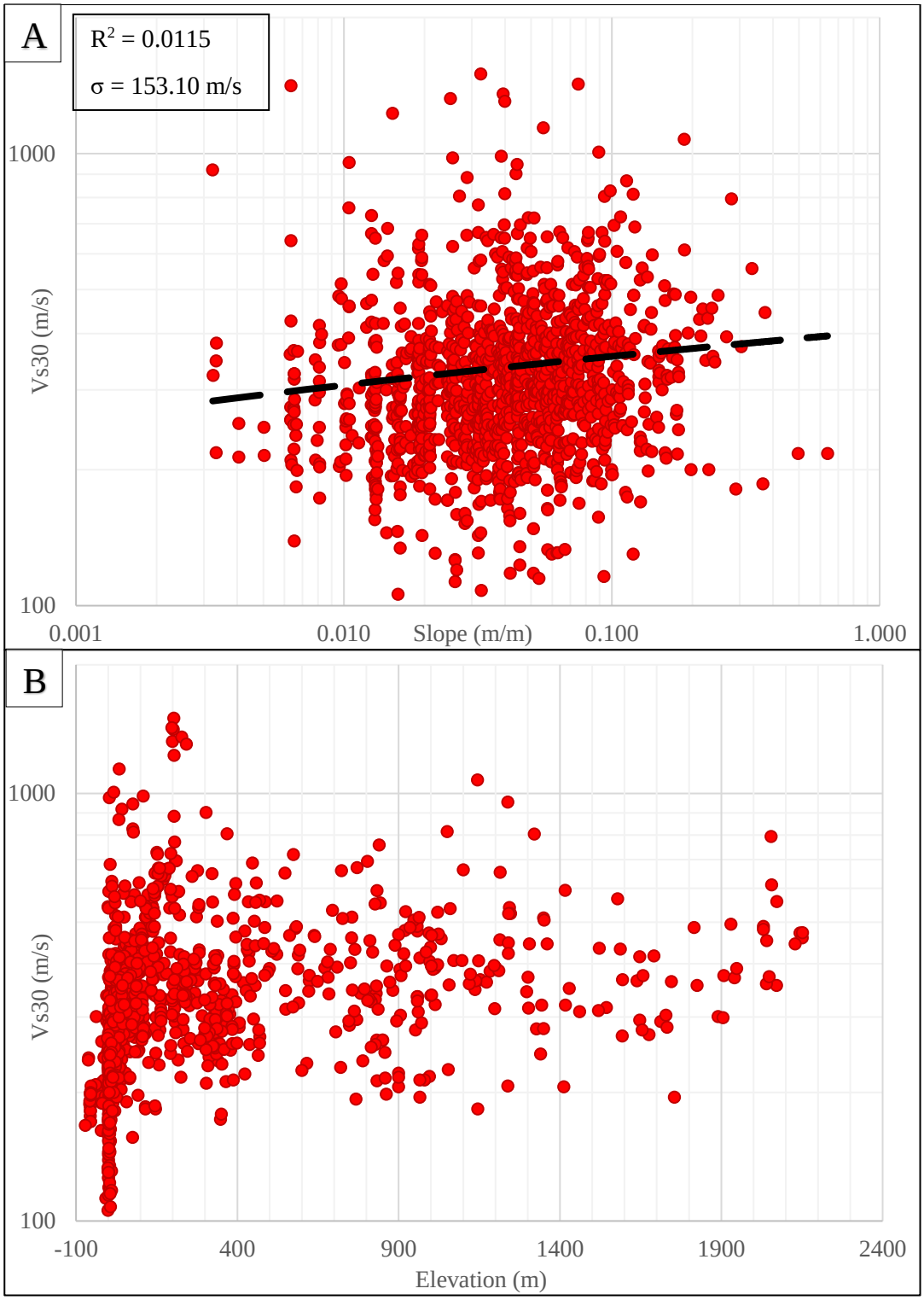


Figure 4-4: Slope vs Vs30 (A) and elevation vs Vs30 (B) graphs of all Vs30 measurements used in this study.

## 4.2 Geologic Classification

Since geology is counted as a strong indicator of Vs30, numerous studies are conducted to develop correlations between geology and shear wave velocity (for example, Wills & Clahan, 2006). In these studies, geologic units displaying similar Vs30 values are identified and categorized into simplified geologic classes to create site condition maps. Both Türkiye and California have different geologic units of various ages. From Proterozoic to Holocene, all different ages with various lithology are present in both regions. Within this variety, surface geology should be simplified to create meaningful relationships.

In general, lithology, which is an important factor for material strength, can be decisive for the seismic velocity of the unit. However, detailed lithology can be highly variable even within short distances and poses a difficulty for categorization, especially in tectonically complex areas. In the absence of sufficient amount of Vs30 measurements from every mapped lithological assemblage, a simplified geologic classification is needed to develop Vs30 maps representative of general site conditions. In this respect, the geologic age of the lithologic unit, which can also be a factor in the compaction and cementation of sedimentary rocks, is one of the parameters spatially defined by geological maps and can be utilized to form simplified geologic classes. In this study, lithology and geologic age are used in combination for geological classification that would serve our purpose.

Initially, geological units are divided into two major classes as sedimentary and non-sedimentary. The seismic properties of non-sedimentary rocks are not as sensitive as the sedimentary rocks to the geologic age but more closely linked to geological processes forming these units. Therefore, non-sedimentary rocks are divided into 3 classes independent of geological age as Intrusive, Extrusive, and Metamorphic rocks which are by-products of essentially different geological processes.

Older sedimentary rocks are generally characterized by higher seismic velocities than young deposits. In order to account for this effect, geologic age is used as a criterion for the differentiation of sedimentary rocks. Considering uncertainties associated to mapped unit ages, sedimentary rocks are divided into 4 geologic age classes as Quaternary-Pliocene, Miocene, Paleogene, and Pre-Paleogene, which also ensures appropriate sampling of each group within the database. The map distributions of the chosen geologic classes in Türkiye and California, which are prepared using QGIS software, are shown in Figure 4-5.

Even though the simplified geological classes are all present in both regions with enough spatial extent and measurements, Vs30 data belonging to the Quaternary-Pliocene sedimentary rock class is vast in quantity (>1000) and thus dominates the Vs30 database (Figure 4-6a). This is due to non-uniform Vs30 sampling concentrated mainly across the residential areas.

In order to minimize the effect of data scattering, outliers that are not within the 90% percentile of each geologic class are also eliminated. Later, group averages with and without outliers are calculated separately with error bounds derived from standard deviations (Figure 4-6b,c).

Sedimentary rocks show a clear, systematic increase in Vs30 with respect to their geologic ages, which supports the basis of our classification. Average Vs30 of Quaternary-Pliocene units, which are mostly unconsolidated, is lowest (just above 300 m/s) among all the classes and represents the poorest site conditions prone to amplification. In contrast, the average Vs30 of Pre-Paleogene sedimentary rocks and all non-sedimentary units largely exceeds 500 m/s indicating better site conditions.

Besides the Quaternary-Pliocene sedimentary rocks, other geologic classes have a relatively small number of measurements. Therefore, any generalization made for these classes may be less reliable and should be treated with caution. In contrast, the large dataset available from Quaternary-Pliocene class provides a unique opportunity to improve Vs30 estimates along young units where site conditions are poorest.

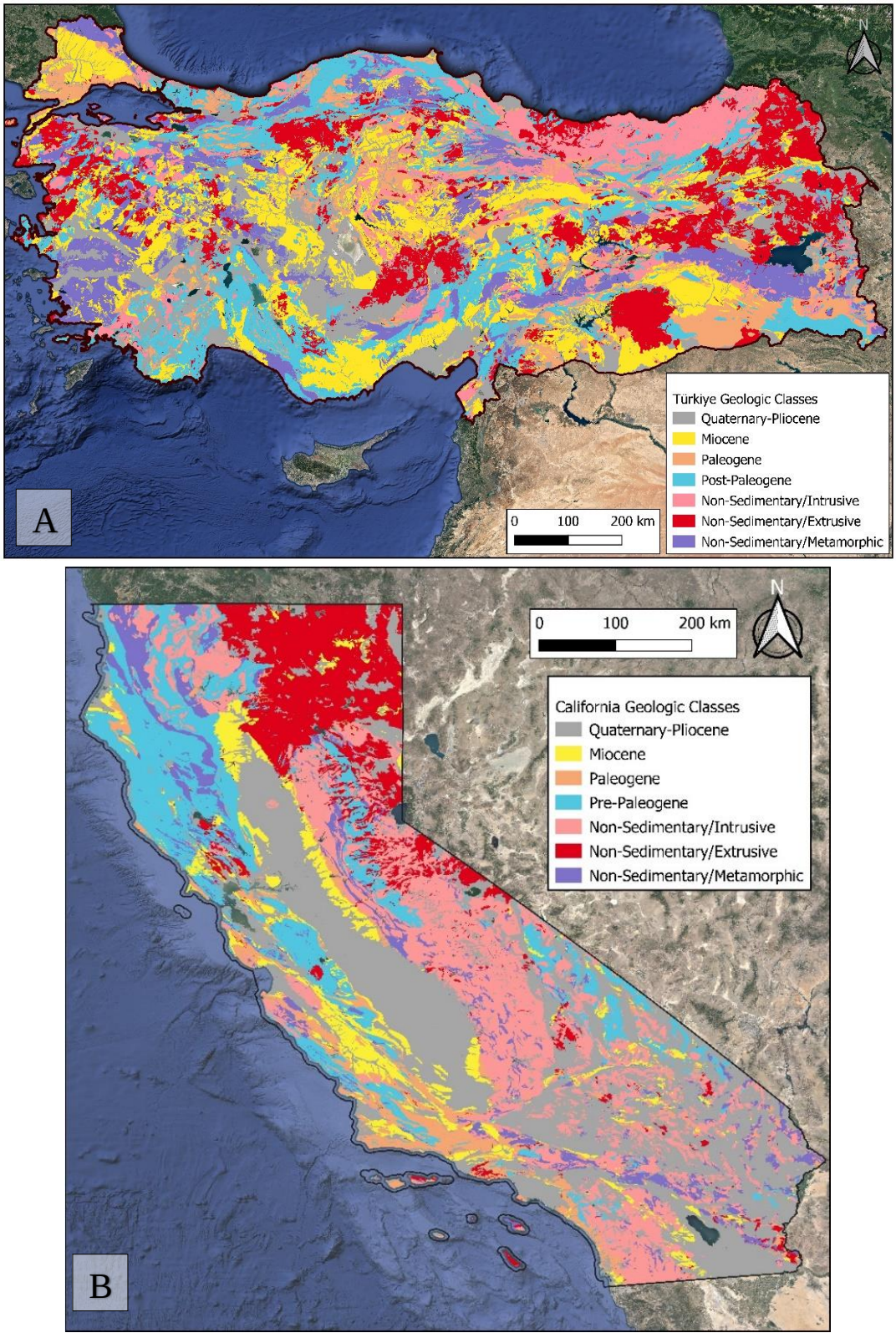


Figure 4-5: Simplified geologic classes map of (A) Türkiye and (B) California, USA

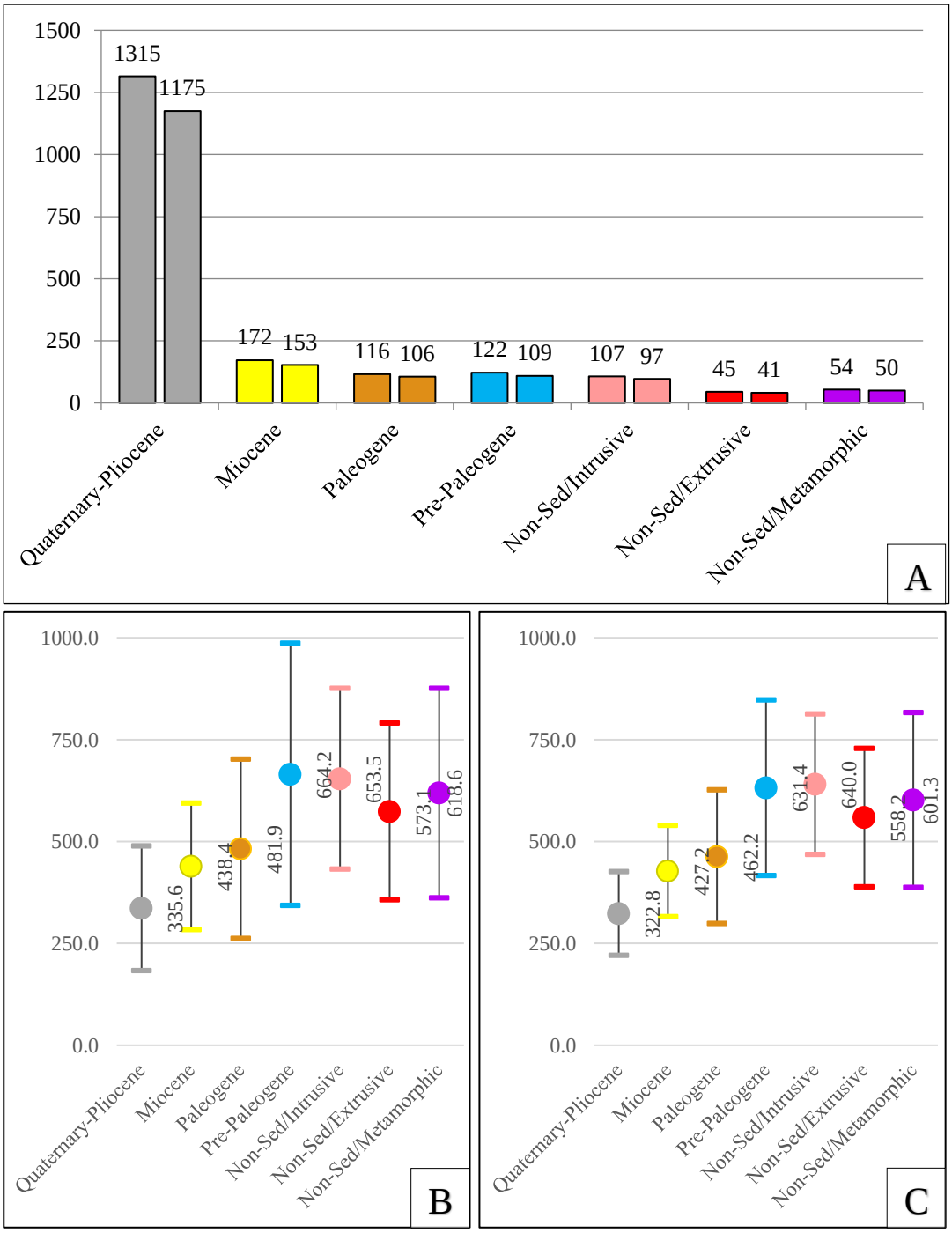


Figure 4-6: (A) Histogram plots showing distribution of Vs30 measurements among simplified geologic classes with and without 90% percentile elimination. Vs30 averages of defined geologic classes before (B) and after (C) outlier elimination. Error bounds are derived from standard deviation of each class.

For each selected geologic class, the sensitivity of Vs30 to slope and elevation are explored by analyzing their data distribution plotted in Figure 4-7, Figure 4-8, and Figure 4-9. Even after geological classification, both slope and elevation still display a large scatter in each class, implying the existence of other unaccounted factors affecting Vs30 measurements. Since data points within each geologic class are rather limited in quantity except for the Quaternary-Pliocene unit (Figure 4-6), older rock classes are excluded from any further classification. Linear regression trendlines are constructed before and after elimination of outliers (outside the %90 percentile) to assess effect of extreme values present in each class. The elimination of outliers only marginally improves the best fit of linear regression and does not change the trends drastically.

In Miocene and Paleogene rocks, Vs30 shows a positive linear correlation with both slope and elevation (Figure 4-7 and Figure 4-8). In contrast, Pre-Paleogene sedimentary rocks and all non-sedimentary rocks display a negative correlation with elevation that has no realistic explanation (Figure 4-8). Among these classes, only metamorphic rocks, which suffer from relatively limited and highly scattered data, show a positive correlation with minimal goodness fit, while others indicate none or minimal sensitivity to the slope (Figure 4-7). Based on these observations, Vs30 estimates of Pre-Paleogene sedimentary rocks and non-sedimentary rocks are fixed to their class averages while using both slope and elevation in multi-variable linear regression for Miocene and Paleogene sedimentary rocks.

Quaternary-Pliocene rocks that have over a thousand Vs30 measurements are statistically more suitable for exploring the relationship of Vs30 values with slope and elevation. However, the data scattering is still very large to establish linear correlations (Figure 4-9). These young deposits are mostly unconsolidated and very much prone to physical and chemical interactions. Moreover, the thickness of these deposits can be closely linked to the morphological setting they are in. Their thickness likely exceeds 30 meters within the basin while can be less than 30 m at rugged terrain. In this respect, their saturation state and terrain class can be employed

during further classification of Quaternary-Pliocene deposits that can help clarify the relationship of Vs30 with slope and elevation.

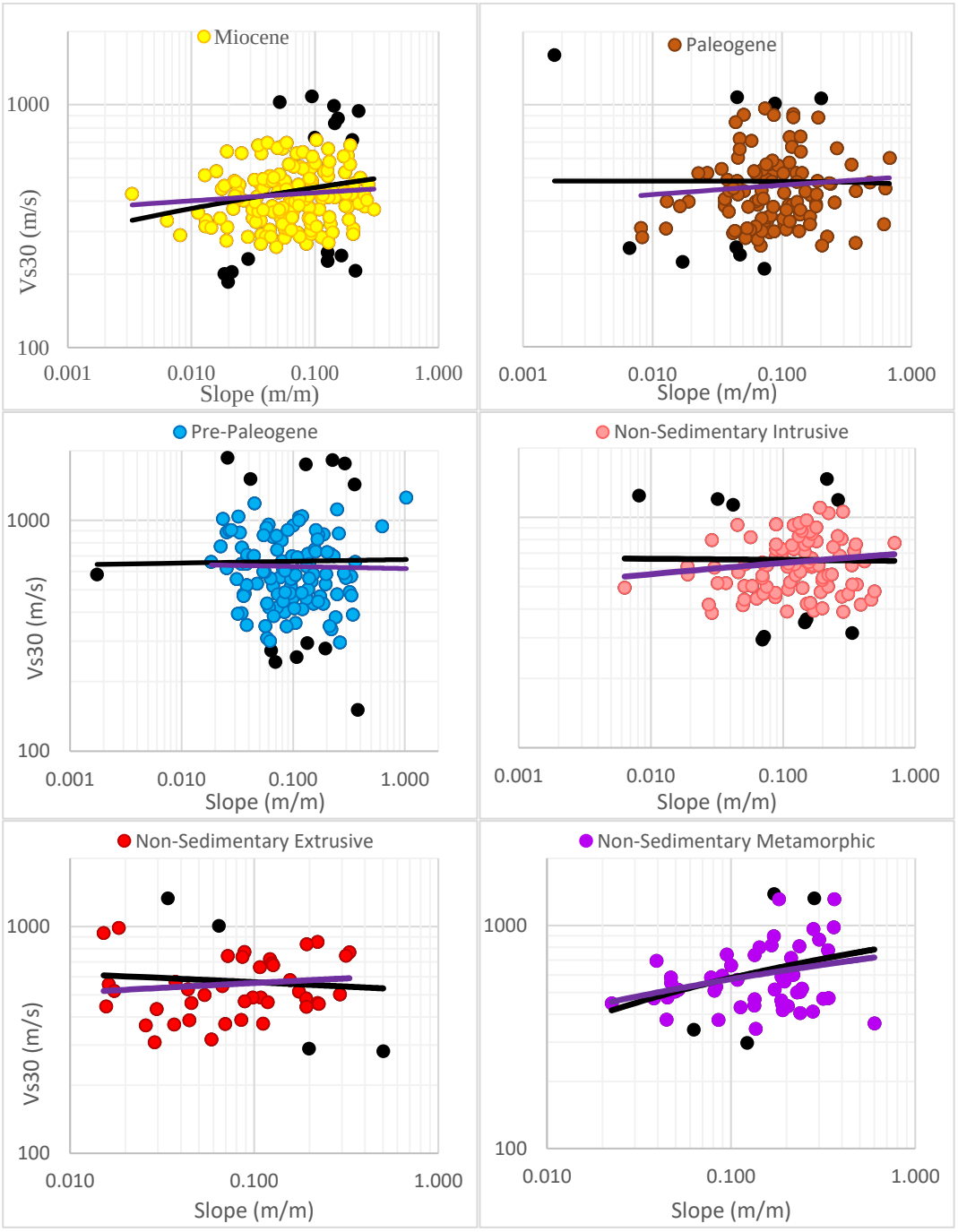


Figure 4-7: Slope vs Vs30 graphs of selected geologic classes. Outliers outside %90 percentile are shown in black. Trendlines calculated using outliers are black and without outliers are purple.

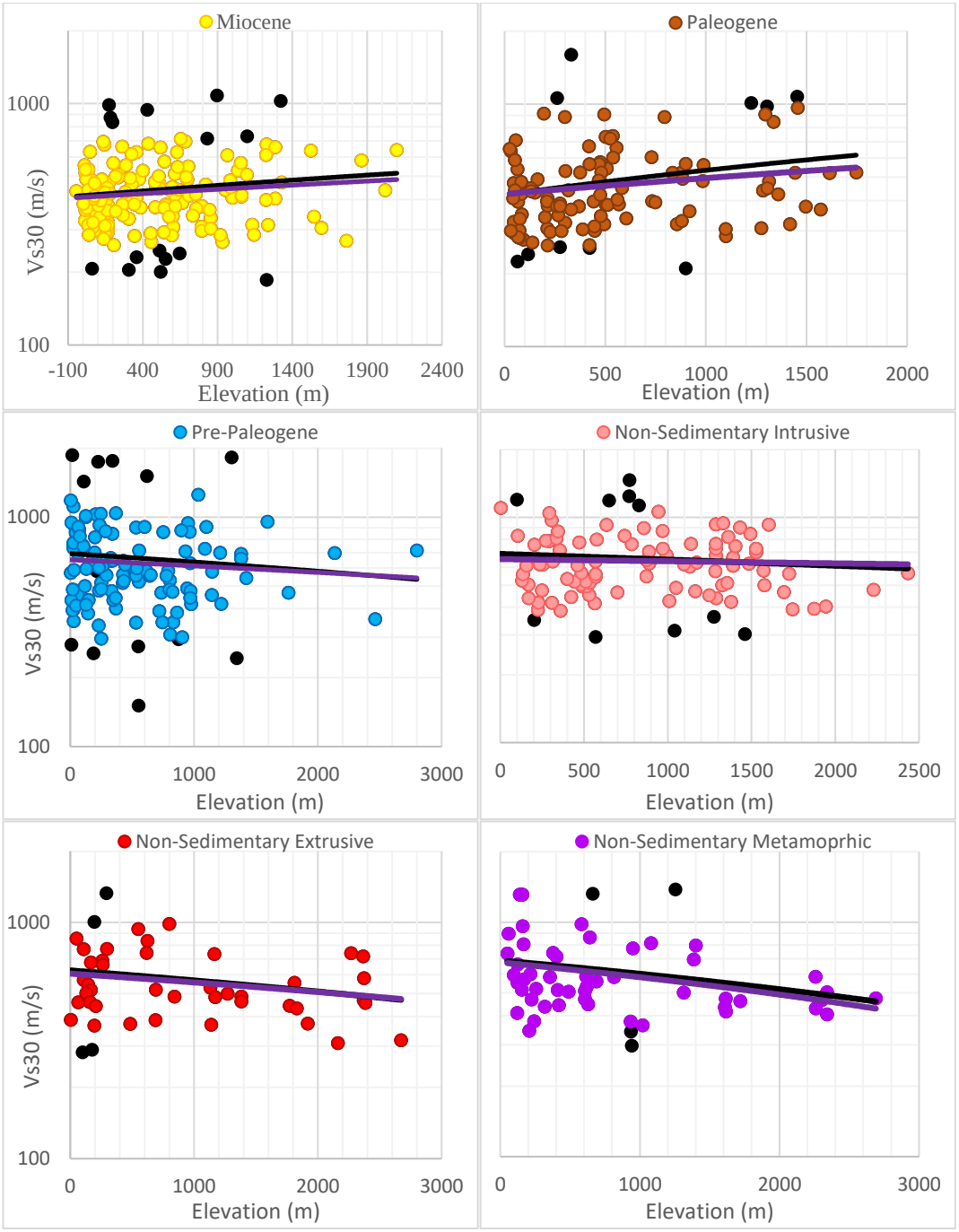


Figure 4-8: Elevation vs Vs30 graphs of selected geologic classes. Outliers outside %90 percentile are shown in black. Trendlines calculated using outliers are black and without outliers are purple

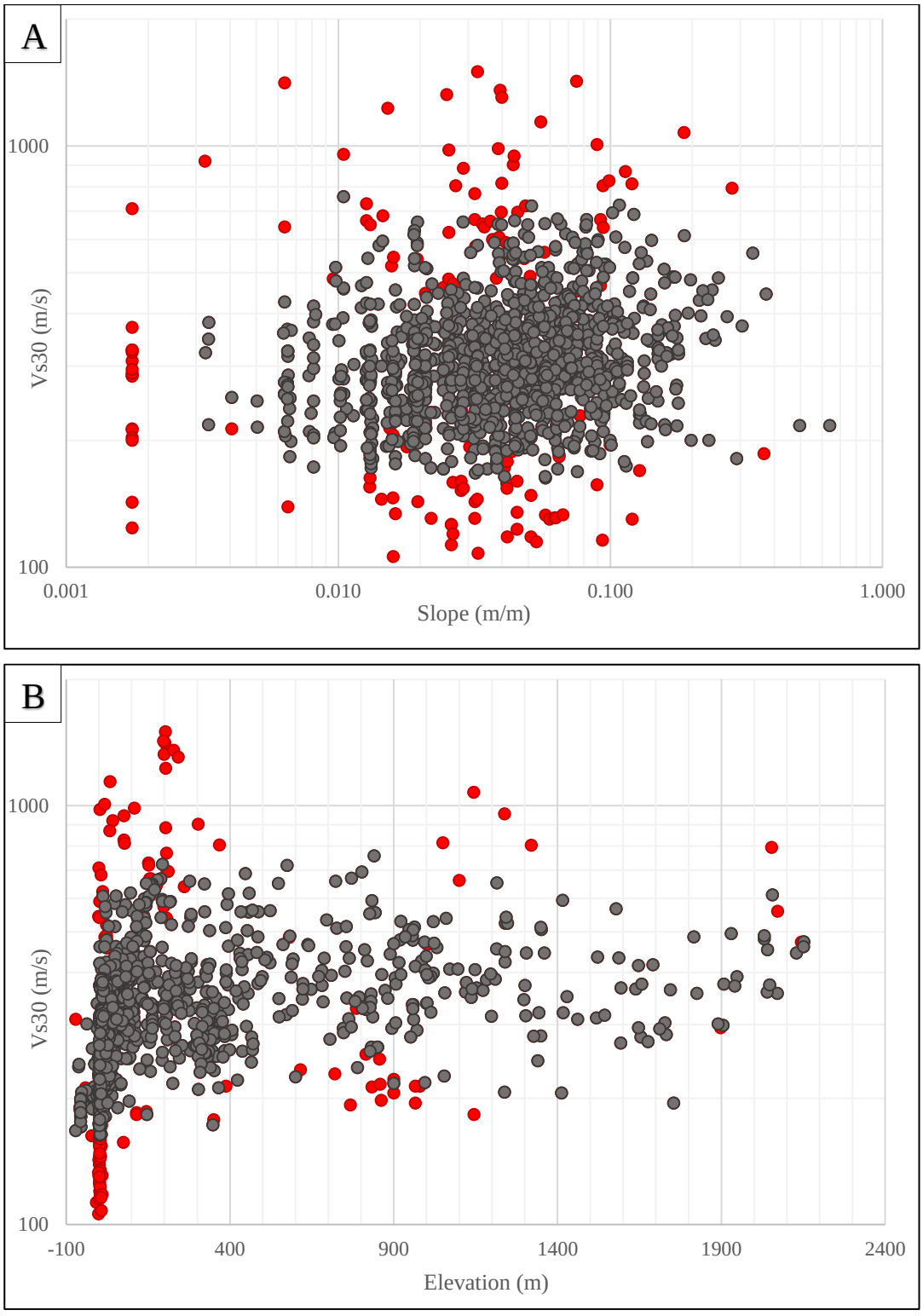


Figure 4-9: Slope vs Vs30 (A) and Elevation vs Vs30 (B) graphs of Quaternary-Pliocene sedimentary rocks. Outlier data points that are outside %90 percentile are shown in red)

## 4.3 Terrain Classification

The global terrain classification of Iwahashi et al. (2018) is made up of 15 individual terrain classes. In our database, several of them are represented with very limited Vs30 measurements (Figure 4-10a). Furthermore, the average Vs30 of these terrain classes overlaps significantly (Figure 4-10b). On the other hand, Vs30 values of terrain classes belonging to two combined terrain categories tend to differ significantly from each other. The first terrain category includes 8 individual terrain classes with average Vs30 values near 500 m/s or above that are mainly associated to mountains and hills (Figure 4-10b). The remaining 7 terrain classes with average Vs30 values near 400 m/s or below belong to plains and terraces (Figure 4-10b). In general, Vs30 values of older geological units are expected to be mainly dependent on major rock types, which is accounted during geological classification. On the other hand, the morphological terrain setting of young deposits can carry information of particle size and shape and more importantly may reveal sections where deposits are possibly very thin (<30 m) that may alter measured Vs30. For these reasons, older geologic rock classes represented with relatively fewer data, are excluded from further terrain classification, whereas Quaternary-Pliocene deposits are divided into two according to their main terrain categories (Mountain/Hill and Plain/Terrace).

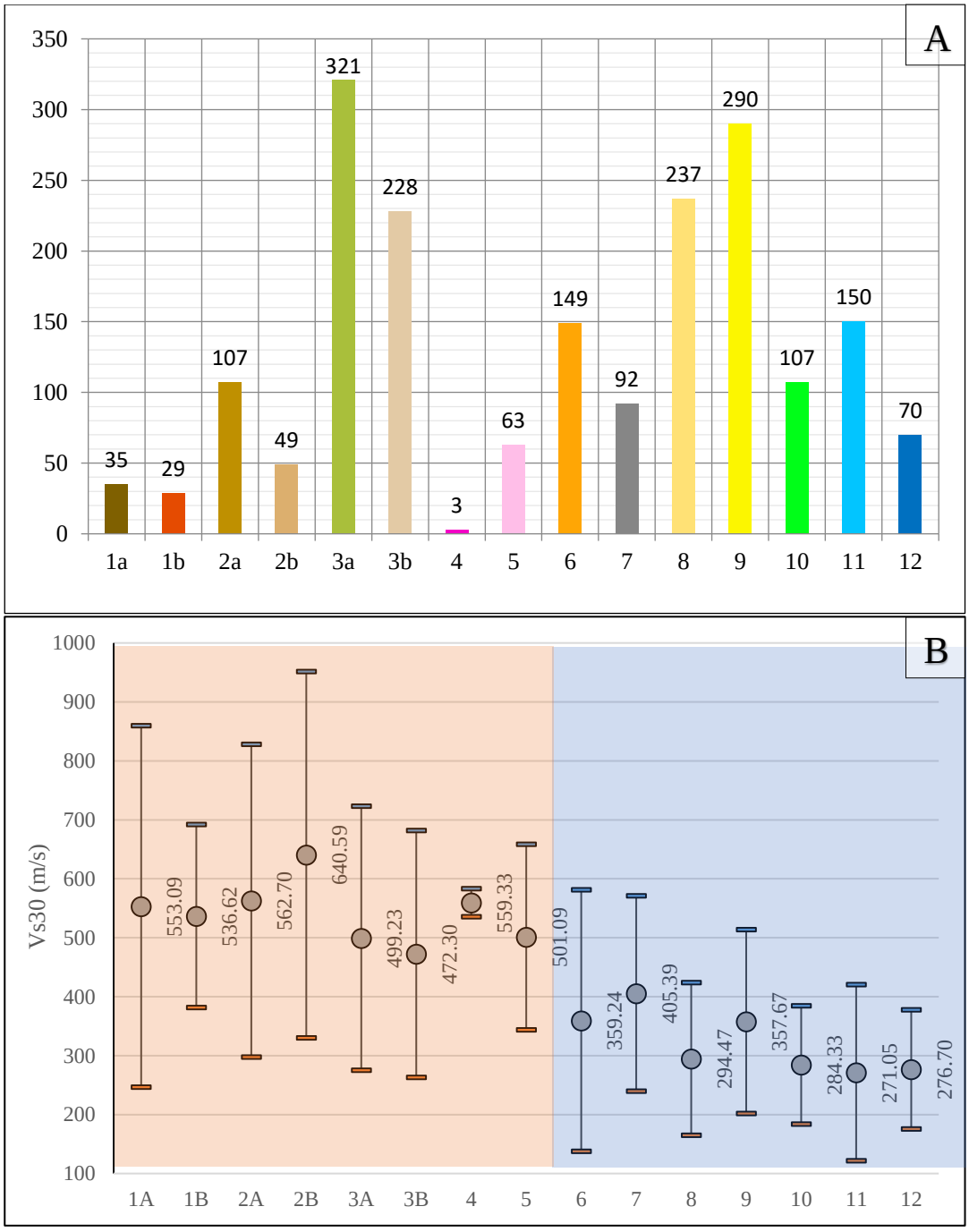


Figure 4-10: (A) Terrain class histogram that shows the amount of data in specific terrain class of Vs30 measurement locations and (B) Mean Vs30 values of terrain classes (orange area indicates “Mountain&Hill” region while blue area represents “Terrace&Plain” in terms of terrain classes)

## 4.4 Assessment of Saturation

Rock mixtures once saturated, are characterized by significantly reduced seismic velocities compared to dry conditions. Young porous sedimentary rock units which have elevated fluid-bearing capacity, are especially more prone to the effect of saturation. Since Vs30 measurements in our database belong predominantly to Quaternary-Pliocene units, further classification of this geologic class based on their saturation state can reduce the present data scatter considerably and allow us to constrain better Vs30 prediction formulations.

As mentioned in previous chapters, Vs30 represents the weighted average shear wave velocity of top 30 meter section. In order to develop any assessment about saturation state, regions, where groundwater is shallower than 30 m depth should be identified. This can be done directly in the presence of water table depth measurements from location of Vs30 data. Fortunately, a larger database including densely collected periodic water table depth measurements across California is made publicly available by California Department of Water Resources (Figure 2-8). The periodic observations of water table depth revealed rather large seasonal fluctuations. By contouring the mean water table depths across California, depth of groundwater at Vs30 measurement sites are estimated. Since, Vs30 measurement times are unknown, temporal variation of water table depth can not be accounted and therefore state of saturation is evaluated using a more simpler discrete approach in which Quaternary-Pliocene units with mean water table depths shallower than 30 m are classified further as saturated and remaining as unsaturated (Figure 4-11).

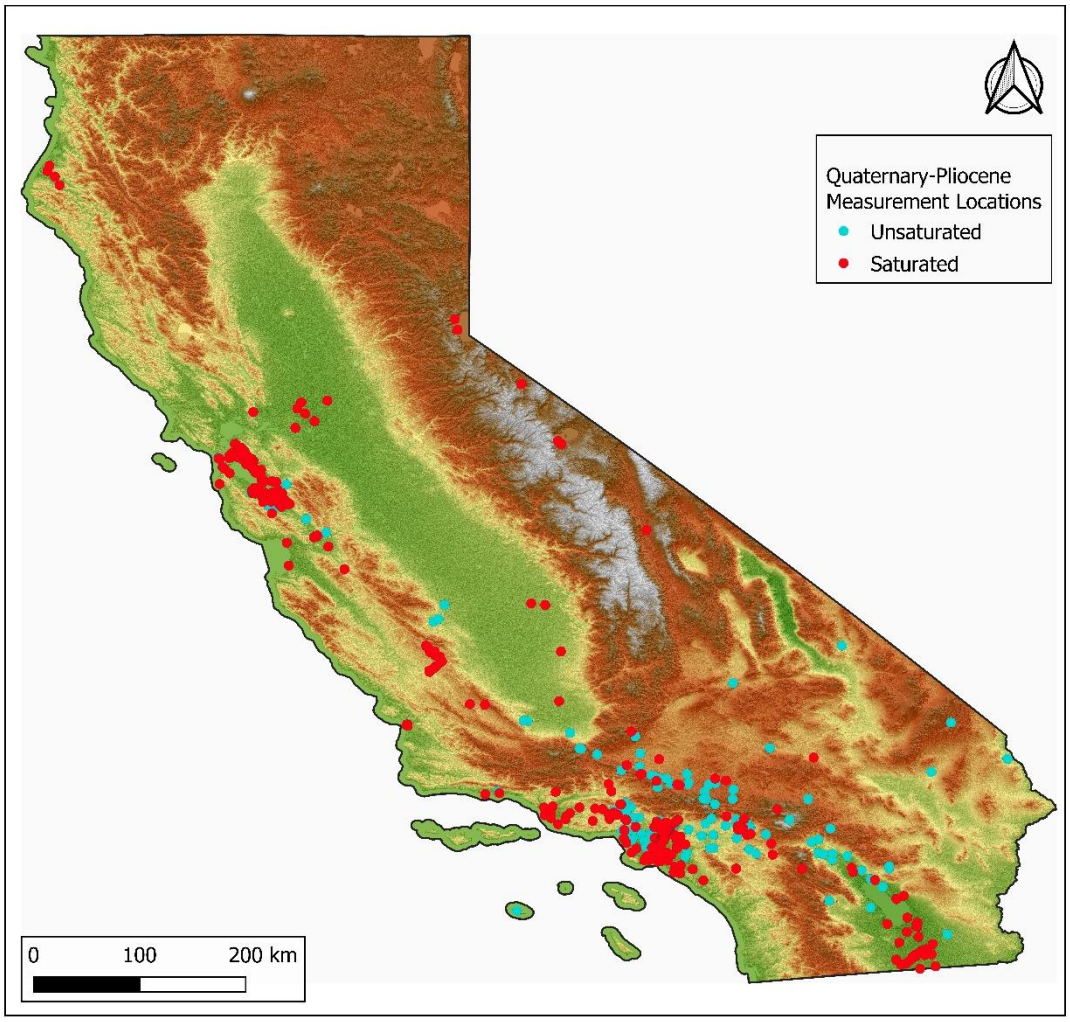


Figure 4-11: Vs30 measurement locations in Quaternary-Pliocene units throughout California.

Unlike California, groundwater data is not available in Türkiye and thus water table depths at Vs30 measurement sites remain unknown. In the absence of such data, the major water bodies (sea, lake and major rivers) are utilized to derive a correlation with saturation state of Quaternary-Pliocene units. For this purpose, water level rise analysis is conducted using 1 arc-second SRTM DEM around surface water bodies of Türkiye. The present levels of surface water bodies are raised 30 m to map the saturated domains where water table likely interferes with Vs30 measurements. According to this implementation, all areas situated up to 30 m above from the nearby surface water bodies are differentiated as saturated. This can be misleading

when sharp topographic changes associated with shallow seated or locally exposed bedrocks are present with height differences less than 30 meters. In order to account this possible scenario properly, we employed 2.5° topographic slope as a threshold to exclude sections from the saturated Quaternary-Pliocene domain.

The assessment of saturation is first applied to Quaternary-Pliocene units at the coastal areas of Türkiye. We raised sea level by 30 meters and identified the flat (slope < 2.5°) saturation area (Figure 4-12). This is applied across the entire coastline of Türkiye. Next, we identified permanent lakes in Türkiye to make the water level rise analysis. Base elevations of the lake are determined using DEM values at the lake center. Water levels of lakes are then raised 30 meters, and the higher slope sections (>2.5°) are filtered out from the resultant Quaternary-Pliocene domains to finalize the saturated area (Figure 4-13).

Unlike other water bodies, rivers are more complicated due to their spatially changing altitudes. In order to conduct water level rise analysis with variable river base elevations, the river base line is converted to a surface that extends both sides of the river and reaches beyond the boundaries of the river basin. This imaginary surface which intersects the river baseline, is raised by 30 m and its intersection with the surface is defined as the boundary between saturated and unsaturated domains (Figure 4-14a). After eliminating sections with slopes above the assigned threshold, the low land regions where the defined surface lies above the Earth's surface are defined as the saturated Quaternary-Pliocene domain (Figure 4-14).

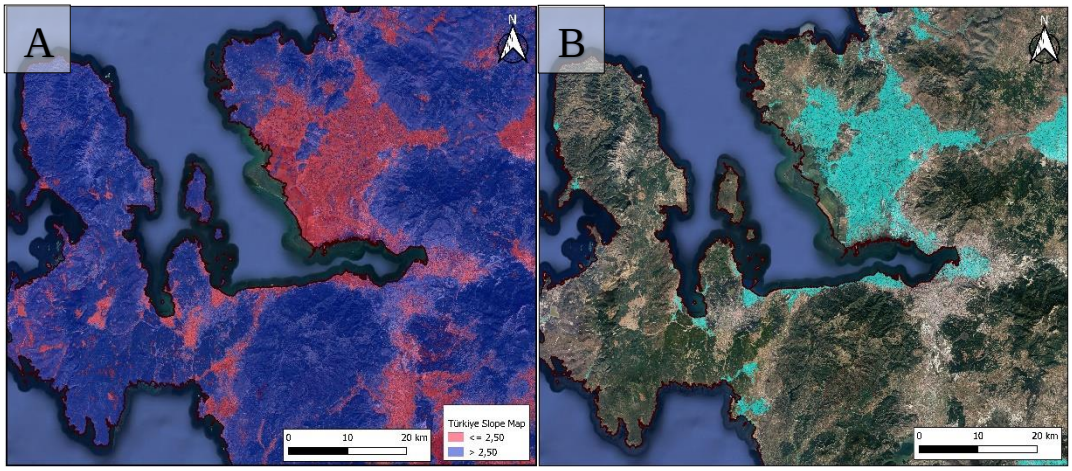


Figure 4-12: (A) Slope map of İzmir area derived from 1 arc-second SRTM DEM, (B) Saturation map of this region derived using elevation difference from water bodies (sea) and slope.

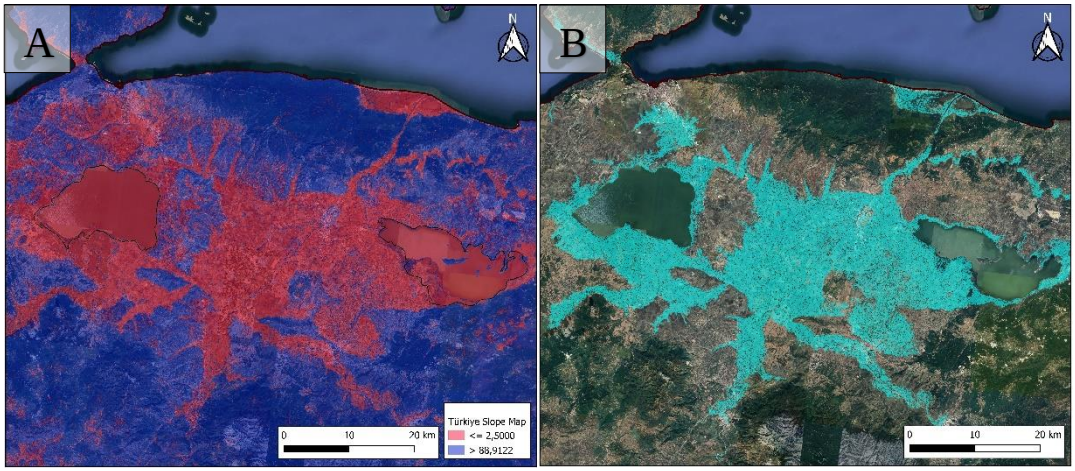


Figure 4-13: (A) Slope map of Kuş Lake (Balıkesir) and Ulubat Lake (Bursa) derived from 1 arc-second SRTM DEM, (B) Saturation map of this region derived using elevation difference from water bodies (lakes) and slope.

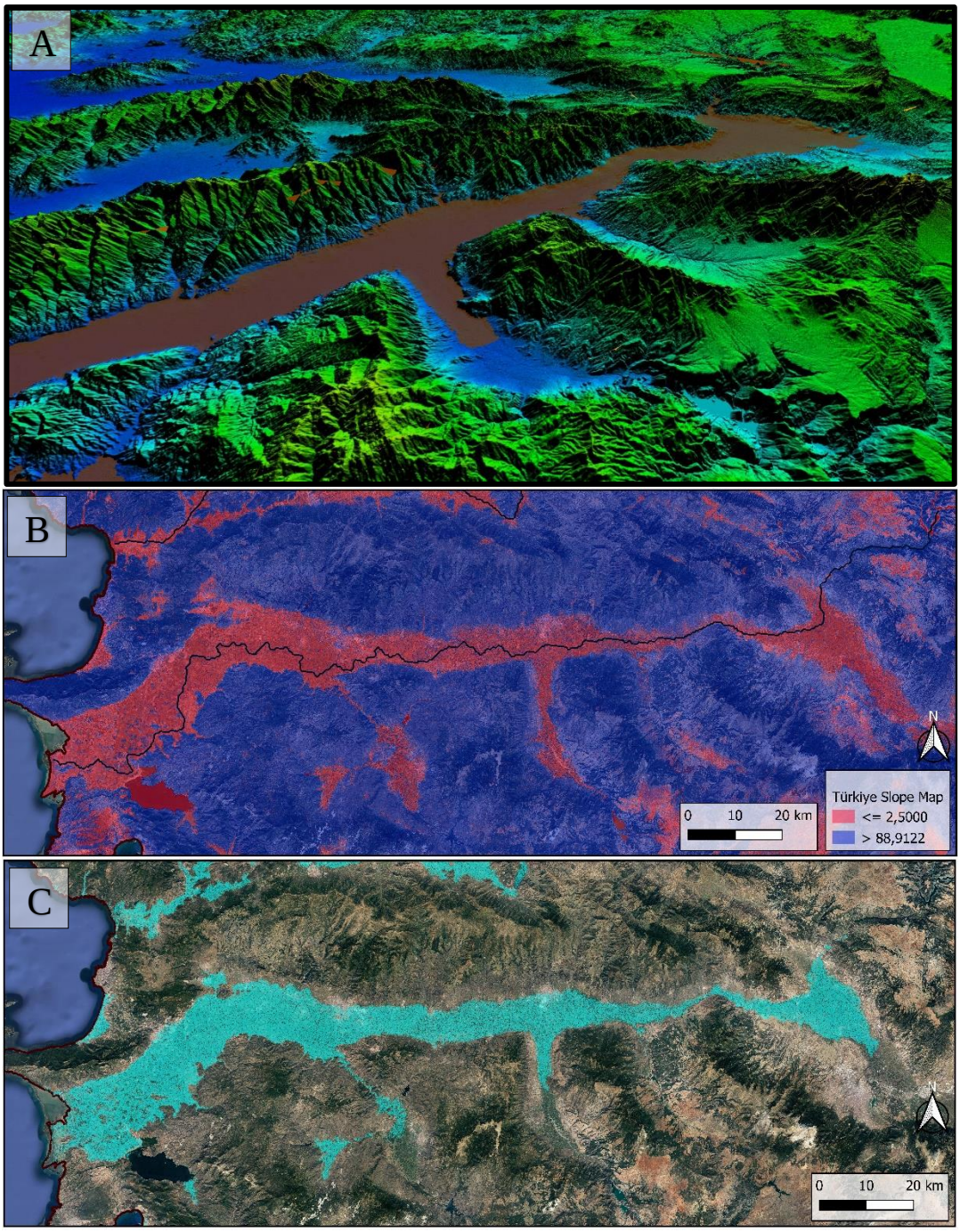


Figure 4-14: (A) 3D model of water level rise analysis along Büyük Menderes River, (B) 1 arc-second slope map and (C) Resultant saturation map derived by elevation difference along river delta and slope.

Unlike California, the developed approach for saturation assessment in the absence of water table depth data provides boundaries of saturated and unsaturated Quaternary-Pliocene units, which is suitable for mapping. Thus a nationwide map of saturated and unsaturated Quaternary-Pliocene units is constructed and shown over the DEM of Türkiye. It is worth to mention that the saturated young deposits do not represent fully saturated surface conditions but outlines the area where Vs30 measurements might have been reduced by the presence of water at depths shallower than 30 meters.

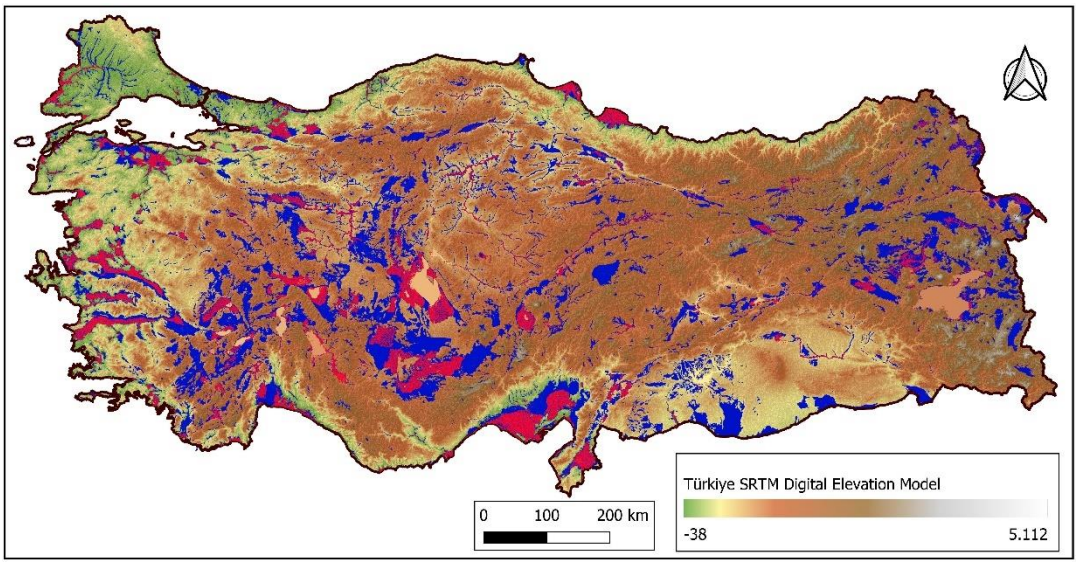


Figure 4-15: Map of saturated (red) and unsaturated (blue) Quaternary-Pliocene aged domains across Türkiye

After classifying Quaternary-Pliocene units into two classes as saturates and unsaturated, their Vs30 correlations with slope and elevation are revisited (Figure 4-16). The distribution of Vs30 measurements belonging to these classes are strikingly different from each other suggesting that Vs30 of young units are strongly controlled by the degree of saturation. As expected unsaturated class representing dry conditions are characterized by higher Vs30 values with a mean value around 400 m/s, while saturated class suffer from significantly reduced Vs30 values averaging just below 300 m/s. Also, this reflects drastically on the regression trends developed both for slope and elevation (Figure 4-16). These results mainly support

the usage of fluid saturation in younger units as a proxy to improve Vs30 prediction models.

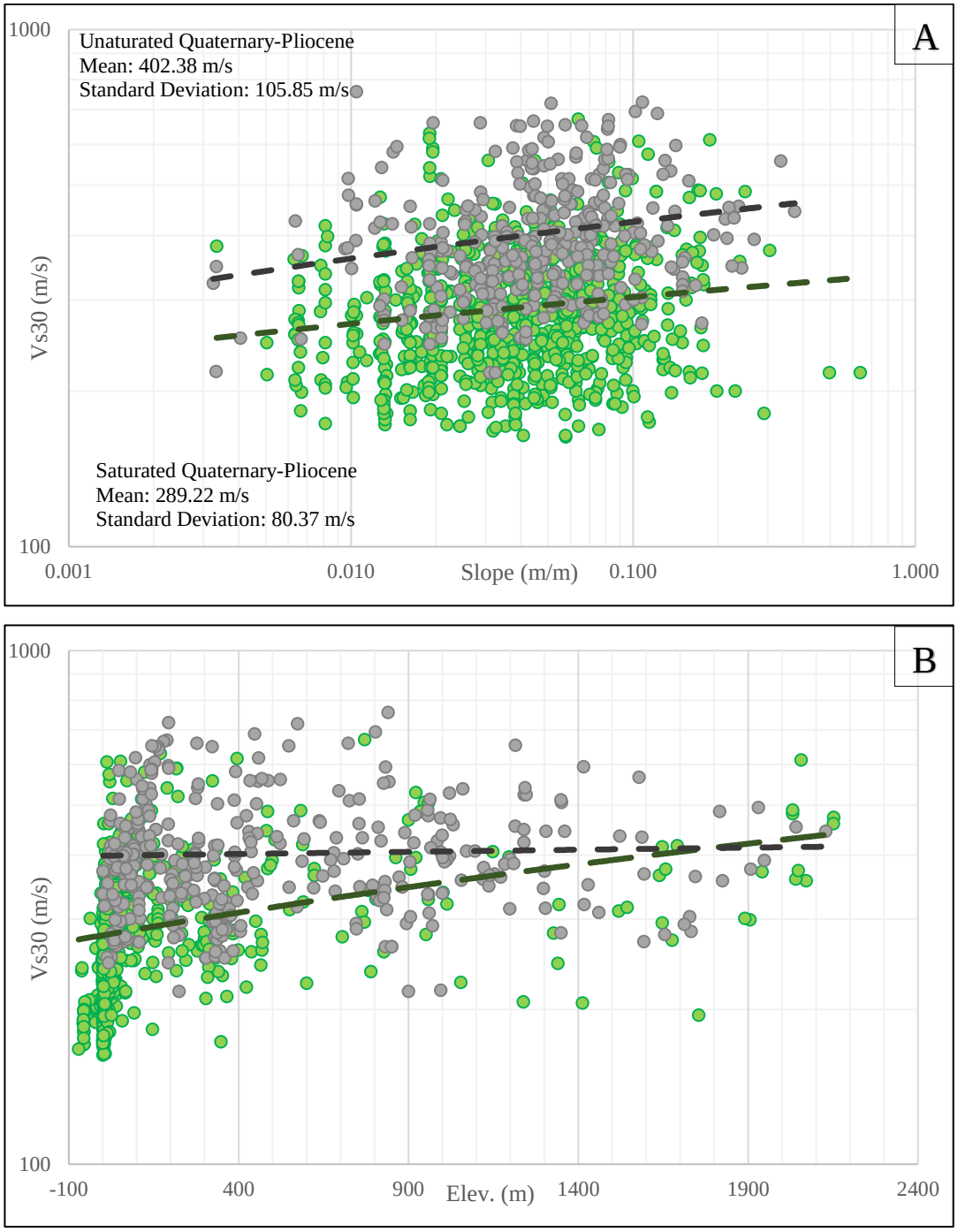


Figure 4-16: Slope vs Vs30 (A) and elevation vs Vs30 (B) graphs of Quaternary-Pliocene geologic class with saturation classification (Green: Saturated – Grey: Unsaturated)

# CHAPTER 5

# RESULTS

Türkiye is an earthquake country, and its seismic hazard map prepared by AFAD, is based on the Vs30 value of 760 m/s (which is equal to a “rock site” in NEHRP classification). The accurate estimation of site responses during earthquakes can be possible only when reliable Vs30 values are available. For this purpose, available Vs30 measurements across the country are sparse and unsuitable for direct usage but provides a unique opportunity to develop a more accurate nationwide Vs30 prediction model.

In this study Vs30 measurements from Türkiye and California are combined to study factors controlling Vs30 values. Throughout both regions slope and elevation are derived from 1 arc-degree SRTM DEM and mapped together with their geologic and morphologic terrain classes using available geology maps and global terrain classification of Iwahashi et al. (2018).

Geologic units are simplified into 4 sedimentary rock classes based on their ages (Quaternary-Pliocene, Miocene, Paleogene, and Pre-Paleogene) and 3 non-sedimentary rock classes based on geological processes forming them. Vs30 measurements taken from oldest (Pre-Paleogene) sedimentary rocks and all non-sedimentary rocks revealed no statistically robust or meaningful correlation with slope and elevation. Therefore, their Vs30 estimates are fixed to the average Vs30 value of each class. In contrast, Miocene and Paleogene rocks which indicated positive Vs30 correlations with both slope and elevation, are selected for multi-variable linear regression analysis.

Quaternary-Pliocene units containing most of the Vs30 measurements are found to be suffering from elevated data scatter that supported the presence of unaccounted factors playing an important role on measured Vs30 values. Terrain class can be

linked to particle distribution and unit thickness of young sedimentary rocks. For terrain classification of Quaternary-Pliocene units, globally defined morphological terrain classes are combined into 2 major terrain categories (Mountain/Hill and Plain/Terrace), displaying distinct average Vs30 ranges.

Fluid saturation that can largely reduce the shear wave velocities of rock mixtures can be one of the key factors controlling Vs30 values measured in unconsolidated porous Quaternary-Pliocene deposits. Using water table depth measurements in California and water level rise analysis around surface water bodies (sea, lake, and major rivers) in Türkiye, young deposits are classified as saturated if groundwater is less than 30 meters deep and as unsaturated otherwise. With this classification, Vs30 measurements are effectively divided into two distinct groups where saturated Quaternary-Pliocene units are mainly made up of the lowest Vs30 values. Since terrain and saturation classifications are both separately responsible for large noticable variations in Vs30 values, Quaternary-Pliocene units are divided into 4 classes using both terrain and saturation proxies at which correlations with slope correlations and elevation will be analyzed by using multi-variable linear regression analysis.

In this new Vs30 prediction strategy, a total of 10 rock classes emerged. For the oldest (Pre-Paleogene) sedimentary rocks and all non-sedimentary rocks, Vs30 is kept fixed to the class average. For younger (Quaternary-Pliocene, Miocene, and Paleogene) sedimentary rocks comprising 6 different rock classes, slope and elevation dependency of Vs30 are further studied. Based on data distributions, Vs30 prediction formulations are developed for each of these 6 classes using single or multi-variable linear regression. Finally, a nationwide predicted Vs30 map of Türkiye is developed based on these proposed formulations and compared with slope based Vs30 model of Allen & Wald (2009), which is the only one covering the whole country.

## 5.1 Regression Analysis and Vs30 Prediction Formulas

The simple linear regression defines a linear relationship between two parameters. Multi-variable or Multiple linear regression is an extension of simple linear regression in which more than one independent variable is used to predict the outcome of a response (dependent) variable by fitting a linear equation. With this method, coefficients of the linear relationship, which belongs to slope and elevation in our case, are identified allowing estimation of Vs30 value.

Theoretically, this method performs well if independent variables have normal distributions and actually display the assumed linear dependency. This would result in minimal normally distributed prediction error. During regression analysis, we used the natural logarithm of dependent and independent variables for normalization and equally weighted the independent variables (slope and elevation). Note that multiple linear regressions are established in "IBM SPSS Statistics" software version 28.0.0.0.

As mentioned before, combined classification of Quaternary-Pliocene rocks based on saturation and terrain proxies led to the formation of 4 distinct rock classes. Vs30 measurement distributions of each resultant class are investigated with respect to slope and elevation by conducting separate multiple linear regression analyses.

Saturated Quaternary-Pliocene rocks are represented by the lowest Vs30 values in the database and after further classification based on their major terrain category formed Vs30 classes which are clearly distinguished from each other (Figure 5-1). Saturated young units located within plain/terrace terrain category display relatively lower slope and elevation values while including lowest Vs30 measurements with a class average less than 300 m/s. In contrast, saturated young units in mountain/hill terrain represented by relatively higher slope, elevation and highest Vs30 values with a class average around 400 m/s. This clear difference in data populations strongly support the applied classification scheme and led to calculation of multiple linear regression trendlines that differ significantly for these rock classes.

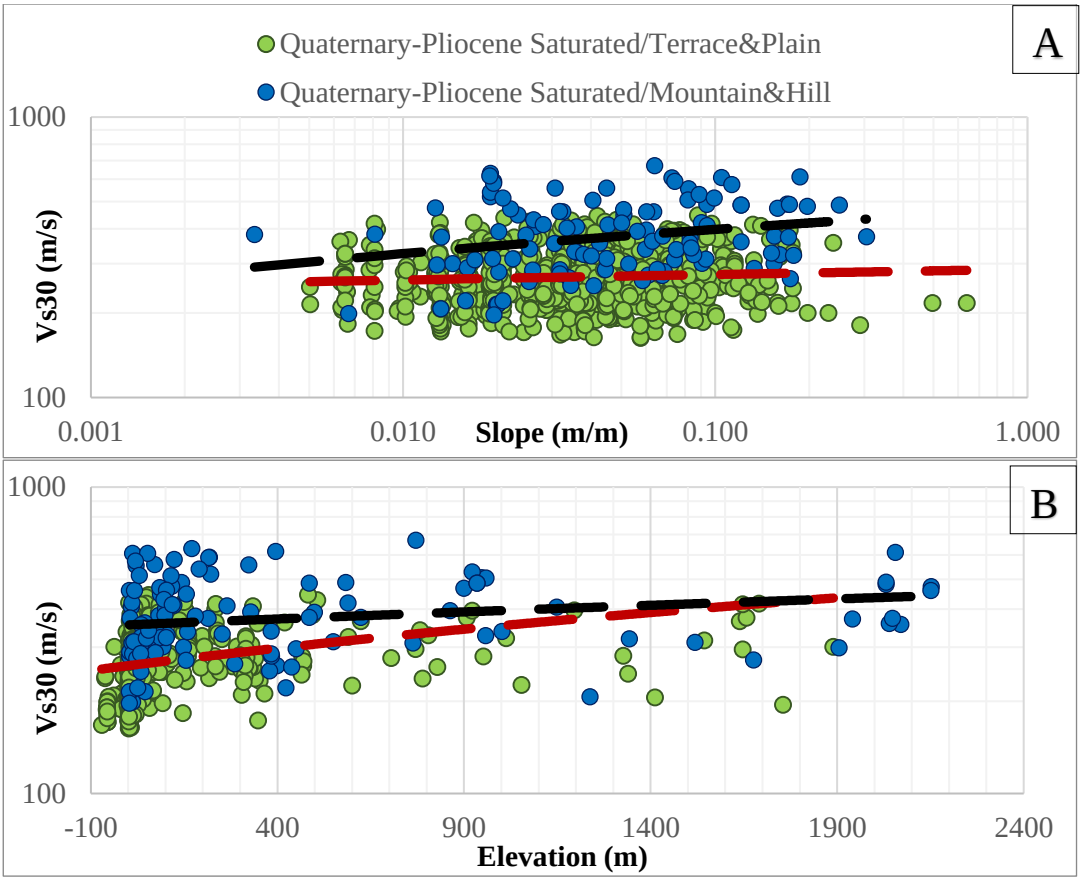


Figure 5-1: Slope vs Vs30 (A) and Elevation vs Vs30 (B) graphs of saturated Quaternary-Pliocene rocks. Measurements from mountain/hill terrain category are shown in blue with black dashed trendlines, and measurements from plain/terrace terrain category are shown in green with red trendlines.

Unsaturated Quaternary-Pliocene rocks which represents significantly higher Vs30 measurements than saturated classes, are also divided into two classes using the proposed major terrain categorization. Unlike saturated classes, unsaturated young rocks showed no statistically viable linear relationship between Vs30 measurements and elevation. Therefore, simple linear regression involving only topographic slope is applied to unsaturated classes separately (Figure 5-2). As expected, unsaturated young units located within mountain/hill terrain category are characterized by higher slope and Vs30 measurements than the ones located within plain/terrace terrain category. In this respect, the applied classification has decreased the data scatter and provided more stable regression results with linear trendlines that differ noticeable for each unsaturated young rock class.

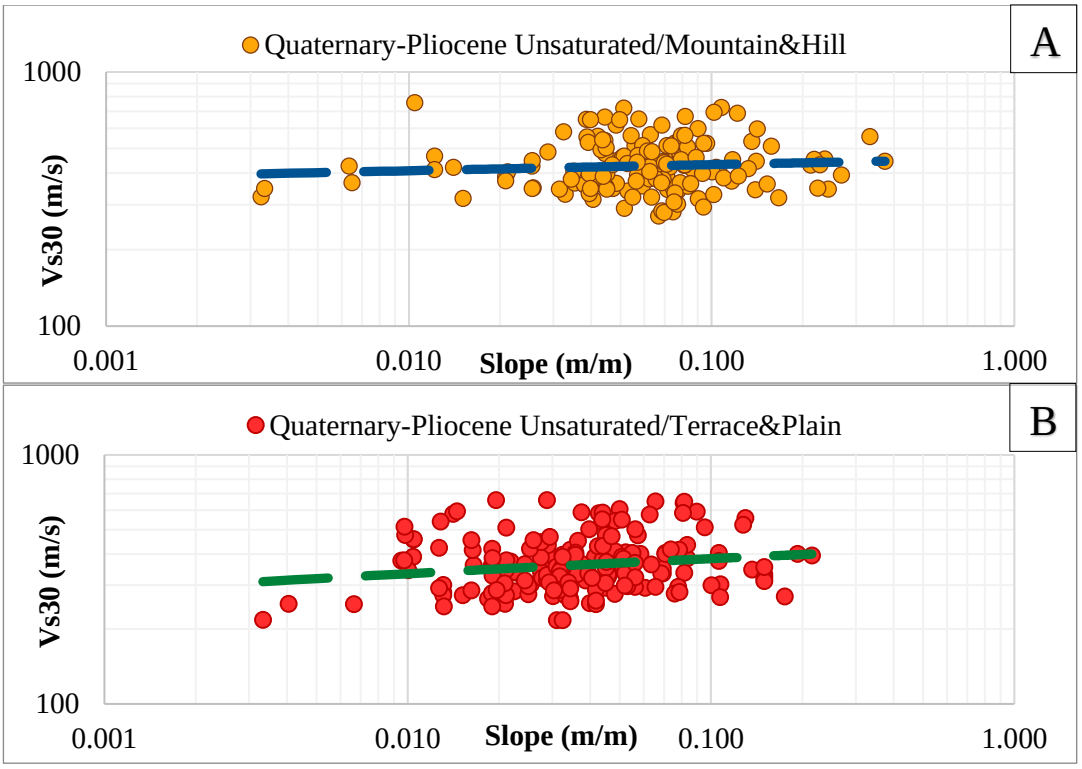


Figure 5-2: Slope vs Vs30 graphs of unsaturated Quaternary-Pliocene rocks located within mountain/hill terrain category (A) and within plain/terrace terrain category (B). Measurements from mountain/hill terrain category are shown in orange with blue dashed trendline and measurements from plain/terrace terrain category are shown in red with green trendline.

Among older sedimentary rocks, Miocene and Paleogene rock units are also showing positive correlation between slope and elevation with Vs30 measurements (Figure 5-3). The data distributions of both age classes do not vary from each other as much as the younger Quaternary-Pliocene rock classes but both have sufficient number of Vs30 measurements to conduct multiple linear regression analysis individually. The resultant regression trends of these groups are much alike but there are still some saddle differences. Since, classification of Miocene and Paleogene maybe needed in other geographic regions, these classes are kept separate in our analysis to ensure enough geologic age variability in Vs30 prediction which can be improved by combining Vs30 data from different geological settings.

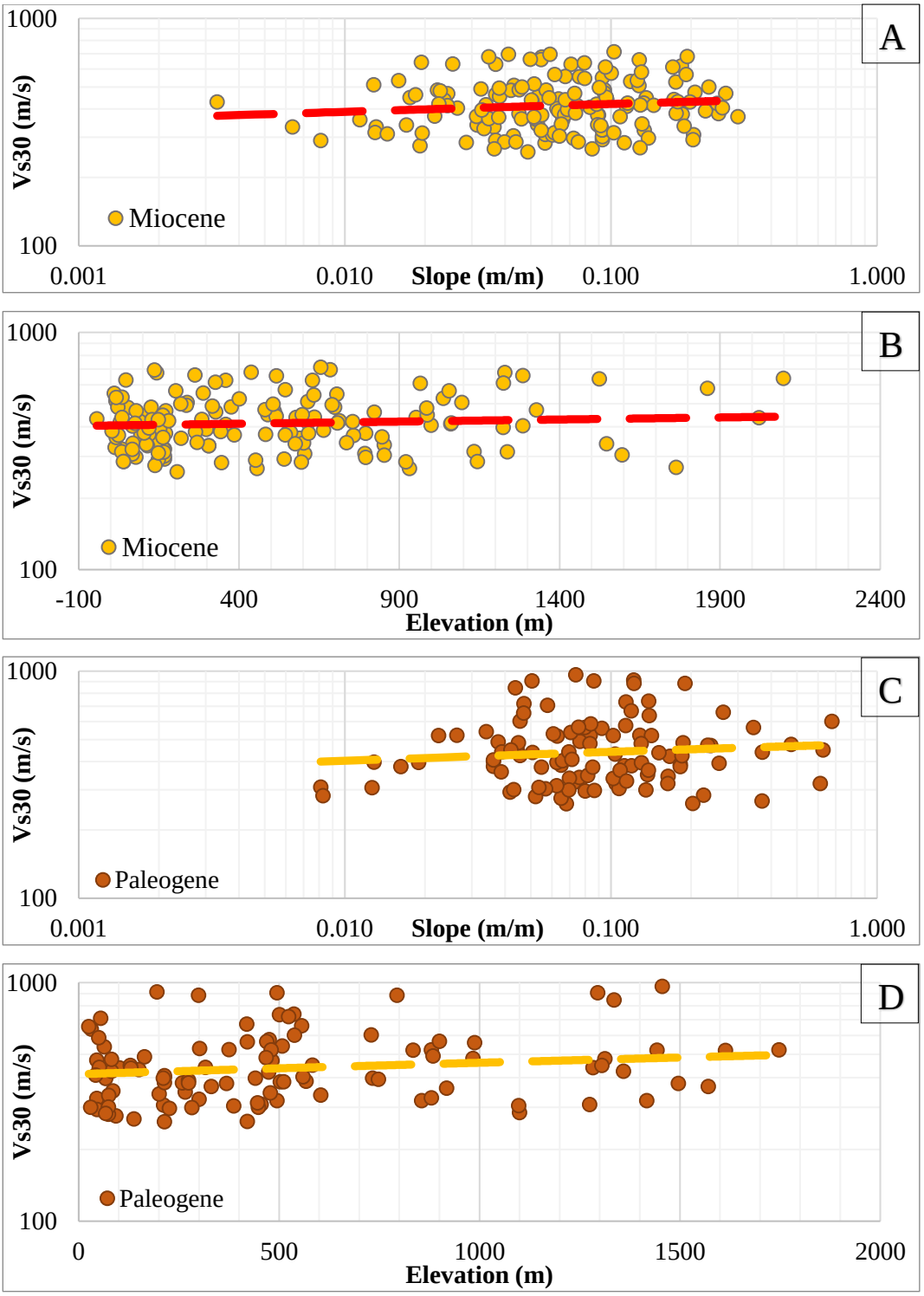


Figure 5-3: Slope vs Vs30 (A & C) and elevation vs Vs30 (B & D) graphs of Miocene and Paleogene rocks. Measurements of Miocene rocks are shown in orange with red dashed trendlines and measurements of Paleogene rocks are shown in brown with orange trendlines.

Vs30 prediction formulas developed in this study for each rock classes is summarized in Table 5-1. As mentioned previously, Pre-Paleogene sedimentary rocks and non-sedimentary rock classes are represented by relatively limited and largely scattered data not suitable for statistically viable regression analysis. For these classes, Vs30 estimate is fixed to the class average as it is given in Table 5-1. For younger sedimentary rocks, applied multiple linear regressions revealed coefficients that differ largely for each rock class especially within youngest units. These derived Vs30 formulas essentially outlines the critical role of saturation state and main terrain category in partly unconsolidated porous young sedimentary deposits.

Table 5-1: Finalized Vs30 prediction formulas of defined rock classes

| $ln(Vs30) = a_0 + a_1 ln(Slope) + a_2 ln(Elevation)$ | | | | | |
|---|---|---|---|---|---|
| **Group** | | | **# of Vs30 data** | **Mean Vs30 (μ) & Std. Dev. (σ) of Measured Vs30** | **Constants of Vs30 equation & Mean Absolute Error (ϵ)** |
| Quaternary-Pliocene | Saturated | Mountain/Hill | 111 | μ = 388,57 m/s<br>σ = 113,72 m/s | $a_0 = 5{,}964$<br>$a_1 = 0{,}065$<br>$a_2 = 0{,}031$<br>ϵ = 90,77 m/s |
| | | Plain/Terrace | 716 | μ = 273,81 m/s<br>σ = 60,85 m/s | $a_0 = 5{,}459$<br>$a_1 = 0{,}015$<br>$a_2 = 0{,}064$<br>ϵ = 42,09 m/s |
| | Unsaturated | Mountain/Hill | 160 | μ = 437,15 m/s<br>σ = 102,12 m/s | $a_0 = 6{,}124$<br>$a_1 = 0{,}024$<br>$a_2 = 0{,}000$<br>ϵ = 77,85 m/s |
| | | Plain/Terrace | 188 | μ = 373,33 m/s<br>σ = 100,20 m/s | $a_0 = 6{,}088$<br>$a_1 = 0{,}060$<br>$a_2 = 0{,}000$<br>ϵ = 75,47 m/s |
| Miocene | | | 153 | μ = 427,15 m/s<br>σ = 111,79 m/s | $a_0 = 6{,}018$<br>$a_1 = 0{,}032$<br>$a_2 = 0{,}017$<br>ϵ = 88,18 m/s |
| Paleogene | | | 106 | μ = 462,16 m/s<br>σ = 163,90 m/s | $a_0 = 5{,}877$<br>$a_1 = 0{,}030$<br>$a_2 = 0{,}048$<br>ϵ = 119,13 m/s |
| Pre-Paleogene | | | 109 | μ = 631,42 m/s<br>σ = 215,29 m/s | |
| Non-Sedimentary | Intrusive | | 97 | μ = 640,01 m/s<br>σ = 173,27 m/s | |
| | Extrusive | | 41 | μ = 558,20 m/s<br>σ = 172,17 m/s | |
| | Metamorphic | | 50 | μ = 601,29 m/s<br>σ = 216,48 m/s | |

## 5.2 Performance Analysis of the Proposed Vs30 Prediction Strategy

Distributions of Vs30 ranges and prediction residuals of our proposed Vs30 prediction strategy are shown in Figure 5-4 along with other alternative previously applied approaches. In our model, number of Vs30 predictions within given discrete ranges below 500 m/s is highly comparable with the Vs30 measurements. On the other hand, Vs30 predictions above 500 m/s poorly resembles the measurements (Figure 5-4a). It is most likely due to the inherited trade-off in regression associated to non-uniform data sampling. Since Vs30 measurements are concentrated in residential areas, observations from large slope areas are very limited and thus developed linear regression may not sufficiently account the measured high values of Vs30. In addition, rock classes with fixed Vs30 estimates represent class averages with large standard deviations which are all below 700 m/s and are not suitable to match the measured distributions at high Vs30 ranges. For these reasons, our models result exceeding 500 m/s should be treated with caution.

Residuals of our model shows a narrow symmetric normal distribution centered at zero which is better than other tested alternative approaches (Figure 5-4b,c). The residual box of our predictions is centered at 0 with symmetric bounds between -60 and 60 m/s which are narrower than others (Figure 5-4d). In short, our Vs30 prediction strategy performs quiet well in Türkiye and California and has considerably improved the accuracy of Vs30 predictions, especially more in younger units (Figure 5-5) which are most prone to site amplifications. Thus, the implementation of this Vs30 model is expected to produce more realistic site response estimations that are vital for reliable seismic hazard assessments.

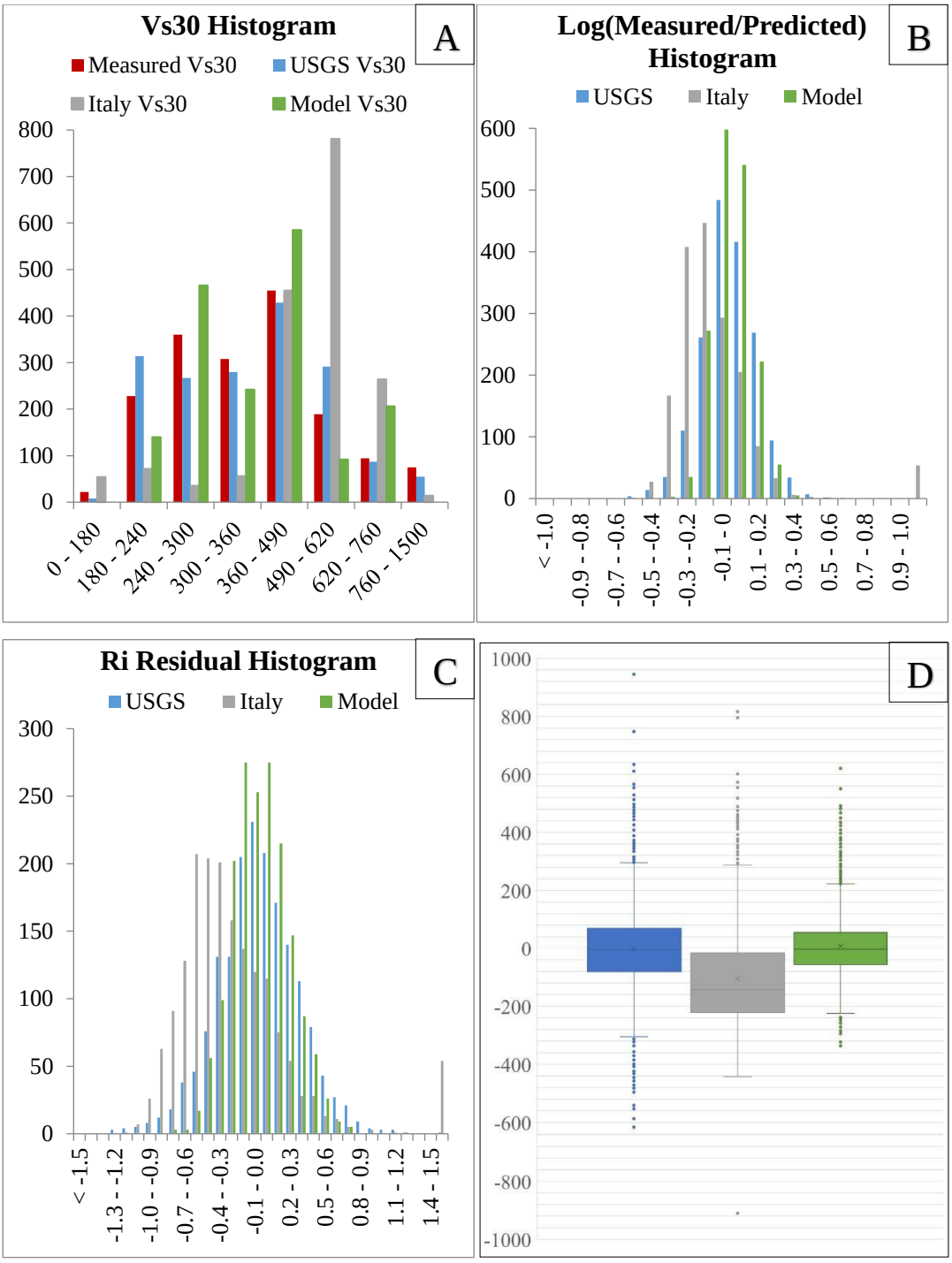


Figure 5-4: Histograms of measured and predicted Vs30 values (A), logarithmic ratio between measured and predicted Vs30 values (B), Ri - Residual (Seyhan et al., 2014) (C) and box plots of residuals (D).

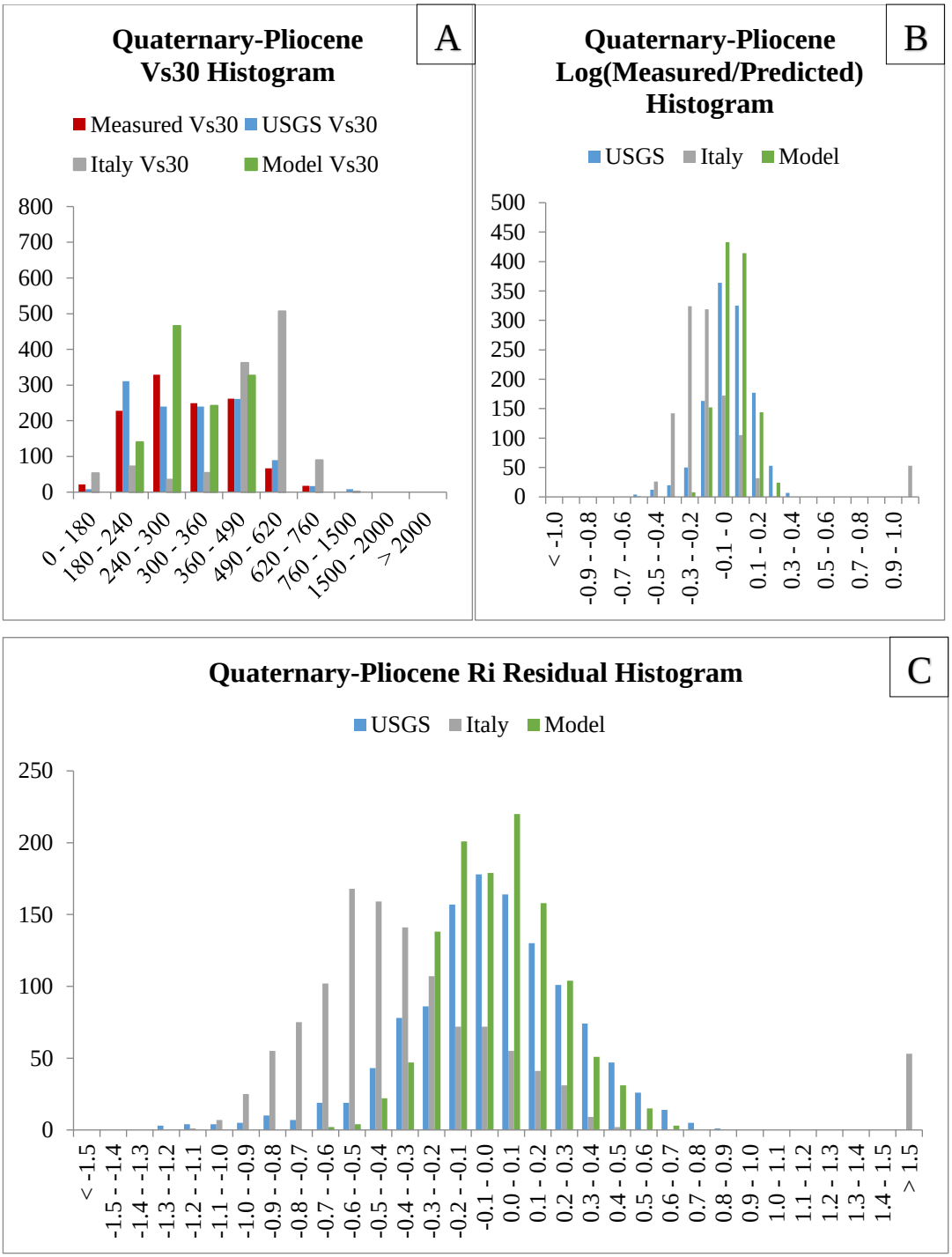


Figure 5-5: Histograms of measured and predicted Vs30 values (A), logarithmic ratio between measured and predicted Vs30 values (B), and Ri - Residual (Seyhan et al., 2014) (C) for Quaternary-Pliocene aged relatively younger units

## 5.3 New Vs30 Model of Türkiye

Türkiye is located in one of the most tectonically active regions in the world and witnessed the devastation of many large magnitude earthquakes in the past. Most recently, the Samos earthquake produced severe damage across the İzmir Bay area where large site amplifications are observed in association with thick basin fill (Cetin et al., 2022; Gülerce et al., 2022). Mitigation of such seismic risks requires reliable knowledge of site conditions. In the absence of a representative amount of Vs30 measurements, it is crucial to have an accurate Vs30 model of the region.

Across Türkiye, only AFAD's Vs30 database collected across strong motion stations is publicly available, which is made up of widespread sparse measurements. Moreover, the region is covered nationwide only by global Vs30 prediction models providing coarse spatial resolution, and unfortunately, none of them employs the local Vs30 measurements collected from Türkiye. In this study, Vs30 data collected from Türkiye is combined with data from California to better represent active tectonic settings and utilized for the development of a new Vs30 prediction strategy. Eventually, the proposed Vs30 prediction formulations computed for 10 different rock classes (Table 5-1) are used to estimate Vs30 values in high spatial resolution across the whole country, which led to the production of a new, more accurate nationwide Vs30 map of Türkiye (Figure 5-6).

According to the resultant Vs30 model of Türkiye, NEHRP site classes displaying Vs30 below 300 m/s (orange to red colored polygons in Figure 5-6a) is spatially limited to basins forming along tectonically active coastal areas, along active grabens containing major rivers and across large deltas formed at the major river and sea intersections. In order to better visualize the spatial variations, our Vs30 model is also mapped with continuous coloring which shows Vs30 patterns developing under the influence of dynamic surficial processes, geomorphology, saturation, and regional tectonism (Figure 5-6a).

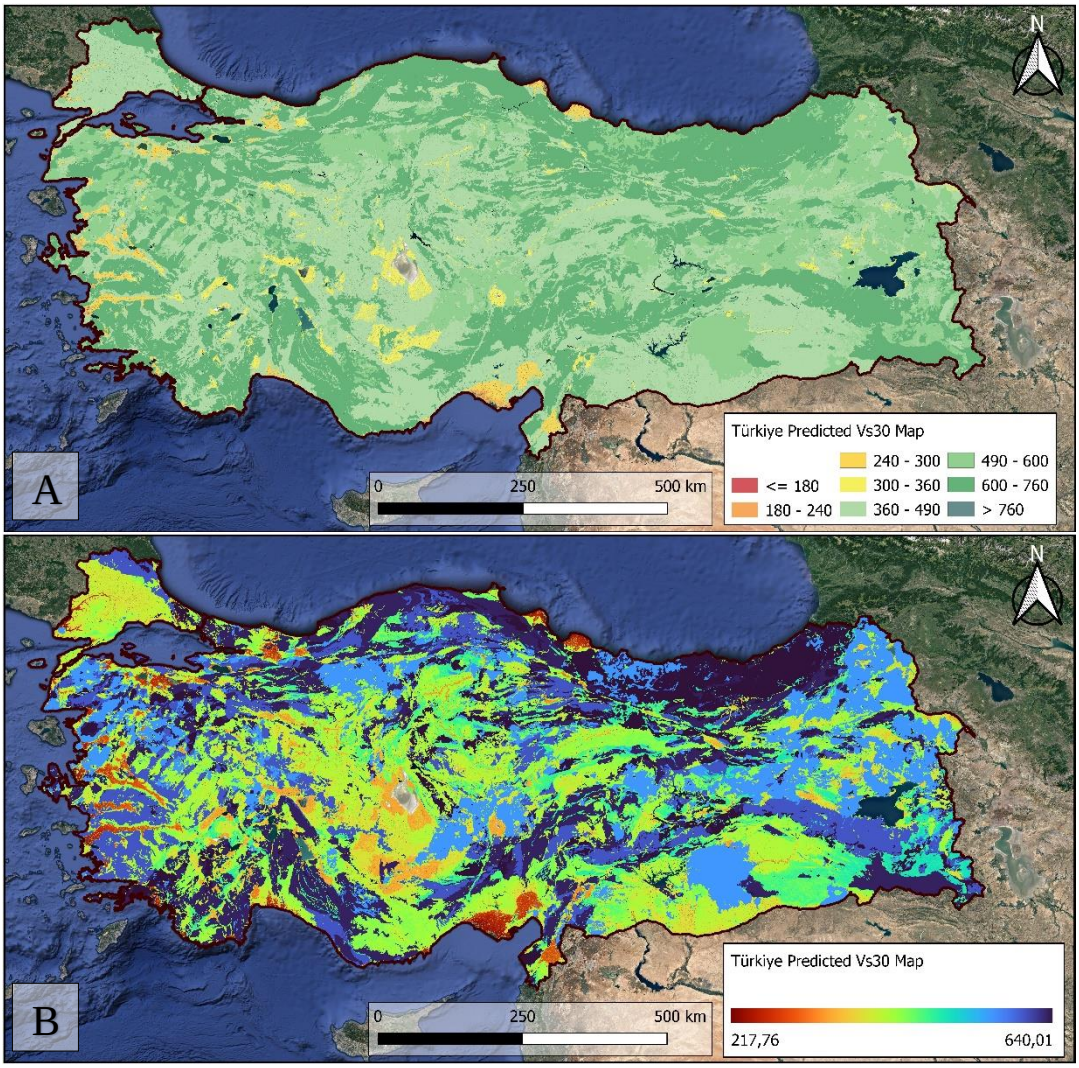


Figure 5-6: Finalized Vs30 map of Türkiye (A) with NEHRP site classification boundaries and (B) with continuous coloring.

# CHAPTER 6

# DISCUSSION

The resolution of the digital elevation model is the key factor in creating an accurate model when the model includes slope and elevation as a parameter. Previous studies use different resolutions and global Vs30 prediction models using 9 and 30 arc-second resolutions for slope calculations (Allen & Wald, 2009; Wald & Allen, 2007). The digital elevation model loses accuracy when the resolution drops due to an increase in pixel size. When pixel size increases, slopes become lower because they represent wider regions compared to the higher resolution. Figure 6-1 illustrates the clear effect of resolution in slope computation where lower resolution DEM creates significantly lower slopes at flat areas. By employing the highest possible resolution in our calculations, we attempted to produce the most detailed result locally.

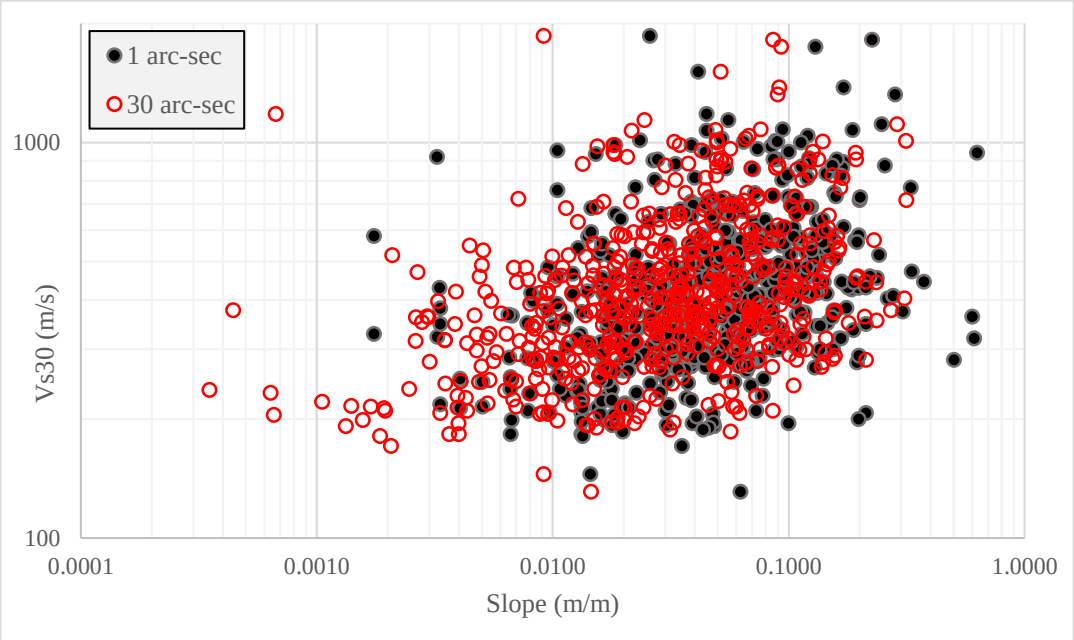


Figure 6-1: Slope vs Vs30 graph displaying the effect of DEM resolution on the slope calculation

The quality and quantity of the measurements in the target area are another factor in developing an appropriate model. In order to obtain more precise findings, we have combined California Vs30 values with AFAD measurements. However, the number of measurements in Pre-Paleogene and Non-Sedimentary units restricts the predictive power of our model. In order to create a more consistent and predictive model, the sampling should be more comprehensive. In other words, non-uniform data sampling affects the classes' reliability. Because we only have a small number of higher Vs30 values, our model's maximum velocity is 640.01 m/s. An increase in the quantity of measurements in these classes directly effecting our model. Pre-Paleogene and Non-Sedimentary units must be averaged under these circumstances because we are unable to forecast measured values as we had anticipated.

When creating the final Vs30 prediction map, we realized that “noise” is present in our model (Figure 6-2). Since we use a high-resolution elevation and slope model in our calculations, high spatial frequency creates this type of noise in the final model. Another reason for this noise is our model itself. Our prediction equations use the natural logarithm of slope and elevation, and the natural logarithm of zero (white cells in Figure 6-2a) is undefined. Because of that reason, our model can not create predictions in flat areas. To overcome this problem, “smoothing” can be applied in flat areas like plains or lowlands.

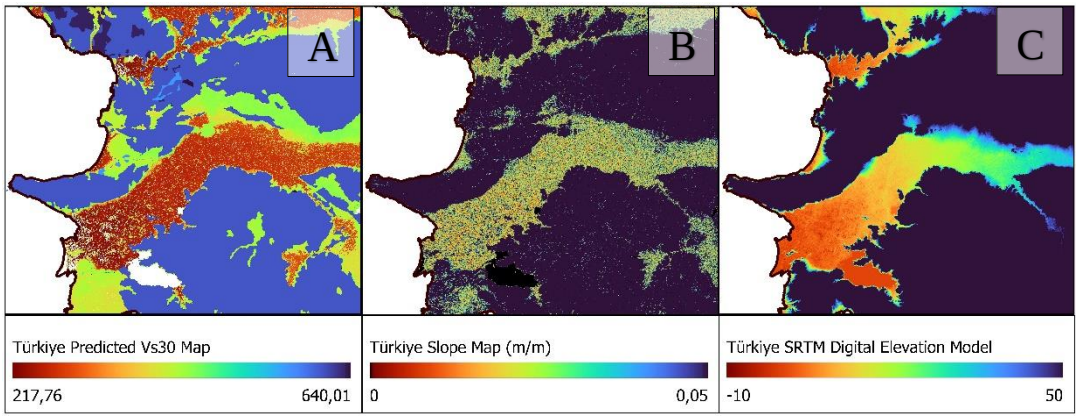


Figure 6-2: (A) Predicted Vs30 map, (B) Slope map, and (C) Elevation map of the sample region

The original resolution and clusters of Iwahashi et al. (2018) are used without any subjective change. Currently used terrain classification is using 280 m DEMs for global usage. Regional-specific terrain classification with higher resolution can improve the discrimination of regions.

In California, water table depths which are measured periodically in different seasons, display significant fluctuations associated to temporary climatic conditions. Since, measurement times of Vs30 are not available in the compiled database, we utilized mean depth of the water table for saturation classification, thus any temporary climatic effect are ignored. If times of the Vs30 measurements is known, a more precise classification of saturation could be established from nearest groundwater observations that will minimize temporary effects.

# CHAPTER 7

# CONCLUSION AND RECOMMENDATIONS

During this study, a new Vs30 prediction strategy is developed and applied to provide a more accurate Vs30 model of Türkiye. Rocks are classified initially based on their major rock type (sedimentary, intrusive, extrusive, and metamorphic) and geologic ages (Quaternary-Pliocene, Miocene, Paleogene, Pre-Paleogene), and then young partly unconsolidated porous sedimentary deposits are further classified based on their saturation states (saturated and unsaturated) and major terrain categories (mountain/hill and plain/terrace) which effectively minimized the data scatter. As a result, prediction equations of 10 different rock classes are formulated using slope and elevation in regression analysis of Quaternary, Miocene, and Paleogene sedimentary rocks while fixing Vs30 estimates to averages of remaining classes (Table 5-1).

Using saturation and terrain proxies with slope and elevation increased Vs30 estimation performance. This newly established Vs30 prediction strategy provided minimum misfits with more narrow normal distribution centered at zero and performed better than other tested alternative approaches, especially in younger units displaying low Vs30 values. Based on these findings, Vs30 measurements of youngest units are found to be strongly controlled also by saturation state and terrain proxies not by topographic slope alone as global models may predict. Finally, a new improved nationwide Vs30 model of Türkiye is established to aid calculations of site responses anywhere across the whole country.

At the end, future recommendations that would help us to improve the performance of our Vs30 prediction strategy are listed shortly as follows:

- Creation of error map for the proposed Vs30 model of Türkiye to quantify location of specific uncertainities of the model.

- Constructing saturation and new Vs30 maps of California combining point based saturation proxy with Quaternary-Pliocene rocks.
- Conducting water level rise analysis also in California and verifying its performance using obtained fits to the present borehole data.
- Developing strategies to enlarge the data collected from rock classes with fixed Vs30 estimates, which would help us construct a statistically viable model.
- Incorporating data from other geographic regions and testing our the robustness of derived Vs30 formulas globally to form global Vs30 models.
- Incorporating more local data collected by microzonation efforts and/or engineering projects to further improve the national Vs30 prediction model.
- Forming regularly updated national Vs30 database that incorporates local data collected by microzonation efforts and/or engineering projects to extend data capability.
- Modeling water table depths of California in a more continuous manner to understand the possible effect of partial saturation in Vs30 measurements. In Türkiye, application of water level rise analysis for multiple depth less than 30 meters to account possible effect of partial saturation.

## REFERENCES


Allen, T. I., & Wald, D. J. (2009). On the use of high-resolution topographic data as a proxy for seismic site conditions (VS30). *Bulletin of the Seismological Society of America, 99*(2 A), 935–943. https://doi.org/10.1785/0120080255

Borcherdt, R. D. (1994). Estimates of Site-Dependent Response Spectra for Design (Methodology and Justification). In *Earthquake Spectra* (Vol. 10, Issue 4, pp. 617–653). https://doi.org/10.1193/1.1585791

Bozkurt, E., & Mittwede, S. K. (2001). Introduction to the geology of Turkey - A synthesis. *International Geology Review*, *43*(7), 578–594. https://doi.org/10.1080/00206810109465034

Bozkurt, E., & Oberhänsli, R. (2001). Menderes Massif (Western Turkey): Structural, metamorphic and magmatic evolution - A synthesis. *International Journal of Earth Sciences*, *89*(4), 679–708. https://doi.org/10.1007/s005310000173

Building Seismic Safety Council (2003) NEHRP Recommended Provisions for Seismic Regulations for New Buildings and Other Structures, Part1: Provisions, FEMA 368, Federal Emergency Management Agency, Washington, D.C.

CA Department of Conservation. (n.d.). California Geological Survey. CA Department of Conservation. Retrieved July 19, 2022, from https://www.conservation.ca.gov/cgs

California Department of Water Resources. (2018, February 12). Periodic groundwater level measurements. California Natural Resources Agency Open Data. Retrieved April 2022, from https://data.cnra.ca.gov/dataset/periodic-groundwater-level-measurements

Castellaro, S., Mulargia, F., & Rossi, P. L. (2008). Vs30: Proxy for Seismic Amplification? *Seismological Research Letters*, *79*(4), 540–543. https://doi.org/10.1785/gssrl.79.4.540

Cetin, K. O., Altun, S., Askan, A., Akgün, M., Sezer, A., Kıncal, C., Özdağ, Ö. C., İpek, Y., Unutmaz, B., Gülerce, Z., Özacar, A. A., Ilgaç, M., Can, G., Cakir, E., Söylemez, B., El-Sayeed, A., Zarzour, M., Bozyiğit, İ., Tuna, Ç., … Karaali, E. (2022). The site effects in Izmir Bay of October 30 2020, M7.0 Samos Earthquake. *Soil Dynamics and Earthquake Engineering*, *152*, 107051. https://doi.org/10.1016/j.soildyn.2021.107051

European Committee for Standardization (CEN) (2004). Eurocode 8: Design of structures for earthquake resistance, part 1: General rules, seismic actions and rules for buildings, EN 1998-1, https://eurocodes.jrc.ec.europa.eu (last

accessed April 2022).

Foster, K. M., Bradley, B. A., McGann, C. R., & Wotherspoon, L. M. (2019). A VS30 map for New Zealand based on geologic and terrain proxy variables and field measurements. *Earthquake Spectra*, *35*(4), 1865–1897. https://doi.org/10.1193/121118EQS281M

Gülerce, Z., Akbaş, B., Özacar, A. A., Sopacı, E., Önder, F. M., Uzel, B., Can, G., Cakir, E., Ilgaç, M., Söylemez, B., Saltoğlu, N., Askan, A., Cetin, K. O., & Unutmaz, B. (2022). Predictive performance of current ground motion models for recorded strong motions in 2020 Samos Earthquake. *Soil Dynamics and Earthquake Engineering*, *152*, 107053. https://doi.org/10.1016/j.soildyn.2021.107053

Hammond, E. H. (1964). Analysis of Properties in Land Form Geography: An Application to Broad-scale Land Form Mapping. *Annals of the Association of American Geographers*, *54*, 11–19. https://doi.org/https://doi.org/10.1111/j.1467-8306.1964.tb00470.x

Heath, D. C., Wald, D. J., Worden, C. B., Thompson, E. M., & Smoczyk, G. M. (2020). A global hybrid VS30 map with a topographic slope–based default and regional map insets. *Earthquake Spectra*, *36*(3), 1570–1584. https://doi.org/10.1177/8755293020911137

Hofierka, J., Mitasova, H., Neteler, M., 2009. Geomorphometry in GRASS GIS. In: Hengl, T. and Reuter, H.I. (Eds), Geomorphometry: Concepts, Software, Applications. Developments in Soil Science, vol. 33, Elsevier, 387-410 pp, http://www.geomorphometry.org

Hunter, J. A., Benjumea, B., Harris, J. B., Miller, R. D., Pullan, S. E., Burns, R. A., & Good, R. L. (2002). Surface and downhole shear wave seismic methods for thick soil site investigations. *Soil Dynamics and Earthquake Engineering*, *22*(9–12), 931–941. https://doi.org/10.1016/S0267-7261(02)00117-3

Iwahashi, J., Kamiya, I., Matsuoka, M., & Yamazaki, D. (2018). Global terrain classification using 280 m DEMs: segmentation, clustering, and reclassification. In *Progress in Earth and Planetary Science* (Vol. 5, Issue 1). Progress in Earth and Planetary Science. https://doi.org/10.1186/s40645-017-0157-2

Iwahashi, J., & Pike, R. J. (2007). Automated classifications of topography from DEMs by an unsupervised nested-means algorithm and a three-part geometric signature. *Geomorphology*, *86*(3–4), 409–440. https://doi.org/10.1016/j.geomorph.2006.09.012

Karimzadeh, S., Feizizadeh, B., & Matsuoka, M. (2019). DEM-based VS30 map and terrain surface classification in nationwide scale—A case study in Iran. *ISPRS International Journal of Geo-Information*, *8*(12). https://doi.org/10.3390/ijgi8120537

Kwok, O. L. A., Stewart, J. P., Kwak, D. Y., & Sun, P. L. (2018). Taiwan-specific model for V S30 prediction considering between-proxy correlations. *Earthquake Spectra*, *34*(4), 1973–1993. https://doi.org/10.1193/061217EQS113M

Li, M., Rathje, E. M., Cox, B. R., & Yust, M. (2021). A Texas-specific VS30 map incorporating geology and VS30 observations. *Earthquake Spectra*. https://doi.org/10.1177/87552930211033622

McPhillips, D.F., Herrick, J.A., Ahdi, S., Yong, A.K., and Haefner, S., 2020, Updated Compilation of VS30 Data for the United States: U.S. Geological Survey data release, https://doi.org/10.5066/P9H5QEAC.

Mori, F., Mendicelli, A., Moscatelli, M., Romagnoli, G., Peronace, E., & Naso, G. (2020). A new Vs30 map for Italy based on the seismic microzonation dataset. *Engineering Geology*, *275*. https://doi.org/10.1016/j.enggeo.2020.105745

Okay, A. I. (2008). Geology of Turkey : A Synopsis. *Annschnitt*, *21*, 19–42.

Pitilakis, K., Riga, E., & Anastasiadis, A. (2013). New code site classification, amplification factors and normalized response spectra based on a worldwide ground-motion database. *Bulletin of Earthquake Engineering*, *11*(4), 925–966. https://doi.org/10.1007/s10518-013-9429-4

Pitilakis, K., Riga, E., Anastasiadis, A., Fotopoulou, S., & Karafagka, S. (2019). Towards the revision of EC8: Proposal for an alternative site classification scheme and associated intensity dependent spectral amplification factors. *Soil Dynamics and Earthquake Engineering*, *126*(March), 105137. https://doi.org/10.1016/j.soildyn.2018.03.030

Prothero, D. R. (2016). *California's Amazing Geology*.

Sandikkaya, M. A., Akkar, S., & Bard, P. Y. (2013). A nonlinear site-amplification model for the next pan-European ground-motion prediction equations. *Bulletin of the Seismological Society of America*, *103*(1), 19–32. https://doi.org/10.1785/0120120008

Sandıkkaya, M. A., & Dinsever, L. D. (2018). A site amplification model for crustal earthquakes. *Geosciences (Switzerland)*, *8*(7), 15–21. https://doi.org/10.3390/geosciences8070264

Seyhan, E., Stewart, J. P., Ancheta, T. D., Darragh, R. B., & Graves, R. W. (2014). NGA-West2 site database. *Earthquake Spectra*, *30*(3), 1007–1024. https://doi.org/10.1193/062913EQS180M

Shapiro, M., & Waupotitsch, O. (2022, April 26). r.slope.aspect Manual. R.SLOPE.ASPECT - Grass Gis Manual. Retrieved July 20, 2022, from https://grass.osgeo.org/grass82/manuals/r.slope.aspect.html

Sheriff, R. E., 2002, Encyclopedic dictionary of applied geophysics: SEG

Geophysical Reference Series No. 13, 4th Ed., Society of Exploration Geophysicists (SEG), Tulsa, Oklahoma, 429 pp.

Stewart, J. P., Klimis, N., Savvaidis, A., Theodoulidis, N., Zargli, E., Athanasopoulos, G., Pelekis, P., Mylonakis, G., & Margaris, B. (2014). Compilation of a local Vs profile database and its application for inference of Vs30 from geologic- and terrain-based proxies. *Bulletin of the Seismological Society of America*, *104*(6), 2827–2841. https://doi.org/10.1785/0120130331

Strahler, A. (1957). Quantitative Analysis of Watershed Geomorphology, Transactions of the American Geophysical Union. *Transactions, American Geophysical Union*, *38*(6), 913–920.

Türkiye Bina Deprem Yönetmeliği (TBDY) (2019) Afet ve Acil Durum Yönetimi Başkanlığı, Ankara, Türkiye

USGS eros archive - digital elevation - shuttle radar topography mission (SRTM) 1 ARC-second global active. USGS EROS Archive - Digital Elevation - Shuttle Radar Topography Mission (SRTM) 1 Arc-Second Global | U.S. Geological Survey. (2018). Retrieved July 19, 2022, from https://www.usgs.gov/centers/eros/science/usgs-eros-archive-digital-elevation-shuttle-radar-topography-mission-srtm-1

United States Geological Survey. (n.d.). *USGS Vs30 Map Viewer*. Vs30 Map Viewer. Retrieved April 1, 2022, from https://usgs.maps.arcgis.com/apps/webappviewer/index.html?id=8ac19bc334f747e486550f32837578e1

Vilanova, S. P., Narciso, J., Carvalho, J. P., Lopes, I., Quinta-Ferreira, M., Pinto, C. C., Moura, R., Borges, J., & Nemser, E. S. (2018). Developing a geologically based VS30 site-condition model for Portugal: Methodology and assessment of the performance of proxies. *Bulletin of the Seismological Society of America*, *108*(1), 322–337. https://doi.org/10.1785/0120170213

Wald, D. J., & Allen, T. I. (2007). Topographic slope as a proxy for seismic site conditions and amplification. *Bulletin of the Seismological Society of America*, *97*(5), 1379–1395. https://doi.org/10.1785/0120060267

Wills, C. J., & Clahan, K. B. (2006). Developing a map of geologically defined site-condition categories for California. *Bulletin of the Seismological Society of America*, *96*(4 A), 1483–1501. https://doi.org/10.1785/0120050179

Wills, C. J., Gutierrez, C. I., Perez, F. G., & Branum, D. M. (2015). A next generation Vs30 map for California based on geology and topography. *Bulletin of the Seismological Society of America*, *105*(6), 3083–3091. https://doi.org/10.1785/0120150105

Wills, C. J., Petersen, M., Bryant, W. A., Reichle, M., Saucedo, G. J., Tan, S., Taylor, G., & Treiman, J. (2000). A site-conditions map for California based on

geology and shear-wave velocity. *Bulletin of the Seismological Society of America*, *90*(6 SUPPL.), 187–208. https://doi.org/10.1785/0120000503

Yamazaki, D., Ikeshima, D., Tawatari, R., Yamaguchi, T., O'Laughlin, F., Neal, J. C., Sampson, C. C., Kanae, S., & Bates, P. D. (2017). A high-accuracy map of global terrain elevations. *Geophysical Research Letters*, *44*, 5844–5853. https://doi.org/10.1002/2017GL072874